inorganics

MDPI

Review

Recent Advances in Low Valent Thorium and Uranium Chemistry

Nikolaos Tsoureas * and Ioannis Vagiakos

Inorganic Chemistry Laboratory, Department of Chemistry, National and Kapodistrian University of Athens, Panepistimioupoli Zografou, 157 72 Athens, Greece
* Correspondence: ntsoureas@chem.uoa.gr

Abstract: The synthesis, isolation, and characterisation of well-defined low-valent actinide complexes are reviewed with a main focus on compounds featuring uranium and thorium metal centres in formal oxidation states $\leq$ +3. The importance of the ligand environment in enabling access to these highly reactive species, as well as its influence on ground state electronic configurations and their reactivity, are emphasised. Furthermore, we highlight cyclic voltammetry (C.V.) studies as a more widely used method that can guide the synthesis of these highly reducing species.

Keywords: actinide; organometallic; uranium; thorium; low valent; small molecule activation

1. Introduction

Historically, the first attempts to access organometallic or similar (e.g., amido) complexes of the actinides date back to the Manhattan Project, when such compounds were investigated as candidates for an isotope separation (e.g., [1,2]). These efforts focused mainly on actinide complexes in oxidation states, usually >+4, especially in the case of uranium.

Unlike the 4f manifold of the lanthanides, the 5f orbitals of the actinides extend radially (one radial node excluding the one at infinity), and as a result, they can be involved in covalent bond formations. Table 1 shows their atomic ground state electronic configuration, and as can be seen, the increase in atomic number Z results in the decrease in the energy of the 5f orbitals, especially after Pu (Z = 94). Nevertheless, this decrease is not as pronounced as in the case of the 4f orbitals in the lanthanide series, and Pa, U, and Np have the general electronic configuration $[Rn]5f^n6d^17s^2$. This means that the 5f, 6d, and 7s valence orbital manifolds are relatively close in energy, and consequently, actinides have a wider accessible range of oxidation states, especially the earlier ones (e.g., +7 for the neptunyl cation [3]).

Herein, we review recent advances in broadening the actinide's extensive oxidation state (O.S.) *repertoire* to isolate organometallic complexes in oxidation states $\leq$ 3. We focus mainly on the organometallic complexes of Thorium (O.S. IIII and III) and Uranium (O.S. II and I), with an emphasis on their synthesis and reactivity, while bringing into focus underlying structural–electronic configurations and ligand environment correlations. The importance of electrochemistry in guiding the synthetic efforts towards isolating low-valent U/Th complexes is also highlighted. U(III) complexes and their extensive reactivity toward small molecules have been thoroughly reviewed recently [4] and, as such, will be discussed in passing; a recent book chapter by Evans et al. highlights the emergence of the +2 oxidation state for both the 4f and 5f elements [5].

It has to be noted that the synthesis and isolation of these highly reactive complexes demand rigorous anaerobic conditions as well as the careful exclusion of H_2O from solvents and reagents since they are easily oxidised and form strong An–O bonds. Coupled with these considerations, research with actinides requires special controls (access, environmental/laboratory/materials monitoring, waste disposal, etc.), and in the case of the trans-uranic elements, manipulations must be conducted only in purpose-built radiological facilities.

check for updates

Citation: Tsoureas, N.; Vagiakos, I. Recent Advances in Low Valent Thorium and Uranium Chemistry. *Inorganics* **2024**, *12*, 275. https://doi.org/10.3390/inorganics12110275

Academic Editors: Francis Verpoort, Shuang Xiao and Axel Klein

Received: 20 September 2024
Revised: 18 October 2024
Accepted: 21 October 2024
Published: 24 October 2024

Table 1. Atomic ground state electronic configuration of actinides; [a] although the radioactive francium and radium do not strictly belong to the An series, they are useful to highlight the 5f/6d/7s orbital energies with increasing Z.

Element	Z	Electronic Configuration
Fr [a]	87	*[Rn] $7s^1$*
Ra [a]	88	*[Rn] $7s^2$*
Ac	89	*[Rn] $6d^1$ $7s^2$*
Th	90	*[Rn] $6d^2$ $7s^2$*
Pa	91	*[Rn] $5f^2$ $6d^1$ $7s^2$*
U	92	*[Rn] $5f^3$ $6d^1$ $7s^2$*
Np	93	*[Rn] $5f^4$ $6d^1$ $7s^2$*
Pu	94	*[Rn] $5f^6$ $7s^2$*
Am	95	*[Rn] $5f^7$ $7s^2$*
Cm	96	*[Rn] $5f^7$ $6d^1$ $7s^2$*
Bk	97	*[Rn] $5f^9$ $7s^2$*
Cf	98	*[Rn] $5f^{10}$ $7s^2$*
Es	99	*[Rn] $5f^{11}$ $7s^2$*
Fm	100	*[Rn] $5f^{12}$ $7s^2$*
Md	101	*[Rn] $5f^{13}$ $7s^2$*
No	102	*[Rn] $5f^{14}$ $7s^2$*
Lr	103	*[Rn] $5f^{14}$ $6d^1$ $7s^2$*

2. Thorium

Thorium is unique among the actinides with an electronic configuration of [Rn]$6d^2 7s^2$, indicating that the 6d manifold is lower in energy than its 5f orbitals. As a result, the most common oxidation state encountered is the +4, and in that respect, thorium resembles Group IV transition metals. Furthermore, it means that 6d orbitals most likely play a dominant role in the bonding interactions, especially in the case of low valent complexes. Nevertheless, the presence of empty 5f orbitals in its valence cell can have a profound impact on the reactivity of Th(IV) complexes compared to U(IV) and Zr(IV)/Hf(IV) analogues [6–9], distinguishing it from either of these two cases. Th(IV) complexes can catalyse a variety of organic transformations [10], and we point the reader to recent reviews [11,12].

2.1. Isolation of Th(III) Complexes

Due to the dominance of the +4 oxidation state and the lack of Th(III) starting materials (unlike U), the number of known thorium complexes in the +3 oxidation state is limited compared to U(III) complexes. One reason for this relative scarcity can be traced to the Th(IV)/Th(III) redox couple value of −3.7 V vs. the corresponding value of −0.6 V for the U(IV)/U(III) couple, as estimated by atomic spectroscopy measurements (i.e., for ions in the gas phase—*vide infra* Section 5) [13]. Given the fascinating reductive reactivity of U(III) complexes, the above values suggest that Th(III) complexes should be even more reactive than their U(III) analogues. In order to overcome this highly reducing Th(IV)/Th(III) redox couple, access to low valent thorium complexes requires strong reducing agents. Furthermore, the choice of ligands is paramount in order to saturate the coordination sphere, reduce the magnitude of this potential and engender kinetic stabilisation [14].

The first reports of Th(III) complexes date back to the 1970s by Kanellakopulos et al., when the Th(IV) complex [Th(η^5-Cp)$_3$Cl] (**1**) (Cp = $C_5H_5^-$) was reduced with Na/napthalene to furnish the violet [Th(η^5-Cp)$_3$] (**2-Th**) based on an elemental analysis, IR spectroscopy and magnetic measurements [15]. These early efforts were followed by attempts to synthesise Th(III) compounds via photolysis of Th(IV) alkyl complexes of the general formula [Th(η^5-L)$_3$R] (**3-R**) (L = $Cp^{R'}$ (R′ = H, Me, D, Me5), R = ^{i}Pr, s-C_4H_9, n-C_4H_9; L = indenyl, R = n-C_4H_9) by Marks et al. [16,17]. These studies lead to the isolation of green microcrystalline solids, which were postulated to be low valent Th(III) complexes based on some magnetic measurements, UV-Vis and IR. Mechanistic studies posited the formation of

$[Th(\eta^5\text{-}L)_3H]$ (**3-H**) hydride complexes as intermediates *en-route* to the formation of these Th(III) complexes.

It was not until 1986 when the first structurally authenticated blue Th(III) complex $[Th(\eta^5\text{-}Cp'')_3]$ (**5**) (Scheme 1) was synthesised and isolated in good yields by Lappert and co-workers from the reductive redistribution of $[Th(\eta^5\text{-}Cp'')_2Cl_2]$ (**4**) (Cp'' = $[1,3\text{-}C_5H_3(SiMe_3)_2]^-$), using Na/K alloy with concurrent formation of Th metal [18]. The synthesis of (**5**) was later achieved starting from $[Th(\eta^5\text{-}Cp'')_3Cl]$ (**6-Cl**) under the same reduction conditions, thus mitigating the lower yields obtained in its initial synthesis [19]. This synthesis was further expanded to other bis-silyl substituted Cp ligands (Scheme 1) [20]. EPR studies in either powder or methylcyclohexane solutions, both at RT and low temperatures, showed that the ground state electronic configurations in both (**5**) and (**8**) are consistent with a $6d^1$ Th(III) metal centre [18,21].

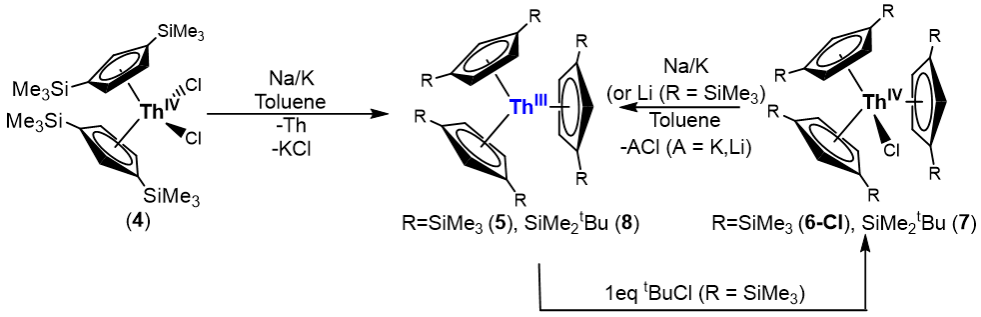

Scheme 1. Synthesis of Th(III) complexes (**5**) and (**8**).

Following the seminal synthesis of Th(III) complexes (**5**) and (**8**), Cloke and co-workers reported on the synthesis of the green–blue ionic Th(III) sandwich complex $[K(DME)_2][Th(\eta^8\text{-}COT^{TBDMS2})_2]$ (**10-Th**) (COT^{TBDMS2} = $[\{1,4\text{-}(SiMe_2{}^tBu)\}_2\text{-}C_8H_6]^{2-}$; DME = 1,2-dimethoxyethane) from the reduction in the neutral Th(IV) precursor $[Th(\eta^8\text{-}COT^{TBDMS2})_2]$ (**9-Th**) with K mirror in DME (Scheme 2) [22]. In a similar manner, the ionic U(III) congener (**10-U**) was also isolated, and a structural comparison between these two An(III) complexes revealed that the Th(III) metal radius in (**10-Th**) is approximately 0.04 Å larger than U(III) in (**10-U**) (0.06 Å larger than in Th(IV) complex (**10-Th**)). Again, EPR studies in powdered samples of (**10-Th**) at 298 K and 110 K revealed a $6d^1$ electronic configuration with the unpaired electron residing in a SOMO of predominantly d_{z2} character.

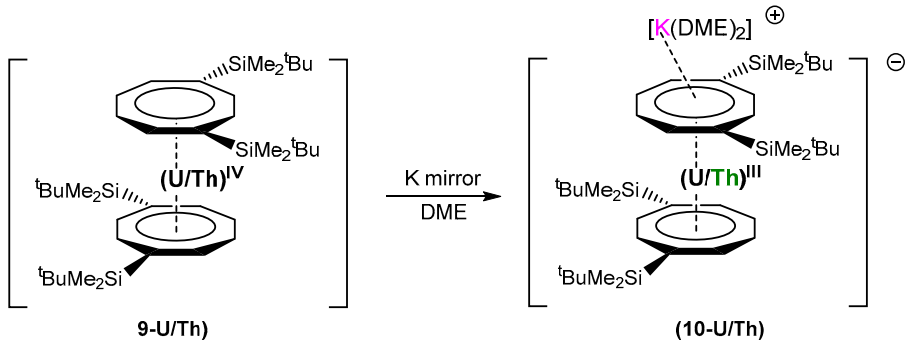

Scheme 2. Synthesis of U/Th(III) complexes supported by silyl substituted COT^{2-} ligands (COT^{2-} = cyclooctatetradienide).

In 2010, Evans et al. reported the synthesis and structural characterisation of the dark purple Th(III) $[(\eta^5\text{-}Cp^*)_2Th(\kappa^2\text{-}^i PrNC(Me)N^i Pr]$ (Cp^* = Cp^{Me5}) (**12**) from the reduction of in situ generated $[(\eta^5\text{-}Cp^*)_2Th(\kappa^2\text{-}^i PrNC(Me)N^i Pr)]^+[MeBPh_3]^-$ (**11**) with KC_8 in THF (Scheme 3) [23]. Based on UV-Vis, EPR and DFT studies, this complex also adopts a $6d^1$ ground-state electron configuration. The Th-Cp* centroid distances shorten from 2.584 and 2.598 Å in precursor (**11**) to 2.541 and 2.545 Å in (**12**), despite Th(IV)'s smaller ionic radius.

Concurrent to this is the shortening of the Th–N bond distances in (**12**) compared to the Th(IV) complex [(η^5-Cp*)$_2$Th(κ^2-^{i}PrNC(Me)N^{i}Pr)Me] (**13**) [24] and the authors attribute this phenomenon to relieving steric hindrance upon removal of the Me ligand.

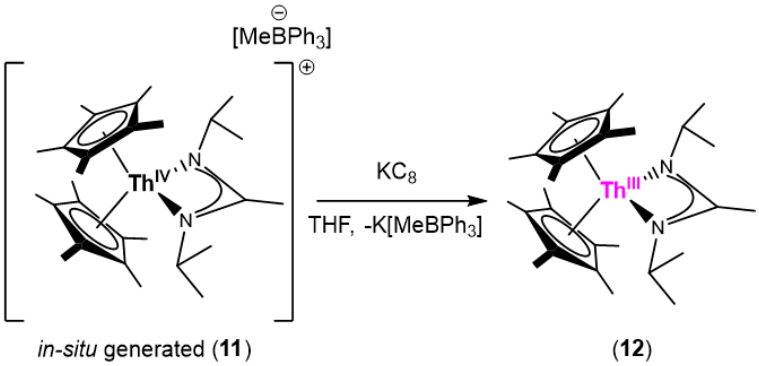

Scheme 3. Synthesis of Th(III) complex (**12**) supported by Cp* and amidinate ligands.

Using the electron donating [Cp^{Me4}]$^-$ and [Cp*]$^-$, Evans and co-workers were able to synthesise the homoleptic purple Th(III) complexes [(η^5-Cp^{Me4})$_3$Th] (**15**) [25] and [(η^5-Cp*)$_3$Th] (**16**) [26] respectively, by reducing the Th(IV) precursors [(η^5-Cp^{Me4R})$_3$Th(THF)$_x$]BPh$_4$ (R = H: x = 0 (**14^H**); R = Me, x = 0, 1 (**14^{Me}**)) with KC$_8$ or in the case of (**15**) by reducing [(η^5-Cp^{Me4})$_3$ThBr] (**15-Br**), using the same reductant (Scheme 4).

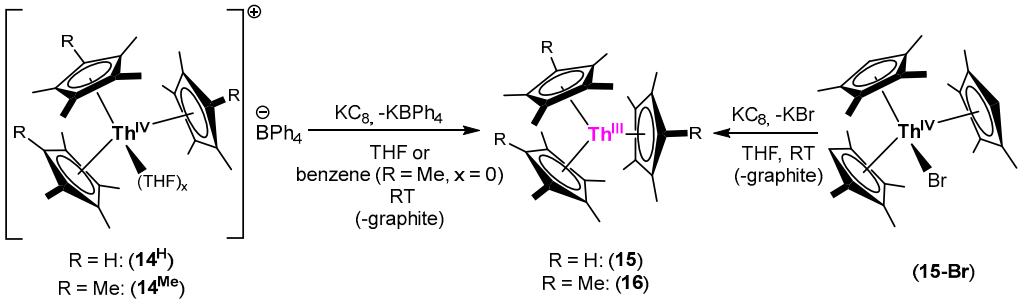

Scheme 4. Synthesis of [(η^5-Cp^{Me4R})$_3$Th] (R = H (**15**), Me (**16**)).

As in the case of (**5**) and (**8**), EPR and UV-Vis studies are consistent with a 6d^1 ground state electronic configuration for both (**15**) and (**16**), while the longer Th-Cp(centroid) distance in (**16**) (2.607 Å) compared to that in (**15**) (2.551 Å) is attributed to the steric crowding imposed by the Cp* ligand in (**16**). Interestingly, when the dimeric Th(IV) complex [{(η^5-Cp*)$_2$ThH}(μ-H)]$_2$ (**17**) [27] is reduced with KC$_8$ in the presence of crown ether 18-crown-6 (18-crown-6 = 1,4,7,10,13,16-hexaoxacyclooctadecane) the blue mixed valence Th(IV)/Th(III) dimer [K(18-crown-6)(THF)][Th(η^5-Cp*)$_2$H$_2$]$_2$ (**18**) [26] is formed, whose identity was confirmed by an elemental analysis as well as its analogous spectroscopic features (EPR, UV-Vis) to the structurally characterised mixed valence Th(IV)/Th(III) blue complex [[K(18-crown-6)(Et$_2$O)] [Th^{III}(η^5-Cp″)$_2$(μ-H)$_3$ Th^{IV}(η^5-Cp″)$_2$(H)] (**44**) (see also below—Section 2.3—Scheme 14) [26].

Using the bulky and electron-rich Cp^{tt-} (Cp^{tt-} = [1,3-^{t}Bu$_2$-C$_5$H$_3$]$^-$) ligand, Mills and co-workers were able to isolate dark blue [(η^5-Cp^{tt})$_3$Th^{III}] (**20-Th**) from the reduction in its Th(IV) precursor [(η^5-Cp^{tt})$_3$ThCl] (**19-Th**) with KC$_8$ in DME (Scheme 5) [28]. Detailed CW and pulsed EPR (HYSCORE) studies on (**20-Th**) and its U(III) congener (**20-U**) revealed that there is a greater degree of covalency between the ligand and the U^{3+} centre in (**20-U**) than in (**20-U**) despite the greater radial extent of 6d orbitals vs 5f. This was attributed to only the singly occupied 6d$_{z2}$^{1} in (**20-Th**) having the correct orientation for the overlap of its annular lobe with ligand frontier orbitals, whereas in (**20-U**), the singly occupied 5f orbitals (5f^3 electronic ground state) have a more in-plane character [28]. A more recent

detailed theoretical and computational study from Chilton et al. [29], which takes into account paramagnetic spin–orbit contributions to model the experimental spectra, arrived at the conclusion that actually (**20-Th**) exhibits a higher degree of covalency between the Cp^{tt} ligands and the Th(III) centre; interestingly the interactions between the Th(III) centre and the ligand extend further from the carbons of the 5-membered Cp^{tt} scaffold to include the H atoms of the ring, while the ^{t}Bu substituents are also involved. A comparison of ^{13}C-HYSCORE spectra of (**20-Th**) and $[Yb^{III}(\eta^5\text{-}Cp)_3]$(**2-Yb**) ($4f^{13}$) [30] surprisingly suggests similar covalency between the two, despite the 4f vs. 6d/5f valence orbitals.

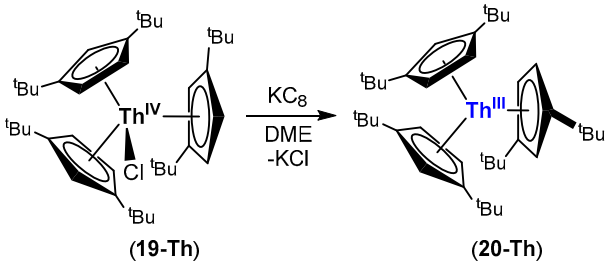

Scheme 5. Synthesis of $[(\eta^5\text{-}Cp^{tt})_3Th]$ (**20-Th**).

Reduction in the Th(IV) alanate complex $[(\eta^5\text{-}Cp^{tt})_3ThCl(\mu\text{-}H)_3AlC(SiMe_3)_3]$ (**21**) with excess KC_8 in n-hexane furnished the purple Th(III) complex $[(\eta^5\text{-}Cp^{tt})_3Th(\mu\text{-}H)_3AlC(SiMe_3)_3]$ (**22-Th**) which co-crystallises with the Th(IV) hydride complex $[(\eta^5\text{-}Cp^{tt})_3ThH(\mu\text{-}H)_3AlC(SiMe_3)_3]$ (**23**) in a 1:0.12 ratio ((**22-Th**):(**23**)) (Scheme 6) [31]. Despite the presence of (**23**), the identity of (**22Th**) as a Th(III) complex was confirmed by magnetic studies, EPR and UV-Vis spectroscopy. The most interesting feature in (**22Th**) is the Th→Al bonding interaction (2.942(2) Å) originating from an overlap of the singly occupied $6d_{z2}$ in (**22Th**) and the antibonding Al-C molecular orbital of the alanate ligand, which has a predominantly Al-3p character. The U(III) analogue (**22-U**) also shows a similar interaction, with Wyberg Bond Indices for the U→Al interaction very similar to that of (**22-Th**), despite the involvement of 5f valence orbitals [31]. This novel bonding interaction was further scrutinised by DFT studies and later by pulsed EPR techniques, and was compared to the Ti(III) complex $[Cp_2Ti(\mu\text{-}H)_3AlC(SiMe_3)_3]$(**22-Ti**), which revealed that in the latter, the Ti→Al interaction is at best minimal due to the 3d orbitals of Ti (i.e., smaller radial extent) being much less diffuse [32].

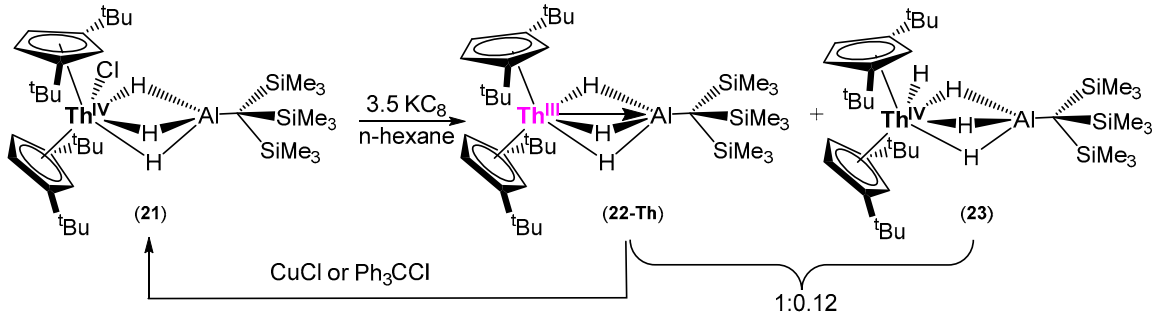

Scheme 6. Synthesis of an alanate Th(III) (**22-Th**) complex.

Liddle et al. reported that $K_2[C_4(SiMe_3)_4]$ (**25**) acts as a reducing agent when it reacts with $[(\eta^8\text{-}C_8H_8)ThCl_2(THF)_2]$ (**24**), leading to the formation of the blue trimetallic thorium cluster $[\{Th(\eta^8\text{-}C_8H_8)(\mu_3\text{-}Cl)_2\}_3\{K(THF)_2\}_2]_\infty$(**26**) (Scheme 7) [33]. This cluster features two Th(III) and one Th(IV) metal centres, and it is diamagnetic according to SQUID (Super Quantum Interference Device) measurements (albeit ~1.3% of an unidentified paramagnetic impurity was also present). The diamagnetism of (**26**) points to a d^2 singlet ground state instead of two non-interacting magnetic singlets (i.e., two d^1-d^1 Th(III) metals centres), which were also supported by theoretical calculations. Computationally, it was found

that a 3c-2e$^-$ HOMO between the three Th centres rationalised the observed magnetic measurements [33], and it was suggested that (**26**) exhibits σ-aromaticity [33–35]. This was challenged by Szczepanik [36], suggesting that a multi-centre charge-shift bonding between the Th and Cl atoms is dominant (i.e., delocalisation along the Th-Cl bridges). A very recent detailed study by Kaltsoyiannis et al. [35] scrutinising different basis sets and employing an extended NBO (Natural Bond Order) analysis (specifically Adaptive Natural Density Partitioning—AdNDP) showed that delocalized electrons are associated unsurprisingly with the COT ligands but also the Th_3 centres. Indeed, the latter showed that the bonding contribution in the Th_3 core resembles the Kohn–Sham HOMO calculated using the most appropriate SARC-TZVPP basis set from the ones scrutinised. Furthermore, calculations examining the responses of electron delocalisation in an applied magnetic field gave further evidence for the aromaticity of the Th_3 core. Lin and Mo have also arrived at the conclusion that (**26**) displays such σ-aromaticity [34]. It is also worth pointing out that unlike the previous examples discussed above, the centres of the Th(III) metals in (**26**) encompass their coordination sphere, bridging chlorides as supporting ligands.

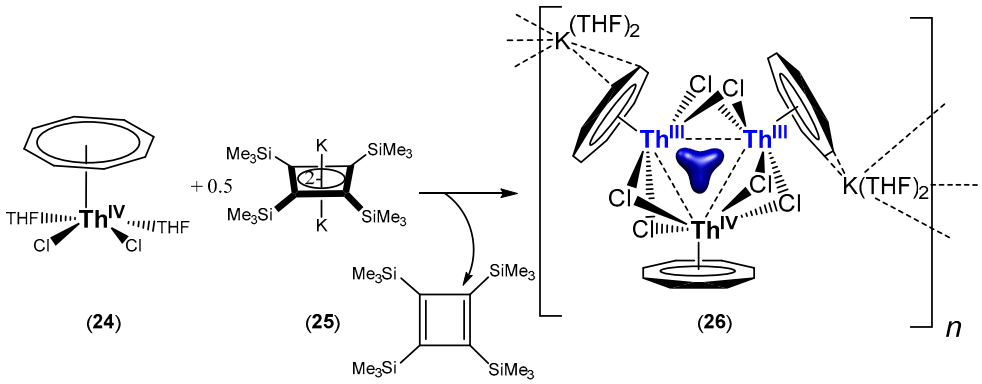

Scheme 7. Synthesis of a mixed-valence trimetallic Th(III)/Th(III)/Th(IV) cluster exhibiting σ-aromaticity between its metal centres (the metal centres in (**26**) are indistinguishable with respect to their formal oxidation centres; between the three metal centres is depicted part of (**26**)'s HOMO isosurface responsible for the σ-aromaticity.).

In 2019, Evans and co-workers reported on the dark purple Th(III) complex $[Th(OAr)_4]^-[A(THF)_x(Et_2O)_y]^+$ (**28**) (Ar = 2,6-^{t}Bu$_2$-4Me-C$_6$H$_2$; A = Li, x = 4, y =0; A = K, x = 5, y = 1) supported by bulky aryloxide ligands, instead of substituted by Cp or COT ligands [37]. Its synthesis was achieved via a reduction in the S_4 symmetric Th(IV) neutral precursor $[Th(OAr)_4]$ (**27**) either with KC_8, Li metal or Cs metal in THF; although in the last case, no molecular structure could be obtained (Scheme 8) and attempts to isolate a Th(III) complex from the dark purple solution led to decomposition. Complex (**28**) is the first example of a square planar Th(III) complex with the unpaired electron residing in the low-lying $6d_{z2}$ orbital (with some of 7s character). The geometric re-arrangement upon reduction of the S_4-symmetric (**27**) to square planar (**28**) occurs because of the significant gain in ligand field stabilisation, partly due to the repulsive interactions between the π-donating aryloxide ligands and the d_{xy} orbital, as well as the degenerate d_{xz} and d_{yz} orbitals of the Th(III) metal centre. Dispersion forces were also found to be important as they can be better facilitated in a square planar environment, where more of the ^{t}Bu methyl groups are near the metal centre, as a result of the longer Th(III)–OAr bond distances (*avg* 2.243 Å) vs. the ones in [Th(IV)-OAr']$_4$ (**29**) (Ar' = 2,6-^{t}Bu$_2$-C$_6$H$_3$ or 2,6-Ph$_2$-C$_6$H$_3$) complexes (*avg* ~2.190 Å). The choice of supporting aryloxide was also found to be crucial in determining the geometry of the Th(IV) precursor, especially since it was found that if (**27**) adopted a *Td* or similar geometry, its 1e-reduction would be endothermic. The square-planar geometry of d^1 (**28**) is usually associated with transition metal complexes with d^7–d^9 electronic configurations and shows that analogies between the early actinides and the transition metals should be better considered as mere parallelisms.

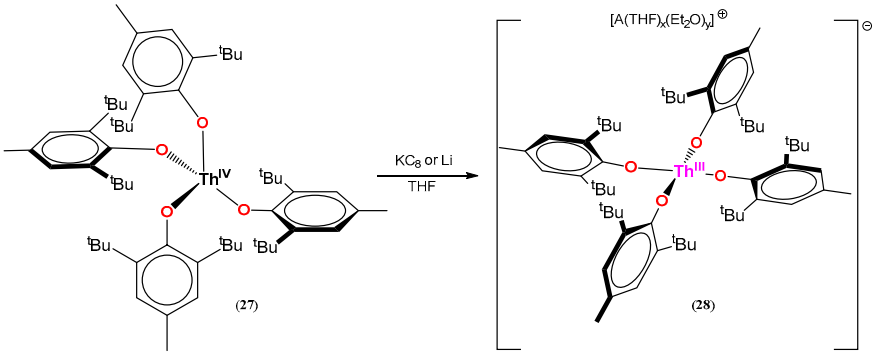

Scheme 8. Synthesis of square planar $d_{z2}{}^1$ Th(III) complex (**28**) (A = alkali metal cation: Li (x = 4, y = 0), K (x = 5, y = 1)).

2.2. Isolation of Th(II) Complexes

The scarcity of Th(III) complexes is even more pronounced in the case of Th(II) complexes. The first evidence of the existence of Th(II) was reported by Lappert et al., when it was observed that during the synthesis of [Th(η^5-Cp″)$_3$] (**5**) using an excess of Na/K alloy, the reaction mixture turned from blue to green. An NMR spectroscopy revealed that this green compound was diamagnetic, but it could not be isolated and fully characterised. Following the landmark isolation of the first U(II) complex [K(2.2.2-crypt)][U^{II}(η^5-Cp′)$_3$] (**68′-U**) (Cp′ = {C_5H_4-$SiMe_3$}$^-$ see below Section 3.1.1) [38], Evans and co-workers tried to access the Th(II) complexes supported by the Cp′ ligand, but unfortunately these attempts were not successful [39]. Following this work, the reduction in (5) with a small excess of KC_8 (*ca* 1.5 mol eq.) in the presence of [2.2.2.-crypt] or 18-crown-6 in THF yielded a green solution, from which the dichroic blue/red Th(II) complex [K(macrocycle)(THF)$_x$]$^+$[Th(η^5-Cp″)$_3$]$^-$ (**30**) (macrocycle [2.2.2-crypt], x = 0; macrocycle = 18-crown-6, x = 2) could be isolated (Scheme 9) [40]. The molecular structure of the anion in (**30**) shows that the Th(II) metal centre adopts a trigonal coordination mode similar to the Th(III) precursor (**5**). The Th-Cp″ (centroid) distances are essentially the same between the two compounds (*avg* 2.523 Å in (**30**) vs. 2.520 Å in (**5**)), signifying that the ground state electronic configuration in (**30**) is most likely $6d^2$. NMR spectroscopy, as well as magnetometric studies both in solution (Evan's method) and in the solid state (SQUID) at RT and low temperatures, show that (**30**) is indeed diamagnetic, confirming Lappert's initial observations. It has to be noted that DFT calculations in the gas phase point to a $5f^1 6d^1$ ground electronic configuration while the experimentally-found $6d^2$ electronic configuration is only 63 cm^{-1} higher in energy; the HOMO in (**30**) has largely $6d_{z2}$ character.

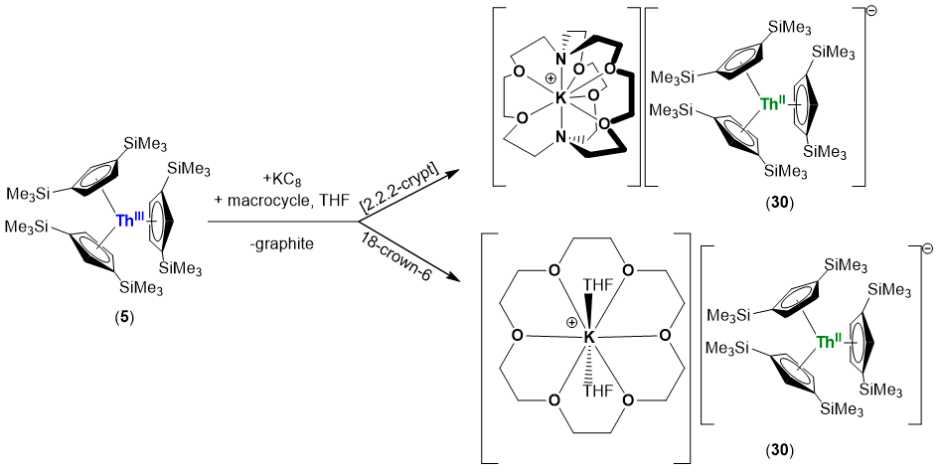

Scheme 9. Reduction in (5) furnishing the Th(II) complexes (**30**).

2.3. Reactivity of Th(III) and Th(II) Complexes

Surprisingly, it was more than three decades after (**5**) [18] was isolated that the reactivity of this seminal Th(III) complex was investigated. Complex (**5**) readily reacts with stoichiometric amounts (i.e., two equivalents) or excesses of CO_2 (gas or supercritical) to give the Th(IV) dimer (**32**) (Scheme 10), which contains a bridging $\{\mu\text{-}\kappa^2\text{:}\kappa^2\text{-}C_2O_4\}$ oxalate di-anion resulting from the reductive coupling of two CO_2 molecules [41]. In this case, the Cp″ ligand is not innocent and undergoes an insertion of a CO_2 molecule into one Th–C(Cp″) bond, followed by $SiMe_3$ migration to form a new carboxylate ligand. As a model of the first steps of this reaction, (**5**) was reacted with 0.5–10 equivalents of CS_2 to form the dinuclear Th(IV) complex (**33**), where the two metal centres are bridged by $\{\mu\text{-}\kappa^2\text{:}\kappa^1\text{-}CS_2\}$ dianion (Scheme 10) [41]. Complex (**5**) also reacts with white phosphorus to yield cleanly the Th(IV) dimer (**31**) featuring a bridging cyclo-P_4 6π aromatic dianion which adopts a $\{\mu\text{-}\eta^1\text{:}\eta^1\text{-}P_4\}$ coordination mode [42]. This coordination mode is most likely due to the steric congestion imposed by the Cp″ ligands, with VT-NMR studies showing restricted rotation of the $\{\mu\text{-}\eta^1\text{:}\eta^1\text{-}P_4\}$ bridging moiety around the Th–P bond. (Scheme 10). The same group also studied the reactivity of (**5**) with pyridine and 4,4′-bipyrine (4,4′-bipy), yielding the Th(IV) complexes (**34**) and (**35**) respectively (Scheme 10) [43]. In both (**34**) and (**35**), the N-heterocycle is no longer aromatic, and the Th–N bond distances are characteristic of Th-amide bond lengths, while at the same time, a new C–C (case of (**35**)) or C=C (case of (**34**)) bond has been formed. Based on the reactivity of (**5**) with 4,4′-bipy and pyridine, the authors were able to gauge the reduction potential of the Th(III) metal centre in (**5**) (*vide infra*) at *ca* −2.76 V vs. Ag/AgCl, although it was noted that for the reduction of a substrate to take place, its coordination to the Th(III) metal centre was a pre-requisite (e.g., no reaction with naphthalene or anthracene). In contrast to the observed reactivity of (**5**) with pyridine and 4,4′-bipy, the U(III) complexes $[U(\eta^5\text{-}Cp')_3]$ (**67′-U**) and $[U(\eta^5\text{-}Cp^t)_3]$ ($Cp^t = \{^tBu\text{-}C_5H_4\}^-$) do not react with these two heterocycles. Interestingly, when crystals of (**34**) are dissolved in hydrocarbons (toluene-d^8, C_6D_6), the appearance of a blue coloration characteristic of Th(III) complexes is observed over a short period of time (<10 min); the authors suggest that a fast equilibrium takes place involving reversible C–C bond formation between the two pyridines in (**35**). From powder X and Q band EPR spectra, the Th(IV) complex $[Th^{IV}(\eta^5\text{-}Cp'')_3(py^{\square-})]$(**36**) containing a pyridine radical anion ligand has been tentatively postulated to be formed, but reactivity studies were not able to substantiate its intermediacy in the formation of (**32**). It is interesting to note that no reactivity is observed between (**5**) and 4-^{t}Bu-pyridine. Complex (**5**) also reacts with the sterically unencumbered N-heterocyclic olefin (NHO) 3-dimethyl-2-methyleneimidazoline (Scheme 10) in toluene at 130 °C to furnish the Th(IV) methyl complex $[Th^{IV}(\eta^5\text{-}Cp'')_3Me]$ (**6-Me**) and $MeImCH_2CH_2MeIm$ (MeIm = 1-methyl-imidazole) as the organic side-product [44]. Complex (**6-Me**) is the result of N-demethylation via a radical pathway involving coordination of the NHO to the Th(III) metal centre in (**5**), according to some preliminary spectroscopic evidence.

The Th(III) complex (**5**) becomes disproportionate following its reaction with MX salts (MX = KH, LiMe, KCl, NaN_3), in the presence of a chelate ([2.2.2-crypt] or 18-crown-6) to afford the Th(II) complex (**30**) along with the corresponding Th(IV) complex $[Th^{IV}(\eta^5\text{-}Cp'')_3X]$(**6-X**) (Scheme 11) [45]. A plausible mechanism for this reactivity involves the initial formation of [M(chelate)] $[Th^{III}(\eta^5\text{-}Cp'')_3X]$ (**37**), which in the presence of neutral (**5**), affords the disproportionation products. This mechanism is supported by electrochemical data and the comproportionation reaction between Th(II) complex (**30**) and $[Th^{IV}(\eta^5\text{-}Cp'')_3Cl]$ (**6-Cl**) that yielded (**5**) as the major product [45].

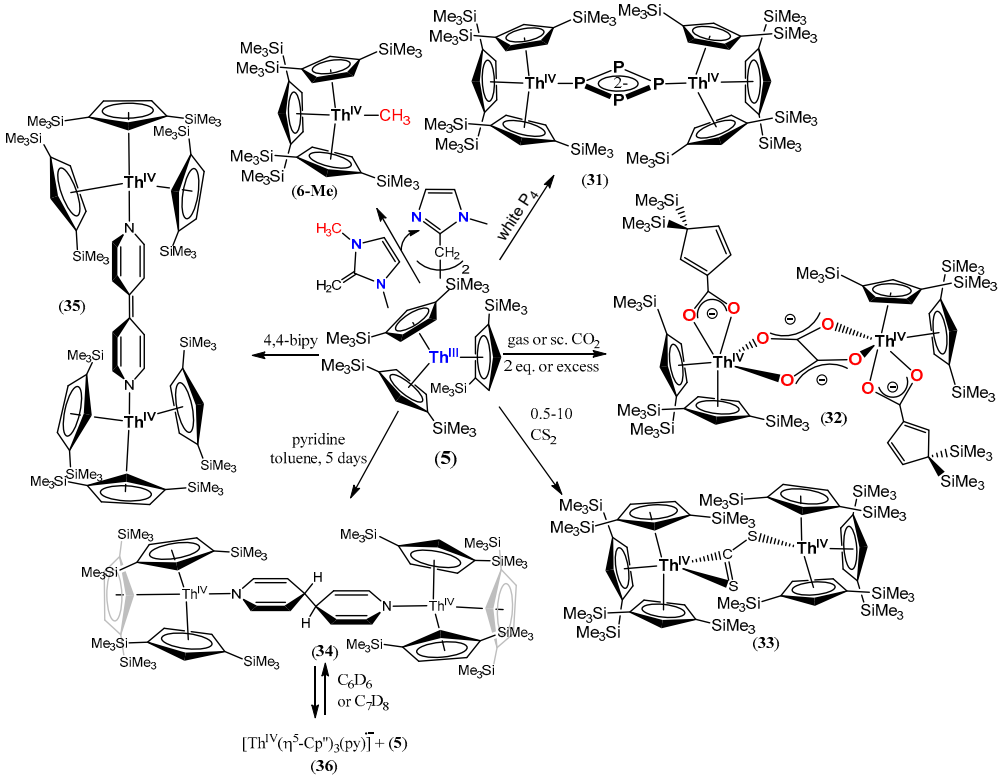

Scheme 10. Reactivity of (**5**).

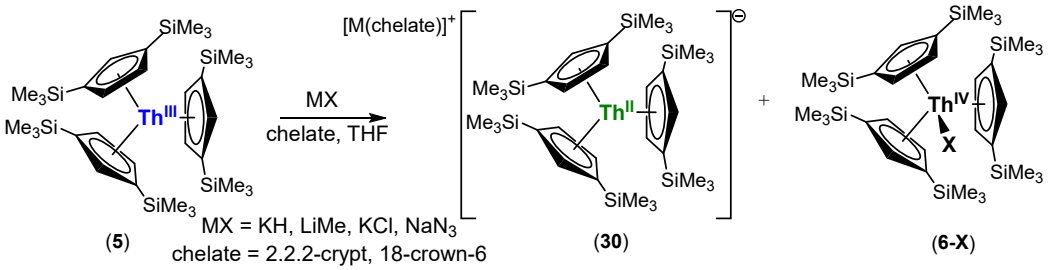

Scheme 11. Disproportionation of (**5**) yielding Th(II) complex (**30**).

When the Th(III) complex (**15**) (Scheme 12) reacted under similar conditions with KH in the presence of [2.2.2-crypt] the only isolable products were $[(\eta^5\text{-}Cp^{Me4})_3Th^{IV}H]$ (**15-H**), $[K(2.2.2\text{-crypt})][Cp^{Me4}]$ and the tuck-in complex $[K(2.2.2\text{-crypt})][(\eta^5\text{-}Cp^{Me4})_2Th^{IV}H(\eta^1{:}\eta^5\text{-}C_5Me_3HCH_2)]$ (**38**). The same product distribution was also observed when (**15**) was reacted with H_2 in the presence of KC_8 and [2.2.2-crypt] (Scheme 12) [46].

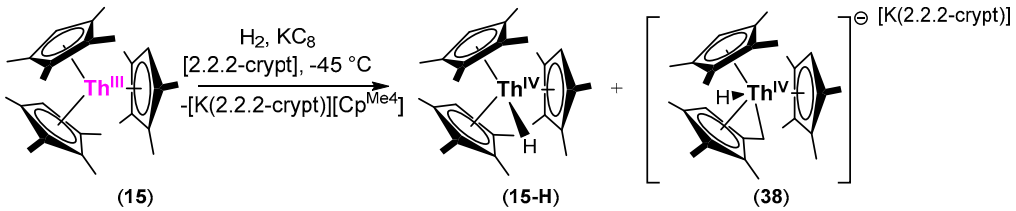

Scheme 12. Reaction of (**15**) with H_2 in the presence of KC_8 yielding Th(IV) hydride complexes (**15-H**) and (**38**).

Complex (**15**) does not react appreciably with just H_2 before the onset of decomposition, while (**5**) shows no reactivity at all. In contrast, complex (**16**) reacts readily with H_2 to give the Th(IV) complex $[(\eta^5\text{-}Cp^*)_3Th^{IV}H]$ (**16-H**) (Scheme 13) [26]. As can be seen from

Scheme 13, complex (**16**) reacts in a manner typical of a reducing complex with various reagents to give sterically crowded Th(IV) products. For example, the Th(IV) methyl complex (**16-Me**) does not react with H_2 to give the hydride complex (**16-H**).

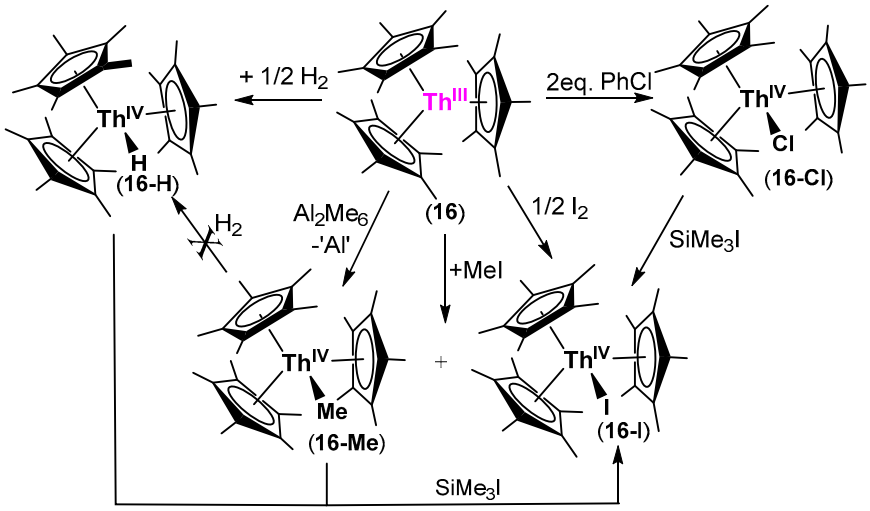

Scheme 13. Reactivity of Th(III) complex (**16**).

The reactivity of (**16**) diverges from that of its U(III) analogue $[(\eta^5\text{-Cp*})_3U^{III}]$ (**39**); for instance, complex (**16**) produces only (**16-Cl**) (Scheme 13) even when it reacts with an excess of PhCl, and even over prolonged periods, while (**39**) ultimately yields $[(\eta^5\text{-Cp*})_2U^{IV}Cl_2]$ (**40**) under these conditions [47]. Furthermore, (**16**), unlike (**39**), does not ring-open THF, nor does it polymerise ethylene-like complexes $[(\eta^5\text{-Cp*})_3M^{III}]$ (M = U (**39**) [48], Ce (**40**), Pr (**41**), Nd (**42**), Sm (**43**) [49]).

The Th(II) complex $[K(18\text{-crown-6})(THF)_2][(\eta^5\text{-Cp}'')_3Th^{II}]$ (**30**) reacts with $[Et_3NH][BPh_4]$ to give the Th(III), complex (**5**), and the Th(IV), complex $[(\eta^5\text{-Cp}'')_3Th^{IV}H]$ (**6-H**) (Scheme 14); as mentioned above, (**5**) does not react with H_2 to give (**6-H**) in a manner analogous to (**16**) (Scheme 13). Furthermore, (**30**) reacts with H_2, with concomitant loss of [K(18-crown-6)][Cp″] furnishing again the Th(III) complex (**5**) and the structurally-characterised mixed-valence Th(IIII)/Th(IV) dimer $[K(18\text{-crown-6})Et_2O][(\eta^5\text{-Cp}'')_2Th^{III}(\mu\text{-H})_3Th^{IV}H(\eta^5\text{-Cp}'')_2]$ (**44**) (Scheme 14). Complex (**44**) (and (**18**)—see Section 2.1—as determined by the analogy of their spectroscopic analyses) is a rare example of a mixed-valence Th(III)/Th(IV) dimer; a spectroscopy and computational analysis advocate a $6d^1$ configuration with the HOMO and LUMO being localised at the Th(III) metal centre, and having predominantly d_{z2} metal characteristics. The isolation of (**44**) signifies that the $[Cp''_2(\mu\text{-H})_3]^{5-}$ ligand set can also provide a suitable coordination environment for this electronic configuration. Complex (**44**) can be oxidised with $AgBPh_4$ or CuX salts to furnish (**6-H**). In contrast, its Cp* analogue (**18**) is oxidised by the same reagents to give the Th(IV) dimeric precursor $[\{(\eta^5\text{-Cp*})_2Th^{IV}H\}(\mu\text{-H})]_2$ (**17**), further demonstrating the role of steric hindrance in the reactivity of these complexes [46].

The formation of (**44**) from (**30**) involves a net four-electron reduction of H_2 to produce four hydride ligands in (**44**). The observation that the Th(III) complex (**5**) is also formed during the reaction suggests that electron processes are also in play. A plausible mechanism involves the formation of a dimeric Th(IV) complex with bridging hydride ligands, similar to (**17**), which is then reduced in the presence of (**5**), ultimately yielding (**44**). Similarly, the reaction of the Th(II) complex (**30**) with $[Et_3NH][BPh_4]$ to give the Th(IV) complex (**6-H**) is also a net two-electron oxidation process (Scheme 14). However, the concurrent formation of the Th(III) complex (**5**) and its lack of reactivity towards either H_2 or $[Et_3NH][BPh_4]$, makes the implication of the one electron process in the overall mechanism apparent.

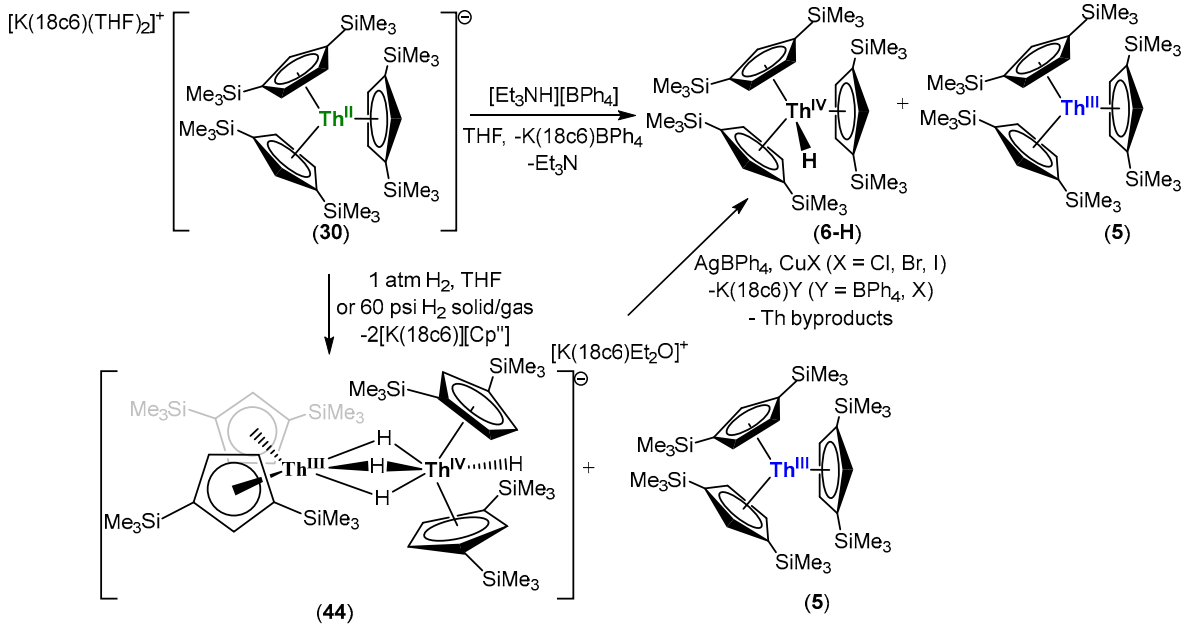

Scheme 14. Reactivity of Th(II) complex (**30**).

Nevertheless, the observed redox transformations of (**30**) distinguish Th(II) complexes from their U(II) analogues (see below Section 3.2). A germane example is the reactivity of (**30**) with COT (C_8H_8) to yield the Th(IV) complex [$Th^{IV}(\eta^5$-Cp″$)_2(\eta^8$-$C_8H_8)$] (**45**), i.e., the result of a two electron reductions in COT, as the only thorium containing product (Scheme 15) [46].

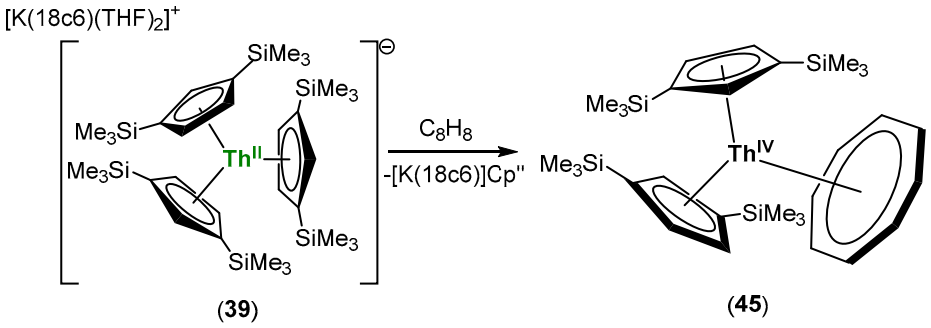

Scheme 15. Net 2e$^-$ reduction in COT by Th(II) complex (**30**).

At this point it is also pertinent to mention that the reactivity of the Th(IV) complexes [$Th^{IV}(\eta^5$-$Cp^{ttt})_2$(2,2′-$bipy^{2-}$)]/[$Th^{IV}(\eta^5$-$Cp^{tt})_2$(2,2′-$bipy^{2-}$)] (**46^{t3}/46^{t2}**) (Cp^{ttt} = {1,2,4-^{t}Bu$_3$-C_5H_2}$^-$) (Scheme 16) with Ph_2C=S [50] parallels that of the U(III) complexes [$U^{III}(\eta^5$-Cp‴$)_2$(2,2′-$bipy^{-\bullet}$)](**47**) (Cp‴ = {1,2,4-(SiMe)$_3$-C_5H_2}$^-$) with the same substrate or of [$U^{III}(\eta^5$-Cp*$)_2$(2,2′-$bipy^{-\bullet}$)] (**48**) with p-chloro-benzaldehyde [51–53]. Magnetometric studies (SQUID) showed that complexes (**46^{t3}/46^{t2}**) exhibit small but positive χ_M's at H > 1T, displaying temperature independent paramagnetism which is indicative of low-lying excited states coupling to their S = 0 ground state (van Vleck paramagnetism). Computational studies further confirmed this, pointing to an S = 1 triplet excited state ($f^0d^1\pi^{*1}$) which can be thermally populated. The observed product is explained with the reaction taking place along this S = 1 energy surface with the first step being the coordination of Ph_2C=S to the Th centre of this triplet state complex [50].

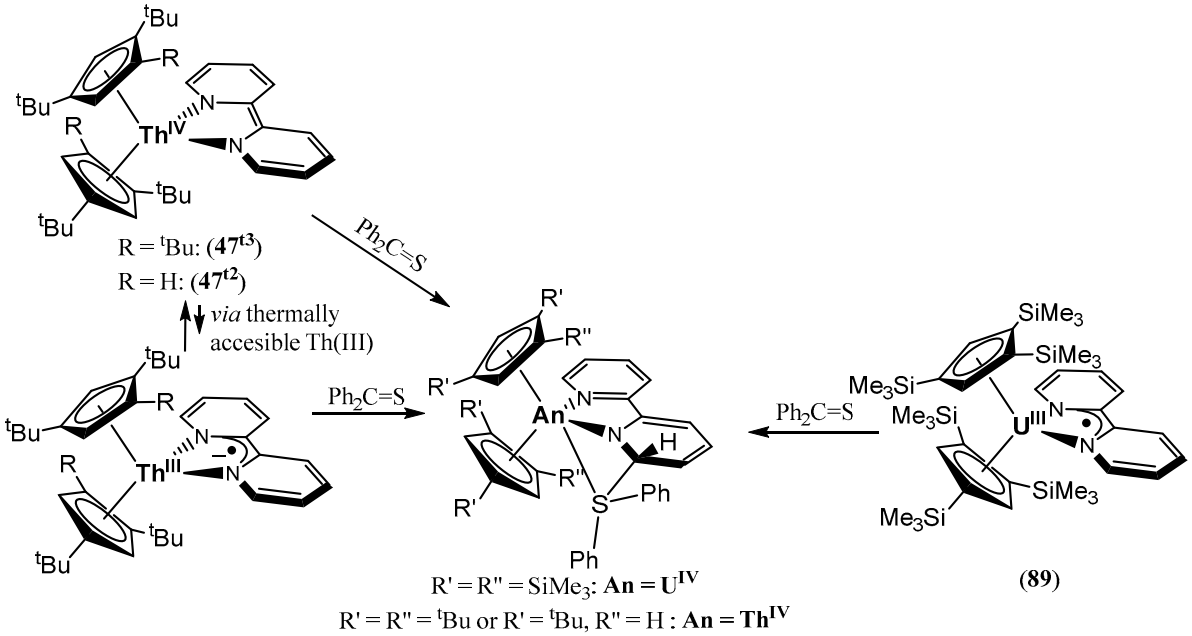

Scheme 16. Reactivity of Th(IV) complexes resembling the one of U(III) complexes.

The intermediacy of a transient Th(III) complex has also been suggested in the reductive transformation of CO_2 to $C_2O_4^{2-}$ (reductive coupling) or CO_3^{2-} (reductive disproportionation) by the Th(IV) complex [Th(η^8-COT^{TIPS})(η^5-Cp*)I] (**53-I**) (COT^{TIPS} = [{1,4-(Si^iPr_3)}$_2$-C_8H_6]$^{2-}$) in the presence of an Na/K alloy in toluene over 12 days to furnish the Th(IV) dimeric complexes [{Th(η^8-COT^{TIPS})(η^5-Cp*)}$_2$(μ:κ^2, κ^2 − C_2O_4] (**54**) and [{Th(η^8-COT^{TIPS})(η^5-Cp*)}$_2$(μ:κ^1, κ^2 − CO_3] (**55**) (Scheme 17), respectively. The intermediacy of the Th(III) complex [Th(η^8-COT^{TIPS})(η^5-Cp*)] (**53**), analogous to the U(III) mixed sandwich complexes, supported by the $[COT^{SiR}{}_3]^{2-}$ (R = ^{i}Pr, Me) and $[Cp^{Me4R1}]^-$ (R1 = H, Me, Et, ^{i}Pr, ^{t}Bu, $SiMe_3$) ligands known to facilitate reductive transformations of CO_2, was based on the absence of reactivity between [Th(η^8-COT^{TIPS})(η^5-Cp*)X] (**53-X**) (X = Cl, I) and Na_2CO_3 or $Na_2C_2O_4$ over prolonged periods of time. Attempts to isolate the Th(III) complex (**53**) by reducing (**53-I**) with Na/K alloy under the same reaction conditions invariably led to the formation of Th metal and [Th^{IV}(η^8-COT^{TIPS})$_2$] (**56**) [54].

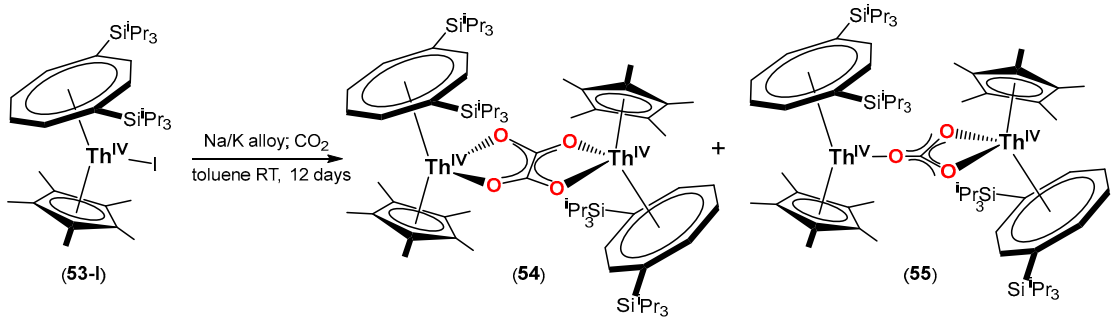

Scheme 17. Reductive coupling and reductive disproportionation of CO_2 involving the intermediacy of a Th(III)(**53**) complex.

Diaconescu et al. have reported on the synthesis and isolation of a series of bimetallic thorium complexes supported by a di-amido ligand, and featuring an aromatic 10π tetra-anionic μ-η^6,η^6 arene symmetrically bridging the two metal centres (**56**) (Scheme 18) [55]. Although these inverse arene sandwich complexes feature Th(IV) metal centres, their reactivity is akin to that of low valent thorium complexes (e.g., the reaction of (**56**) with COT, Scheme 18).

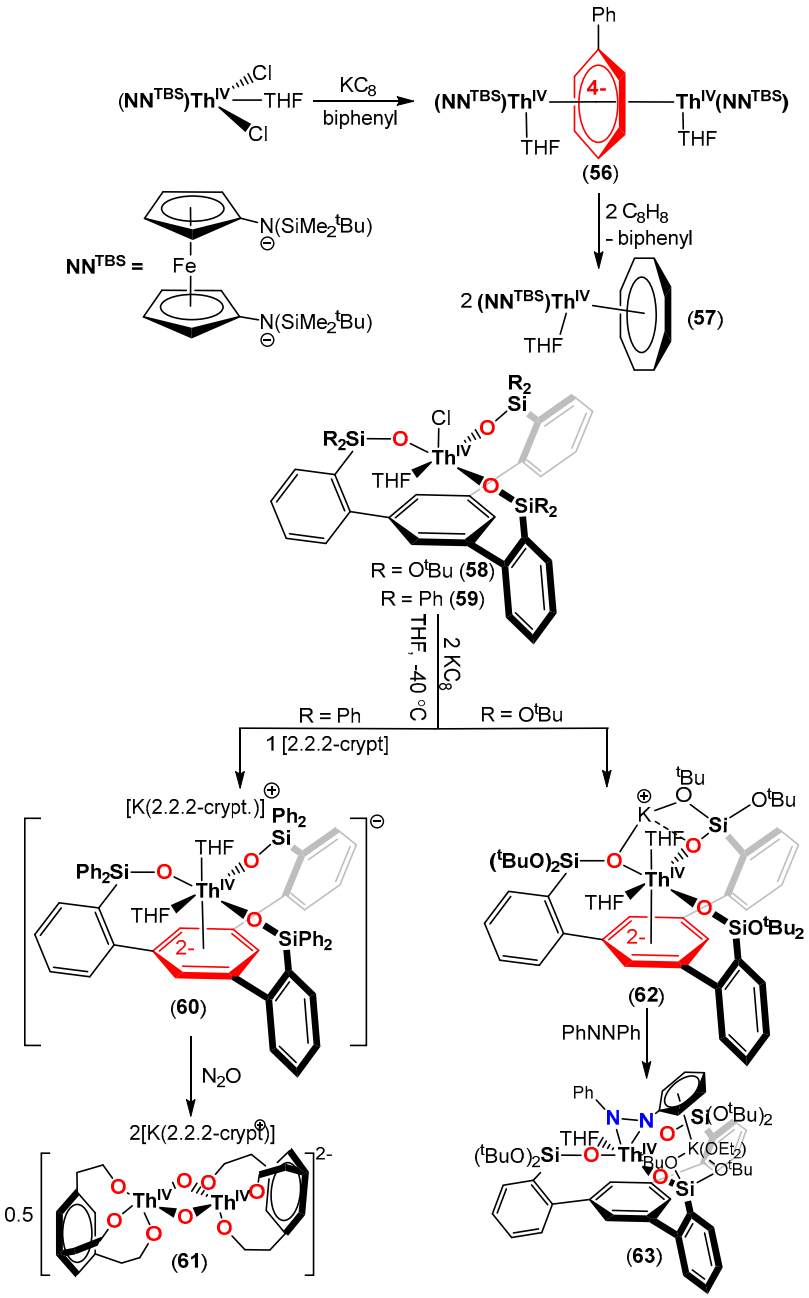

Scheme 18. Inverse sandwich arene complexes of Th(IV) reacting as 'Th(II)' synthons. In the case of (**56**), only the biphenyl is shown as an example, but analogous complexes where arene = toluene, benzene and naphthalene have also been synthesised, isolated and characterised.

Mazzanti and co-workers, in an effort to access Th(III) complexes supported by a tripodal ligand scaffold featuring silyl oxide moieties of varying electron-donating abilities tethered to a basal arene, isolated complexes (**60**) and (**62**), both featuring Th(IV) metal centres with a doubly reduced non-planar basal arene [56]. CV studies of both (**60**) and (**62**) showed that two reduction events are ligand-centred and further confirmed structural data advocating the description of these two complexes as [Th^{IV}-(arene)$^{2-}$]. Representative examples of the reactivity of (**60**) and (**62**) shown in Scheme 18, resemble those of Th(II) complexes, but as in the case of the Th(IV) dimers (**56**) (see above), are the consequence of a highly reduced arene ligand.

3. Uranium

The organometallic and non-aqueous coordination chemistry of uranium has been extensively studied, especially due to the relevant abundance of depleted-uranium with respect to the nuclear fuel cycle. Its $[Rn]5f^3 6d^1 7s^2$ electronic configuration means that all the oxidation states from +3 all the way to +6 are accessible.

From the standpoint of low valent uranium chemistry, the +3 oxidation state is the most explored, especially due to the well-established methods for accessing a variety of U(III) precursors [48,57–68] and starting materials [58,62,63,69–77]. Furthermore, the reducing nature of [U(III)] complexes enables fascinating reactivity with a variety of small molecules and substrates. Some characteristic examples include the reductive transformations of carbon oxides [78–99] (including C_3O_2 [100]), phosphorus [101], phospha-alkynes [102], ECO^- (E = P [103], As [104]), nitrogen fixation [97,105–110], multi-electron N≡N bond activation-cleavage and its subsequent transformation to ammonia and silyl-amines [111–119], electrocatalytic water splitting [120,121], arene activation [122,123], isolation of a CO_2 radical anion [99,124], activation of ethylene and its catalytic hydrogenation [125], activation of CS_2 [93,96,98,126,127], COS [128], activation of NO [129,130] and NO/CO conversion to isocyanate [131,132], SO_2 [90], as well as novel insertion chemistry [64,133,134]. Moreover, [U(III)] complexes offer a gateway to high valent complexes, allowing for the isolation of terminal chalcogenides [135–147], nitride [119,136,148–160], amido [161]and imido complexes [133,147,159,162–171] in oxidation states $\geq$ +4. The scope of this review is focused mainly on $[U^{n+}]$ complexes where n < 3, and we would like to point the reader to the following reviews [4,123,172–178] delving into the reactivity of uranium complexes in oxidation states $\geq$ +3.

3.1. Isolation of U(II) and U(I) Complexes and Their Reactivity

3.1.1. U(II) Compounds Supported by Cyclopentadienyl Ligands

The first evidence for this oxidation state came from matrix isolation experiments and similar observations in the gas phase [179]. In the condensed phase, early attempts to access U(II) complexes via the reaction of UCl_4 with two equivalents of KCp (Cp = $C_5H_5^-$) in the presence of two equivalents of Na metal as a reductant in THF were unsuccessful, yielding instead the U(IV) complex $[U(\eta^5\text{-Cp})_3O\text{-}^n\text{Bu}]$ (**64**) [180]. Counter-intuitively, in the complexes $[\{NAr(R)\}_2U]_2(\mu^2{:}\eta^6,\eta^6\text{-arene})$ (**65**) (R = ^{t}Bu, Ad; arene = 3,5-Me_2-C_6H_3) [170,181] and $[(\eta^5\text{-Cp}^*)_2U]_2(\mu^2{:}\eta^6,\eta^6\text{-benzene})$ (**66**) (Cp* = $C_5Me_5^-$) [182], although each U metal centre can be assigned the +2 formal oxidation state, detailed spectroscopic studies show instead that the bridging arene has been reduced. Therefore, these complexes belong to the wider class of inverted uranium arene complexes [183], and each U centre adopts a $\geq$+3 formal oxidation state depending on the degree of the bridging arene reduction, which acts as a redox-active ligand (RAL).

Following their success in accessing the +2 oxidation state for the whole lanthanide series (except Pm) [5,184–188], Evans and co-workers reported the first successful synthesis, isolation and crystallographic characterisation of the dichroic maroon/green U(II) complex $[K(2.2.2\text{-cryptand})][U^{II}(\eta^5\text{-Cp}')_3]$ (**68′-U**) (Cp′ = $\{SiMe_3\text{-}C_5H_4\}^-$), prepared by the reduction in green $[U^{III}(\eta^5\text{-Cp}')_3]$ (**67′-U**) [58] with KC_8 in the presence of the chelate 2.2.2-cryptand in THF/Et_2O at −35 °C [38]. Complex (**68′-U**) is stable at RT in the solid state for several days, but its THF solutions have a $t_{1/2}$ of *ca* 1.5 hrs owing to its high reactivity (Scheme 19). In contrast, its analogues (**68′-U**) supported by the Cp″ (Cp″ = $\{1,3-C_5H_4(SiMe_3)_2\}^-$) (Scheme 19) ligand are more stable ($t_{1/2}$ of 15 to 20 hrs in THF) [189]. The increased steric protection and the incorporation of an extra electron withdrawing $SiMe_3$ group per Cp are believed to play some role, but unfortunately, due to the insufficient quality of structural data for (**68″-U**) the comparison of pertinent metric parameters with (**68′-U**) is not possible.

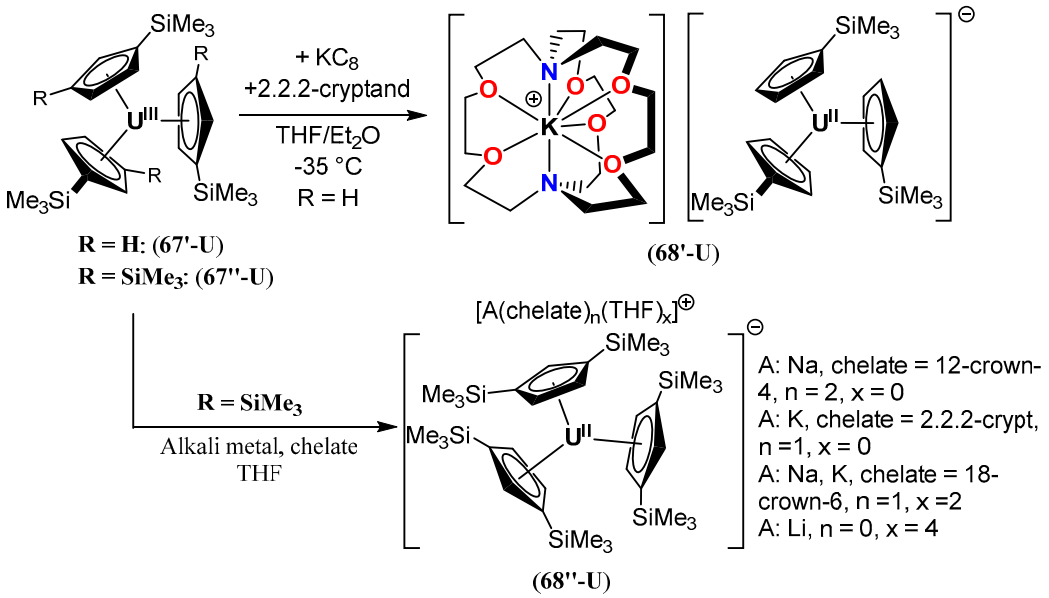

Scheme 19. Synthesis and isolation of the first U(II) complexes (A = Alkali-metal cation).

Upon reduction in (**67′-U**) to (**68′-U**), the U-Cp′(centroid) distance increases (*avg.* 2.521 Å in (**68′**) vs. *avg.* 2.508 Å in (**67′-U**)); such an increase is also observed during the reduction in [$Ln^{(III)}(\eta^5\text{-}Cp')_3$] (**67′-Ln**) to [$Ln^{(II)}(\eta^5\text{-}Cp')_3]^-$ (**68′-Ln**) [5,184–188] and is attributed to the $4f^{n-1}5d^1$ electronic configuration of the Ln(II) metal centre. In the case of (**68′-U/68′′-U**), DFT, magnetometric and UV-Vis studies support a $5f^36d^1$ ground state electronic configuration, rather than the $5f^4$ expected for a U(II) ion. The formation of U(II) complexes (**68′-U/68′′-U**) was also confirmed as a ground state electronic configuration, rather than the 5fs of paramagnetic uranium complexes are very sensitive to changes in oxidation state [190]. In both cases, a significant upfilled shift to the region of −320 to −330 ppm was recorded for these two U(II) complexes compared to −163 ppm for (**67′′-U**) and −165 ppm for (**67′-U**). The possibility of (**68′-U**) being the anionic U(III) hydride complex [K(2.2.2-cryptand)][$HU^{III}(\eta^5\text{-}Cp')_3$] (**69′**), was excluded by the independent synthesis of the latter from (**67′-U**) and KH in the presence of 2.2.2-cryptand and it displayed distinctly different spectroscopic and structural features compared to (**68′-U**) (*vide infra*) [38]. It is also interesting to note that the family of the ionic U(II) complexes (**68′′-U**) can be accessed using Na and Li metal as well as K, an observation which is in agreement with CV studies which have determined the U(III)/U(II) redox couple for (**68′′-U**) to be −2.71 V vs. Fc/Fc+ (see also Section 4) [191,192]. Furthermore, the use of chelating agents (i.e., crown-ethers) is not strictly necessary for the preparation of U(II) complexes as shown by the synthesis and isolation of [$Li(THF)_4$] [$U^{II}(\eta^5\text{-}Cp'')_3$] (**68′′-U**) or the polymeric [$(\eta^5\text{-}Cp'')U^{II}(\mu\text{:}\eta^5, \eta^5\text{-}Cp'')_2Cs(THF)_2]_n$ (**70**) (Figure 1) [192]. It has to be noted though, that when the preparation of (**68′-U**) was attempted using 18-crown-6 instead of [2.2.2-crypt], the reaction mixture furnished instead the bridging hydride di-metallic complex [$K(18\text{-c-6})(Et_2O)$][$\{U^{III}(\eta^5\text{-}Cp')_3\}_2(\mu\text{-H})$] (**71**) even at −35 °C. The bridging hydride in (**71**) presumably originates from solvent activation by the in situ generated highly reactive [K(18-c-6)(solvent)][$U^{II}(\eta^5\text{-}Cp')_3$] (**72**) [189]. Reduction in (**67′′-U**) with Rb metal in THF, in the absence of chelates, also results in the same solution colour changes (green to maroon), however the reduction products were not isolable. Reductions in (**68′-U**) with different alkali metals also undergo the same colour changes, but the thermal instability of the U(II) products prohibited their isolation [189].

The above series of Cp stabilised U(II) complexes was further expanded to include strong electron donating Cp ligands: reduction in dark brown [$U^{III}(\eta^5\text{-}Cp^{Me4})_3$] (**73**) [72,193] with K smear in the presence of 2.2.2-crypt, in THF, at −35 °C, furnishes the U(II) complex [K(2.2.2-crypt)][$U^{II}(\eta^5\text{-}Cp^{Me4})_3$] (**74-U**) [194]. The isolation of (**74-U**) parallels the synthesis

of the crystallographically characterised series $[Ln^{II}(\eta^5\text{-}Cp^{Me4})_3]^-$ (**74**-Ln) complexes [195]. The ground state electronic configuration is again $5f^36d^1$, with the extra electron residing in an orbital of significant $6d_{z2}$ character. The U-Cp^{Me4}(centroid) distance in (**74-U**) (*avg* 2.564 Å) has increased compared to (**73**) (*avg* 2.522 Å) and is also longer than the one found in the U(II) complex (**68′-U**) (*avg.* 2.521 Å—see above). One possible reason for this latter increase is to counteract the electron donating characteristics of the $(Cp^{Me4})_3{}^{3-}$ ligand environment.

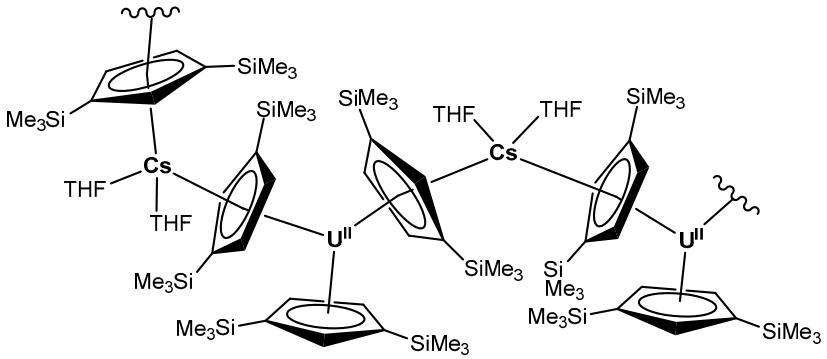

(**70**)

Figure 1. Polymeric structure of $[(\eta^5\text{-}Cp'')U^{II}(\mu{:}\eta^5, \eta^5\text{-}Cp'')_2Cs(THF)_2]_n$ (**70**).

Using the penta-isopropyl substituted Cp, Cp^{iPr5}, Layfield et al. were able to access the neutral U(II) complex $[U^{II}(\eta^5\text{-}Cp^{iPr5})_2]$ (**76-U**) (Scheme 20) [196]. Complex (**76-U**) adopts in the solid state the staggered confirmation of the D_{5d} polymorph of ferrocene with a Cp^{iPr5}(cent)-U(II)- Cp^{iPr5}(cent) angle of 180° and thus can be given the moniker of the '2nd generation uranocene', 51 years after the isolation of $[U^{IV}(\eta^8\text{-}C_8H_8)_2]$ (**77**) [197].

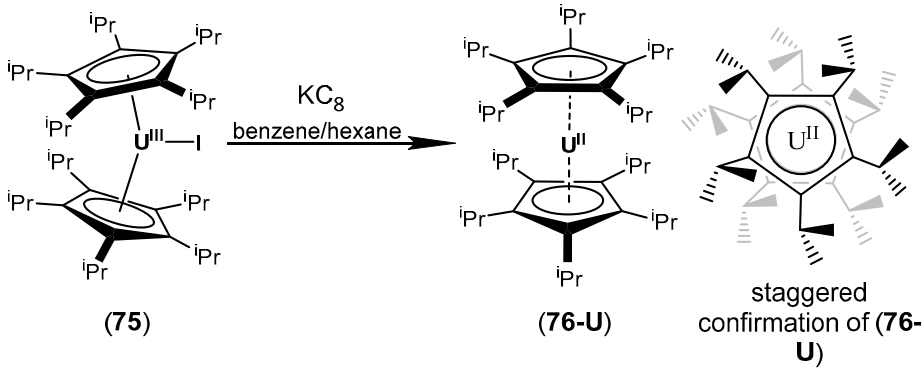

(**75**) (**76-U**)

Scheme 20. Synthesis of the '2nd generation' of U(II) uranocene.

The Cp^{iPr5}(cent)-U distance in (**76-U**) is elongated to 2.504 Å compared to the ones found in the bent U(III) uranocene cations $[U^{III}(\eta^5\text{-}Cp^{iPr4R})_2]^+[B(C_6F_5)_4]^-$ [198,199] (R = H (**77-H**): Cp^{iPr4}(cent)-U-Cp^{iPr4}(cent) = 142.5(2)°; R = ^{i}Pr (**77-^{i}Pr**): Cp^{iPr5}(cent)-U-Cp^{iPr5}(cent) = 167.82°) of 2.472 Å for (**77-^{i}Pr**) and *ca* 2.42 Å for (**77-H**) As a comparison, the linear (i.e., Cp^{iPr5}(cent)-Nd(II)- Cp^{iPr5}(cent) = 180°) neutral Nd(II) congener $[Nd^{II}(\eta^5\text{-}Cp^{iPr5})_2]$ (**76-Nd**) [200], reported by Long et al., that has a $4f^35d^1$ ground state electronic configuration, has a Nd-Cp^{iPr5}(Cent) distance of 2.477(6) Å (average of two disordered Cp^{iPr5} components in the molecular structure). Based on magneto-metric studies, UV-Vis spectroscopy and detailed computational investigations, the four unpaired electrons in (**76-U**) are distributed in three orbitals of predominately 5f character with the fourth electron occupying a non-bonding orbital originating from strong mixing of the 7s and $6dz^2$ atomic orbitals (*ca* 60:40 respectively) of the U(II) metal centre. This latter orbital extends in the empty equatorial

region between the Cp^{iPr5} ligands and is most likely the reason behind the observed geometry in (**76-U**). The lowest unoccupied orbitals in (**76-U**) are $6d_{xy}$ and $6d_{x2-y2}$ orbitals (see also below Section 3.3). It is worth pointing out that the synthesis of (**76-U**) takes place in the absence of coordinating solvents or chelates. CV studies have shown that the $E_{1/2}$ redox couple for the process: (**75**) + e^- → (**76-U**) + I^- is *ca* −2.33 V vs. Fc^+/Fc (Fc = ferrocene; see also Sections 3.2 and 4) [196].

3.1.2. U(II) Complexes Supported by Amido and RO^- Ligands

In 2014 Meyer and co-workers reported the isolation of the U(II) complex [K(2.2.2-crypt)][U^{II}{(^{Ad,Me}ArO)$_3$Mes}] (**78-U**) [201] supported by δ-backbonding from the basal mesitylene anchor of the multidentate [{(^{Ad,Me}ArO)$_3$Mes}]$^{3-}$ ligand (Scheme 21) [202]. Cyclic voltammetry studies showed that the reduction in the U(III) precursor [U^{III}{(^{Ad,Me}ArO)$_3$Mes}] (**77**), is nearly reversible and takes place at −2.495 V vs. Fc^+/Fc (see also Section 4) [203]. The temperature of the reduction reaction is crucial for the isolation of (**78-U**), since at higher temperatures, in benzene and in the presence of 18-crown-6, products resulting from C–H activation of the ligand scaffold are only isolated [203].

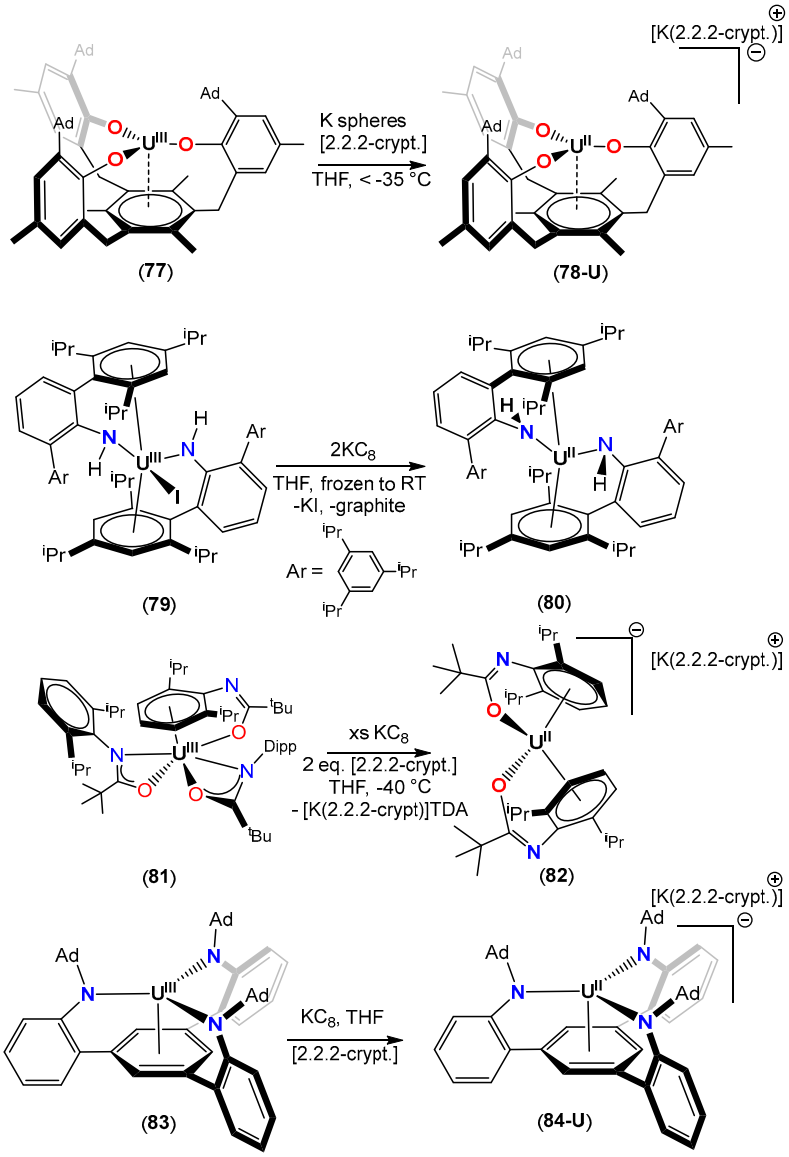

Scheme 21. *Cont.*

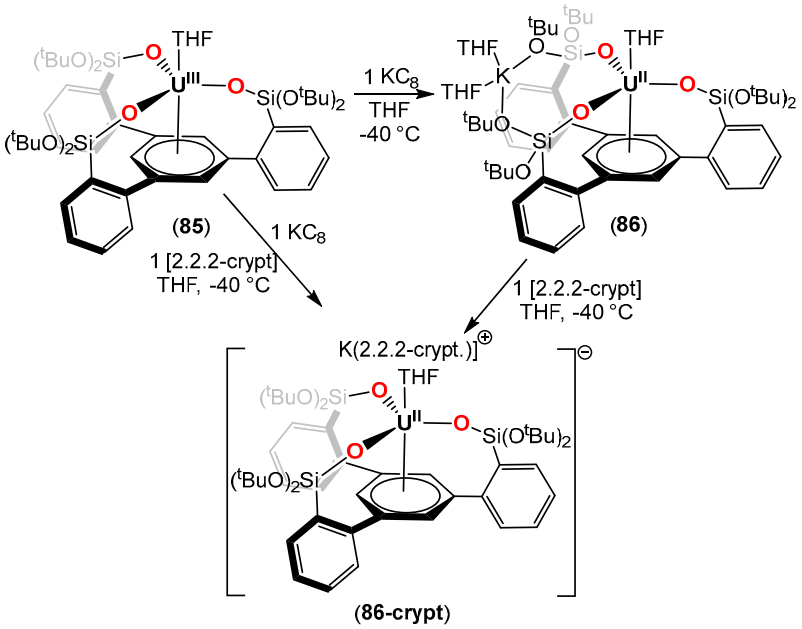

Scheme 21. Synthesis of U(II) complexes stabilised by U-arene δ-backbonding.

The U—O bond distances in (**78-U**) are elongated (2.236(4) Å) compared to U(III) precursor (**77**) (2.158(2)-2.178(2) Å); in contrast the U–Arene(Cent) distance in (**78-U**) contracts to 2.18 Å from 2.35 Å in (**77**). The C–$C_{(arene\text{-}anchor)}$ bond distances in (**78-U**) are slightly longer (1.432(7) Å vs. *avg*. 1.42 Å in (**77**)); nevertheless, the aromatic framework of the basal arene is planar and is effectively undisturbed. The most salient feature of (**78-U**) is its electronic configuration of $5f^4$ which is in stark contrast with the $5f^36d^1$ configuration observed for U(II) complexes supported by Cp ligands (vide supra). The X-band EPR spectrum of (**70**) is silent while its UV-Vis spectrum is devoid of strong absorptions due to f→d transitions. DFT calculations suggest a metal centred reduction in (77) to (**78-U**); it has to be noted though that the π-system of the central arene has the right spatial orientation to interact with the 5f orbitals. Nevertheless, the importance of the U-arene interaction to stabilise the family of U(II) complexes shown in Scheme 21, is still unclear. The isostructural $4f^4$ Nd(II) congener [K(2.2.2.-crypt)][Nd^{II}{(^{Ad,Me}ArO)$_3$Mes}] (**78-Nd**) displays a Nd—O bond length of 2.237(4) Å and a Nd(II)-Cent(arene) distance of 2.366 Å [204].

Similarly, the neutral U(II) complex [U^{II} ($NHAr^{iPr6}$)$_2$] (**80**) [205], as well as the ionic complexes [K(2.2.2-crypt)][U^{II}(κ^1-O:η^6-TDA)$_2$] (**82**) (TDA = N-(2,6-di-isopropylphenyl)pival amido) [206], [K(2.2.2-crypt)][U^{II} (^{Ad}TBPN$_3$)] (**84-U**) [146] and the *ate* U(II) complex [K(THF)$_2$-U^{II}[{OSi(O^tBu)$_2$Ar}$_3$-arene](THF)] (**86**) as well as its ion separated congener [K(2.2.2-crypt.][U^{II}[{OSi(O^tBu)$_2$Ar}$_3$-arene](THF)] (**86-crypt**) (Scheme 21) [207], all featuring U-η^6 arene interactions, exhibit a $5f^4$ electronic ground state.

The reason behind the different ground state electronic configurations between the family of complexes [K(chelate)][U^{II}(η^5-Cp^R]$_3$] (**68-U**) and the η^6-arene U(II) complexes in Scheme 21 was investigated computationally by Furche and Evans [208]. It was concluded that the symmetry imposed from the ligand environment is crucial in determining if the extra electron, upon [U(III)] → [U(II)] reduction, occupies a 5f or a 6d orbital. From the model and reported complexes scrutinised computationally in this study it was found that ligand environments imposing a close to planar geometry around the U(II) metal centre, like Cp ligands, favour a $5f^36d^1$ ground state electronic configuration, regardless of the nature of the ligand. For example, complex [K(2.2.2-crypt)][$U^{(II)}N''_3$] (**88-U**) (N″ = $N(SiMe_3)_2^-$) [194] featuring a U(II) metal centre and stabilised by three amido ligands in a D_3 symmetric environment (Scheme 22), features a $5f^36d^1$ ground state electronic configuration. The average U-N amido bond distance of 2.373 Å in (**88-U**) is longer than the one found in the U(III) precursor [$U^{(III)}N''_3$] (**87**) (2.320 Å) [57], and is reminis-

cent of the elongation observed in the Ln(II) series of complexes [M(2.2.2-crypt)][LnN″$_3$] (**88-Ln**) (M = Rb, K) featuring a $4f^{n-1}5d^1$ electronic structure. On the other hand, for the U(II) complexes and their corresponding U(III) precursors in Scheme 21 where the ligands impose a pseudo-octahedral environment, it was found that a $5f^4$ ground state electronic configuration is favoured.

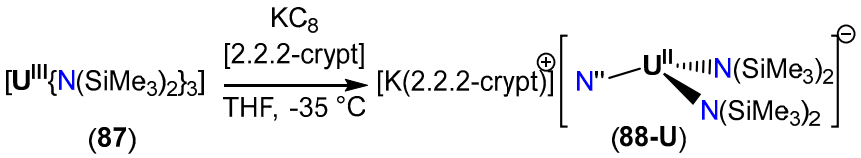

Scheme 22. Synthesis of a U(II) complexes supported by electron donating amido ligands.

Table 2 summarises the salient bond distances of the U(II) complexes stabilised by amido or aryloxido ligands, compared to their U(III) precursors.

Table 2. Comparison of selected bond distances of U(II) and U(III) complexes: [a] [BARF24]-: [B{3,5-(CF3)2-C6H3}4]-; [b] see also Section 3.2 (Scheme 29); [c] κ1-O-U distance(s); [d] two molecule s in the asymmetric unit, average of 6 U-N bond distances ranging from 2.463(3) to 2.504(3) Å.

Compound	U-E (Å) (E = N, O)	U-Arene(Cent) (Å)
[U^{III}{(^{Ad,Me}ArO)$_3$Mes}] (**77**)	2.158(2), 2.178(2), 2.169(2)	2.35
[K(2.2.2)-crypt)][U^{II}{(^{Ad,Me}ArO)$_3$Mes}] (**78**)	2.236(4)	2.18
[U^{III}(NHAr^{iPr6})$_2$I] (**79**)	2.390(3), 2.372(3)	2.777(1), 2.790(1)
[U^{II}(NHAr^{iPr6})$_2$] (**80**)	2.330(2)	2.405(1)
[U^{III}(NHAr^{iPr6})$_2$]$^+$[BARF^{24}]$^-$ (**113**) [a,b]	2.283(6), 2.583(3)	2.573(3), 2.583(3)
[U^{III}(κ^1-O:η^6-TDA)(κ^1, κ^1-N,O-TDA)$_2$] (**77**)	2.310(2) [c]	2.602(2)
K(2.2.2-crypt)][U^{II}(κ^1-O:η^6-TDA)$_2$] (**82**)	2.339(3), 2.356(4) [c]	2.334(6) (see also below)
[U^{III}(^{Ad}TBPN$_3$)] (**83**)	2.413(2), 2.427(2), 2.429(2)	2.34
[K(2.2.2)-crypt)] [U^{II}(^{Ad}TBPN$_3$)] (**84**)	2.477(avg) [d]	2.18
[U^{III}[{OSi(O^{t}Bu)$_2$Ar}$_3$-arene](THF)] (**85**)	2.201(3); 2.209(3); 2.210(3)	2.485(2)
[K(THF)$_2$-U^{II}[{OSi(O^{t}Bu)$_2$Ar}$_3$-arene](THF)] (**86**)	2.236(5); 2.241(5); 2.250(5)	2.255(9) (see also below)
[K(2.2.2-crypt.][U^{II}[{OSi(O^{t}Bu)$_2$Ar}$_3$-arene](THF)] (**86-crypt**)	2.2181(18); 2.2183(18); 2.2197(18)	2.256(1)
[U^{III}N″$_3$] (**87**)	2.320 (avg)	N/A
[K(2.2.2-crypt)][U^{II}N″$_3$] (**88-U**)	2.373 (avg)	N/A

As Table 2 demonstrates, the reduction in the U(III) centre results in the elongation of the U–O or U–N bond, while the U-Arene centroid distance shortens. The latter is attributed to the δ-back-donation between the metal centre and the arene ring. It is also worth pointing out that in the case of the U(II) complex [K(2.2.2-crypt)][$U^{(II)}$(κ^1-O:η^6-TDA)$_2$] (**82**), there are two types of arene rings. One is a planar with minimal torsion angles and C–C bond lengths ranging from 1.389(7) to 1.440(6) Å. The second arene shows a significant distortion from planarity (torsion angles of 11.5(4) and 15.5(4)°), with other metrics characteristic of a mono-reduced arene ligand, with a U-Arene(Cent) distance of 2.274(6) Å [183,206]. The stoichiometry of the reaction implies that two equivalents of KC_8 are needed for the preparation of (**82**), with one equivalent facilitating the U(III)→U(II) reduction, while the second one is consumed to reduce the arene ligand with concomitant loss of one TDA^- ligand. Detailed EPR studies agree with the structural data, further confirming the two decoupled spin systems in the ground state: a S = 2 for the U(II) metal centre (i.e., $5f^4$) and a S = 1/2 for the mono-reduced arene. The requirement for an excess of KC_8 to access the U(II) complex (**82**), was demonstrated by the reduction in (81,) with one equivalent of KC_8 which yielded the U(III) ionic complex [K(chelate)][U(κ^1-O-TDA)$_4$] (**89**) (chelate = 18-crown-6 or 2.2.2-crypt) [206]. As a comparison, when the reduction in the Th(IV) complex [Th^{IV}(κ^2-N,O-TDA)$_4$] (**90**) was performed under similar conditions to the preparation of

(**82**), reductions occurred at the ancillary arene exclusively, yielding the Th(IV) complex (**91**), with the loss of one TDA^- ligand (Scheme 23) [206].

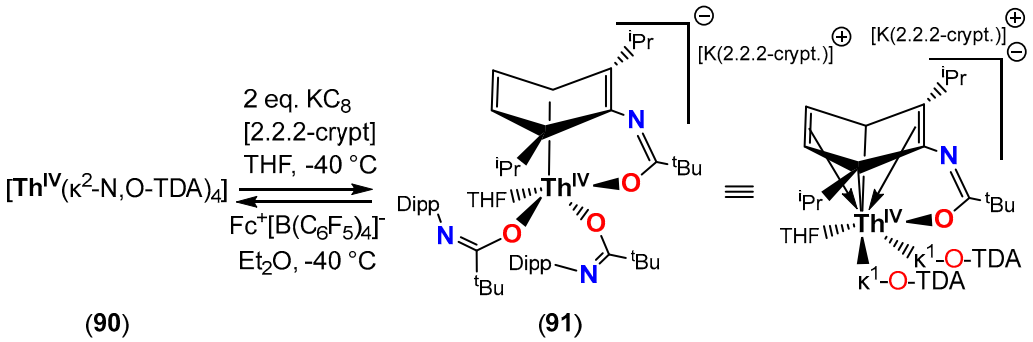

Scheme 23. Attempt at isolating a Th(II) complex supported by a Th-arene interaction (the reduced arene is an L_2X_2 ligand (structure on the right) according to the CBC model [209] with negative charges localised; as such it is best described as a cyclohexa-1,4-diene-3,6 diyl ligand with loss of aromaticity).

In the case of the U(II) inner sphere ion-pair complex [K(THF)$_2$-U^{II}[{OSi(O^{t}Bu)$_2$Ar}$_3$-arene](THF)] (**86**), the structural data show a distorted basal arene with torsion angles and C–$C_{basal\text{-}arene}$ bond distances in the range of 1.1–22° and 1.405(10)–1.455(10) Å respectively [207]. In the case of its U(II) separated ion complex (**86-crypt**), these ranges of values are less pronounced at 3.0–8.7° for the torsion angles and 1.409(4)–1.440(4) Å for the $CC_{basal\text{-}arene}$ bond lengths. The X-band EPR spectra for both (**86**) and (**86-crypt**) are silent, characteristic of a $5f^4$ non-Kramer U(II) ions in both cases. Computational investigations of (**86**) and (**86-crypt**) show that triplet (S = 1) and quintet (S = 2) states have very similar energies. In the case of (**86**), these are very close, giving rise to (**86**), and being described as either a [U(IV)-$(arene)^{2-}$] complex (S = 1; due to 1st-order Jahn–Teller effect, the reduced arene has no unpaired e^- density) or a [U(II)-$(arene)^0$] (S = 2). On the other hand, (**86-crypt**) can be best described as a true [U(II)-$(arene)^0$] complex (i.e., S = 2). Nevertheless, SQUID magnetometry, UV-Vis spectroscopy, and cyclic voltammetry in a solution (see also Section 4) demonstrate that both (**86**) and (**86-crypt**) are best described as U(II) species [207].

3.2. Small Molecule Activation and Reactivity of U(II) Compounds

Due to their high reduction potential (see also Section 4), U(II) complexes can potentially precipitate two electron transfers (i.e., [U(II)] → [U(III)] followed by [U(III)] → [U(IV)]), and thus open new avenues in the reductive transformation of substrates and small molecules.

The U(II) complexes (**68′-U**)/(**68″-U**) both react with H_2 (1atm) or $PhSiH_3$ to furnish the U(III) hydride complexes (**69′**)/(**69″**), respectively (Scheme 24) [189]. The reactivity of the (**68′-U**) with H_2 contrasts with the one observed for the analogous Th(II) complex [K(18-c-6)(THF)$_2$] [$Th^{III}(\eta^5$-Cp″$)_3$] (**30**), which yields the mixed-valence Th(III)/Th(IV) complex [K(18-crown-6)Et$_2$O][$(\eta^5$-Cp″$)_2Th^{III}(\mu$-H$)_3Th^{IV}$H$(\eta^5$-Cp″$)_2$] (**44**) (Scheme 14), along with the Th(III) complex [$Th^{III}(\eta^5$-Cp″$)_3$] (**5**), which does not react with H_2 [46]. Complexes (**69′**) and (**69″**) can also be synthesised via the reaction of (**67′-U**) and (**61″-U**) with KH, in the presence of a [2.2.2-crypt], respectively [38,189]. In contrast, the Th(III) complex [$Th^{III}(\eta^5$-Cp″$)_3$] (**5**) becomes disproportionate when it reacts with KH salts in the presence of a chelate ([2.2.2-crypt] or 18-crown-6) to afford the Th(II) complex (**30**) along with the corresponding Th(IV) complex [$Th^{IV}(\eta^5$-Cp″$)_3$H] (**6-H**) (Scheme 11).

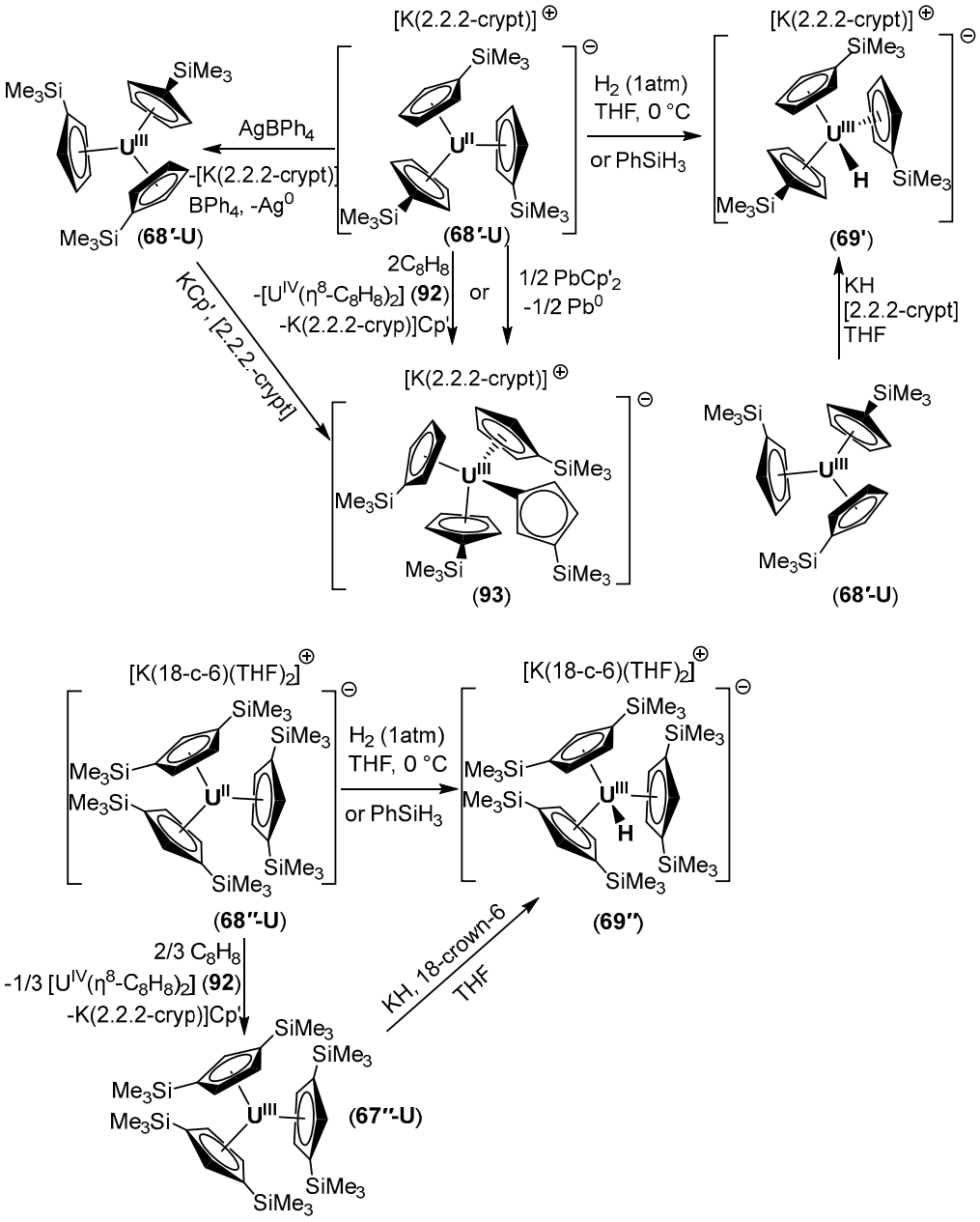

Scheme 24. Reactivity of (**68′-U**)/(**68″-U**).

One electron oxidation of (**68′-U**) with $AgBPh_4$ regenerates its U(III) neutral precursor (**67′-U**) [38]. Both (**68′-U**) and (**68″-U**) react with cyclooctatetraene (COT–C_8H_8) to give either the U(III) ionic compound [K(2.2.2-crypt)][$U^{III}(\eta^5$-Cp′$)_3(\eta^1$-Cp′)], (**88**), or in the case of (**68″-U**), and its U(III) precursor [$U^{III}(\eta^5$-Cp″$)_3$], (**68″-U**), respectively, concomitant losses of [$U^{IV}(\eta^8$-$C_8H_8)_2$] (**92**) and [K(2.2.2-crypt)]$Cp^{(SiMe3)n}$ (n = 1, 2) in both cases [189]. These two different outcomes underline the importance of sterics in controlling reactivity and product distribution. Furthermore, the formation of [$U^{IV}(\eta^8$-$C_8H_8)_2$] (**92**) as a side product suggests that two electron transfers are likely to take place. In contrast, the Th(II) complex [K(18-c-6)$(THF)_2$] [$Th^{III}(\eta^5$-Cp″$)_3$] (**30**) reacts with COT (C_8H_8) to yield the Th(IV) complex [$Th^{IV}(\eta^5$-Cp″$)_2(\eta^8$-$C_8H_8)$] (**45**) (Scheme 15), as the only thorium-containing product [46]. It is also worth noting that the U(III) complex (**93**) can be prepared from (**68′-U**) and 0.5 equivalents of $PbCp'_2$, with metallic lead being the by-product (Scheme 24) [189].

The reduction of the heteroleptic U(III) complexes [$(\eta^5$-Cp*$)_{3-n}U^{III}$(N″$)_n$] (n = 1: (**94**); n = 2: (**95**)) in THF at −35 °C ultimately produces the U(III) ionic complexes (**98**) and (**99**), respectively (Scheme 25). The reaction is thought to proceed via the corresponding

ionic U(II) complexes (**96**) and (**97**), which cannot be isolated, but whose intermediacy is supported by in situ UV-Vis spectroscopy and computational studies. Complexes (**98**) and (**99**) are the result of facile C–H activation of one of the $SiMe_3$ disilylazide substituents by the respective U(II) centre, probably because of the inadequate steric protection offered by these ligand environments. According to the aforementioned computational studies, both (**96**) and (**97**) adopt a $5f^3 6d^1$ ground electronic configuration [210].

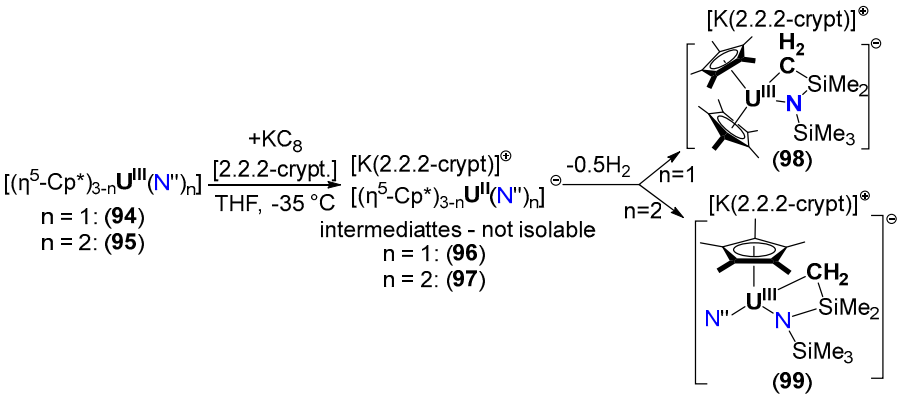

Scheme 25. Intermolecular C–H activation by transient U(II) complexes.

In the same vein, intramolecular C–H activation has been reported by Mazzanti et al. during the reduction of $[U^{III}N''_3]$ (**87**) with one equivalent of KC_8 in THF at RT, yielding instead the U(III) cyclometallated complex $[K(2.2.2\text{-crypt})][U^{III}(N'')_2(\kappa^2\text{-C,N}-CH_2SiMe_2NSiMe_3)]$ (**100**) (Scheme 26). The preparation of (**100**) most likely proceeds via its initial formation in the solution of the U(II) complex $[K(2.2.2\text{-crypt})][UN''_3]$ (**88-U**). This is supported by the observation that cold (−40 °C) solutions of (**88-U**) decompose to (**100**) over prolonged periods of time or upon warming to RT [211].

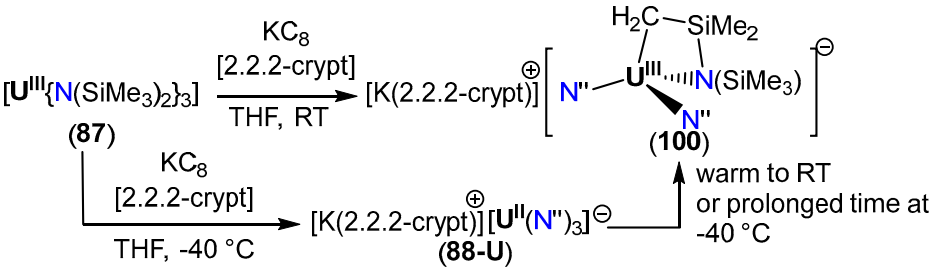

Scheme 26. Intramolecular C–H activation by U(II) complex (**88-U**).

The same group have investigated the reactivity of $[K(2.2.2\text{-crypt})][U^{II}N''_3]$ ($N'' = N(SiMe_3)_2^-$) (**88-U**) (Scheme 26) with diphenyl-acetylene [212], PhN=NPh [212], and N-aromatic heterocycles [213]. In the first two cases, the products $[K(2.2.2\text{-crypt}))][(\eta^2\text{-PhC=CPh})U^{IV}N''_3]$ (**101**) and $[K(2.2.2\text{-crypt}))][(\eta^2\text{-PhN-NPh})U^{IV}N''_3]$ (**102**) are formed, respectively [212], as the result of the transfer of two electrons from (**88-U**) to the corresponding substrate (Scheme 27). THF solutions of compound (**101**) react further upon warming to RT to yield the 5-coordinate diamagnetic U(VI) bis-imido complex $[K(2.2.2\text{-crypt})][N''_3U^{VI}(=NPh)_2]$ (**103**); i.e., overall a $4e^-$ reduction of Ph_2N_2 [212]. When (**88-U**) reacts with pyridine or 4,4′-bipy, the dimeric U(III) complexes (**104**) and (**105**) can be isolated, where in both cases, the N-aromatic heterocycle has lost its aromaticity [213]. This reactivity resembles the one observed with these two substates with the Th(III) complex $[Th^{III}(\eta^5\text{-Cp}'')_3]$ (**5**) [43]. In both these cases, the U(III) complex $[K(2.2.2\text{-crypt}][U^{III}(N'')_4]$ (**106**) is observed amongst the by-products, while in the case of the reaction with 4,4′-bipy the dinuclear-bridged cyclometallated U(IV) complex (**107**) is also observed. Interestingly, the same uranium products are observed when the oxo-bridged bi-metallic U(III) complex

[K(2.2.2-crypt)]$_2$[{N″$_3$U^{III}}$_2$(μ-O)] (**108**) is reacted under similar conditions with the organic substrates mentioned above (Scheme 26) [212,213]. In this latter case, the reactions proceed with concomitant loss of the U(IV) terminal oxo complex [K(2.2.2-crypt)][(O)U^{IV}N″$_3$] (**109**) [138,171], signifying that compound (**108**) can be viewed as a masked U(II) synthon.

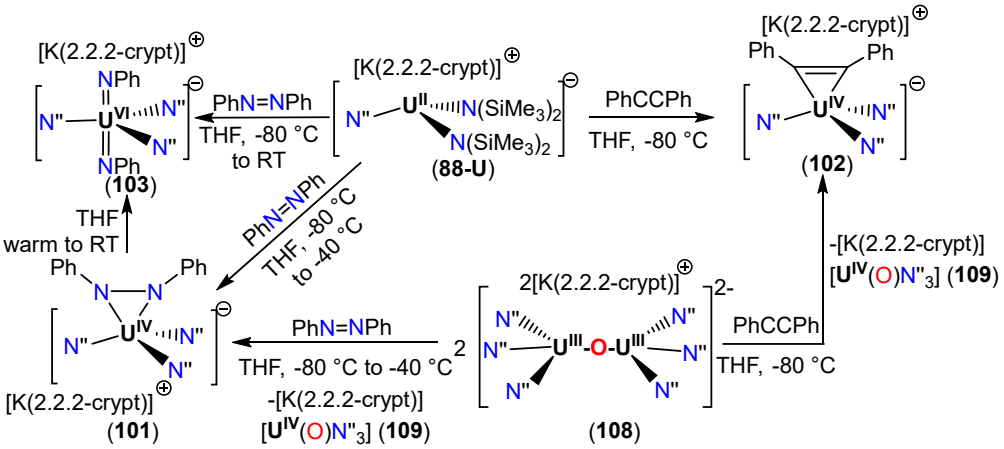

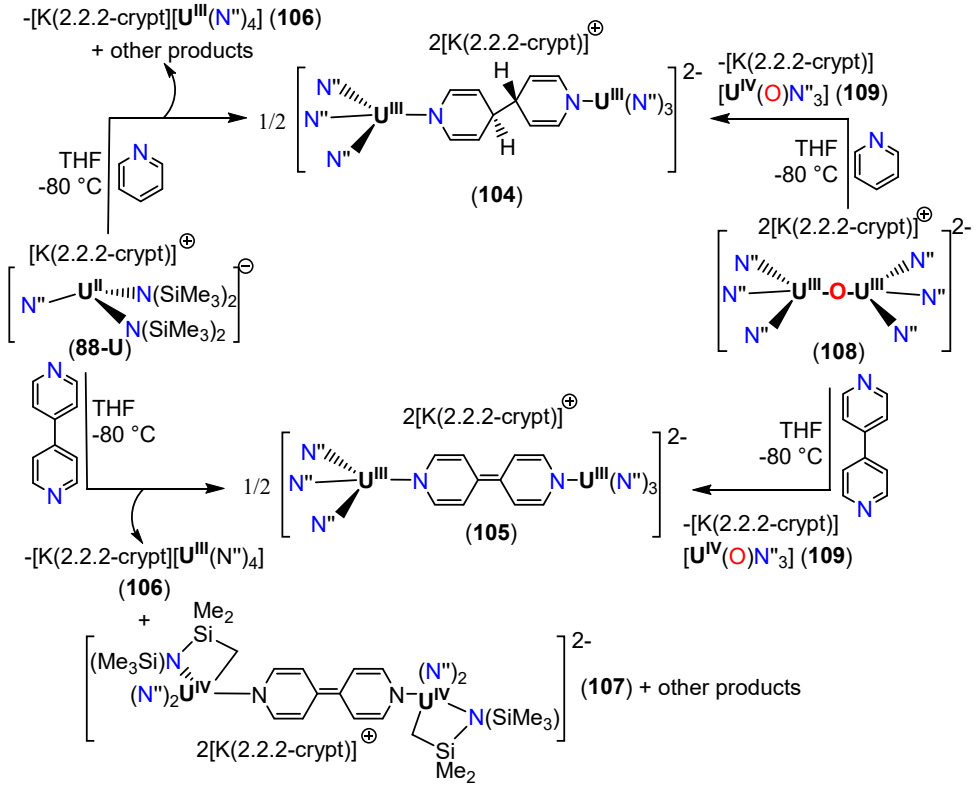

Scheme 27. Two and four electron reactivity of (**88-U**) and the masked U(II) synthon (**108**).

The U(II) complex [K(2.2.2-crypt)][U^{II}(κ^1-O:η^6-TDA)$_2$] (**82**) (Scheme 21) reacts with cycloheptatriene (CHT) to furnish the U(IV) complex [K(2.2.2-crypt)][(η^7-C$_7$H$_7$)U^{IV}(κ^1-O-TDA)$_2$(THF)] (**110**) containing a C$_7$H$_7^{3-}$ ligand (Scheme 28). Complex (**110**) is a rare example of a U–cycloheptatriene complex [214–216], and results from an overall [U(II)] → [U(IV)] 2e$^-$ metal-centred oxidation, with the third electron for the C$_7$H$_7$ → C$_7$H$_7^{3-}$ reduction most likely originating from the reduced arene in (**82**). During this reaction, gas evolution is observed, presumably H$_2$ gas. As a result of this overall 3e$^-$ redox reactivity due to the ligand's non-innocence, (**82**) can be viewed as a masked U(I) synthon. Complex

(**82**) also reacts with COT in a manner similar to (**68″-U**) (Scheme 24) to produce the homoleptic complex[K(2.2.2-crypt)][U^{II}(κ^1-O-TDA)$_4$] (**111**) (vide supra), with a concomitant loss of [U^{IV}(η^8-C_8H_8)$_2$] (**92**). Finally, (**82**) is readily oxidised with I_2 to the iodo-bridged bimetallic U(III) complex (**112**) [206].

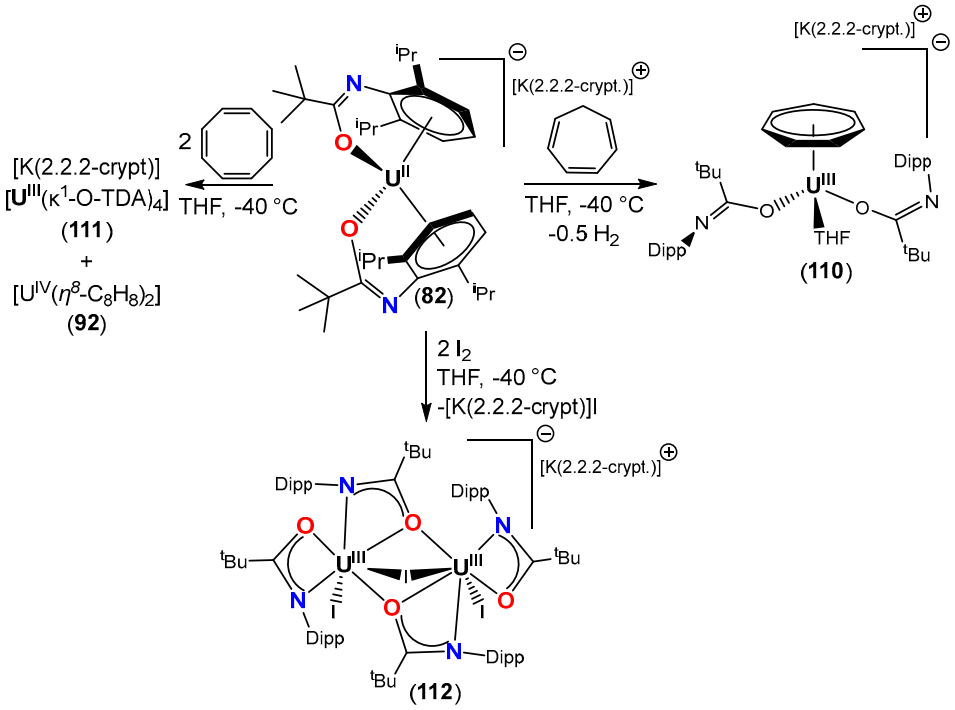

Scheme 28. Multi-electron reactivity of U(II) complex (**82**).

The neutral bis-amido U(II) complex, (**80**), undergoes facile 1e- oxidation with $Fc^+[BARF^{24}]^-$ (Fc^+ = $[Fe(\eta^5\text{-}C_5H_5)_2]^+$; $[BARF^{24}]^-$: $[B\{3,5\text{-}(CF_3)_2\text{-}C_6H_3\}_4]^-$) to yield the U(III) complex (**113**) (Scheme 29) [205]. Complex (**84**) undergoes a facile O transfer reaction from either N_2O or pyridine N-oxide (C_5H_5NO) to produce the U(IV) ionic complex [K(2.2.2-crypt)][(O)U^{IV}(^{Ad}TBPN$_3$)] (**114**) (i.e., a 2 e- oxidation, Scheme 29) [146].

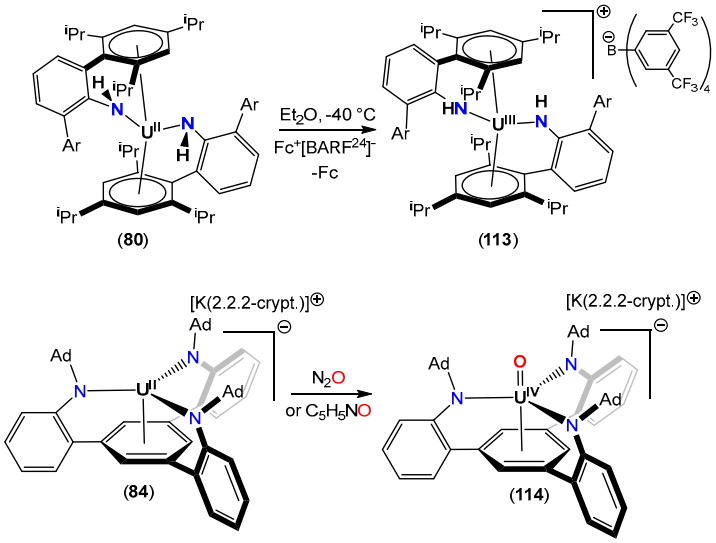

Scheme 29. Reactivity of η^6-arene U(II) complexes (**80**) and (**84**).

Remarkably, the U(II) complexes [K(THF)$_2$-U^{II}[{OSi(O^{t}Bu)$_2$Ar}$_3$-arene](THF)] (**86**) and [K(2.2.2-crypt.][U^{II}[{OSi(O^{t}Bu)$_2$Ar}$_3$-arene](THF)] (**86-crypt**) react with two equivalents of

KC_8 to furnish complexes (**115**) and (**115-crypt**), respectively (Scheme 30). Computational studies, X-band EPR spectroscopy and SQUID magnetometry show that the U–metal centre in (**115**)/(**115-crypt**) is in the +3 oxidation state. The extra two unpaired electrons singly occupy U-arene δ-bonds, with their spins either both antiparallel or one parallel and the second one antiparallel to the unpaired electron density of the U(III) centre, giving rise to a doublet or a quartet ground state, respectively, which were found to be almost degenerate. This also explains the experimentally observed planarity (SC-XRD) of the basal arene and, thus, complexes (**115**)/(**115-crypt**) can be described as [U^{III}-(arene)$^{2-}$]. Both (**115**)/(**115-crypt**) can also be prepared from the reaction of the U(III) neutral precursor (**85**) with three equivalents of KC_8 in the absence or presence of [2.2.2-crypt.], respectively [207].

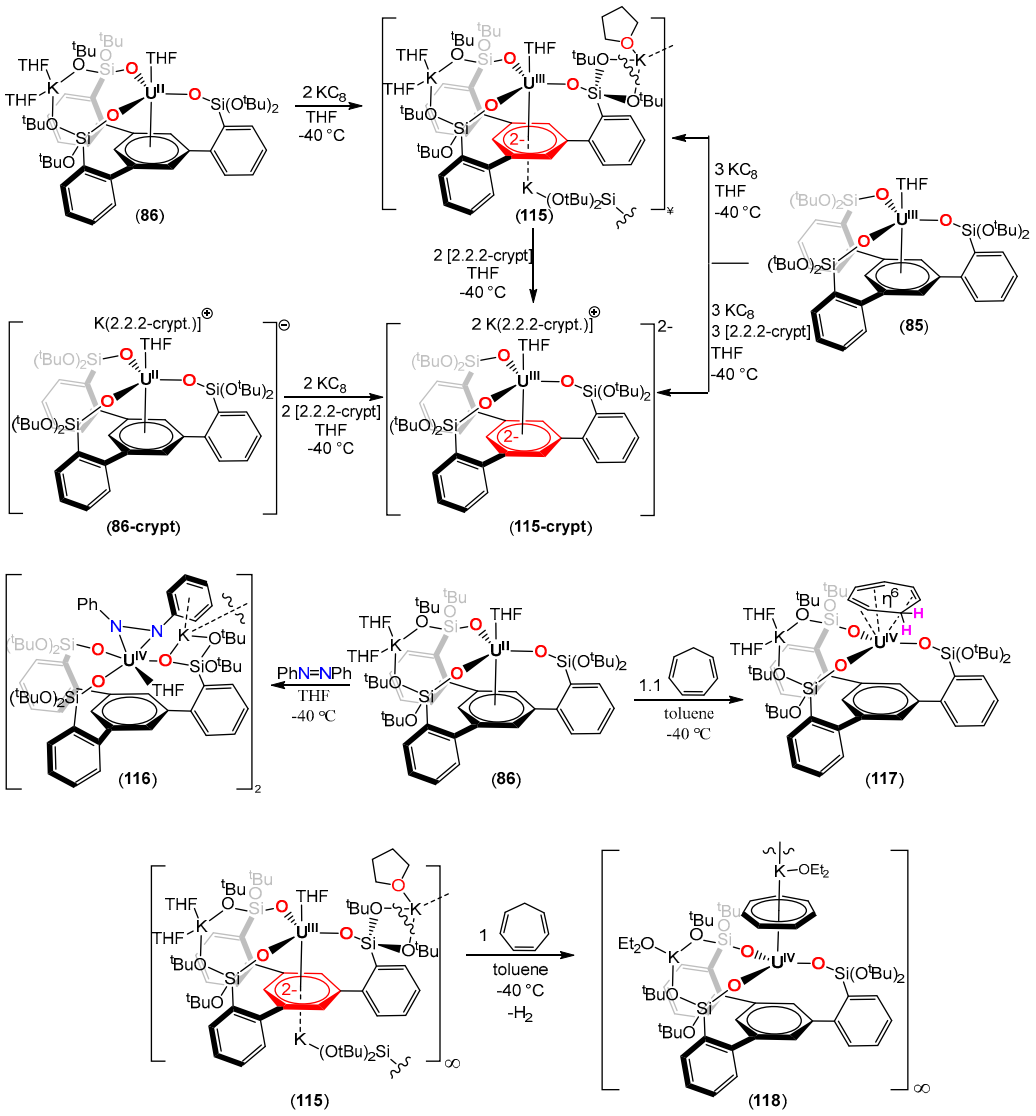

Scheme 30. Reactivity of (**86**)/(**86-crypt**) and (**115**).

Complex (**115**) reacts with CHT (cyclo-heptatriene) to yield the U(IV) complex (**118**), which adopts a polymeric solid-state structure (Scheme 30). The CHT ligand has been reduced triply to $\{C_7H_7\}^{3-}$, and coordinates to the U(IV) centre in an η^7-fashion. The overall $3e^-$ transfer from (**115**) is reminiscent to the reactivity of [K(2.2.2-crypt)][U^{II}(κ^1-O:η^6-TDA)$_2$] (**78**) (Scheme 21) [206] and, thus, (**115**) can be considered as a masked U(I) synthon. In contrast, the reaction of CHT with the U(II) complex (**86**) results in a $2e^-$ transfer, yielding the inner sphere U(IV) ionic complex [Et_2OK-U^{IV}(η^6-C_7H_8)\{(OSi(O^tBu)$_2$Ar\}$_3$-arene}] (**117**). The η^6 coordinated CHT in complex (**117**) is reduced doubly (i.e., $\{C_7H_8\}^{2-}$), and is the

first example of CHT coordinating in this fashion to a uranium metal centre [207]. Finally, (**86**) and (**86-crypt**) reduce PhN=NPh by double, to produce either the inner spere ionic complex (**116**) or its separated ion pair analogue (**116-crypt**) (the latter has only been spectroscopically characterised) [212].

The examples shown in Scheme 30 point to a very delicate interplay of metal centre vs. arene/ligand-based reduction. This is further accentuated in complexes $[(THF)_4K_2\{(Ph_3SiO)_2U\}(\mu\text{-}O)(\mu\text{-}\kappa^2\text{:}\eta^6\text{-}Ph,O\text{-}PhSiPh_2O)\text{-}\{U(THF)\text{-}(Ph_3SiO)_3\}]$ (**120**) and $[K(THF)_2(18\text{-}c\text{-}6)]_2[K\{(Ph3SiO)U\}(\mu\text{-}O)\ (\mu\text{-}\kappa^2\text{:}\eta^4\text{-}Ph,O\text{-}PhSiPh_2O)\text{-}\{U(THF)\text{-}(Ph_3SiO)_3\}]$ (**121**), the synthesis of which is shown in Scheme 31 [217].

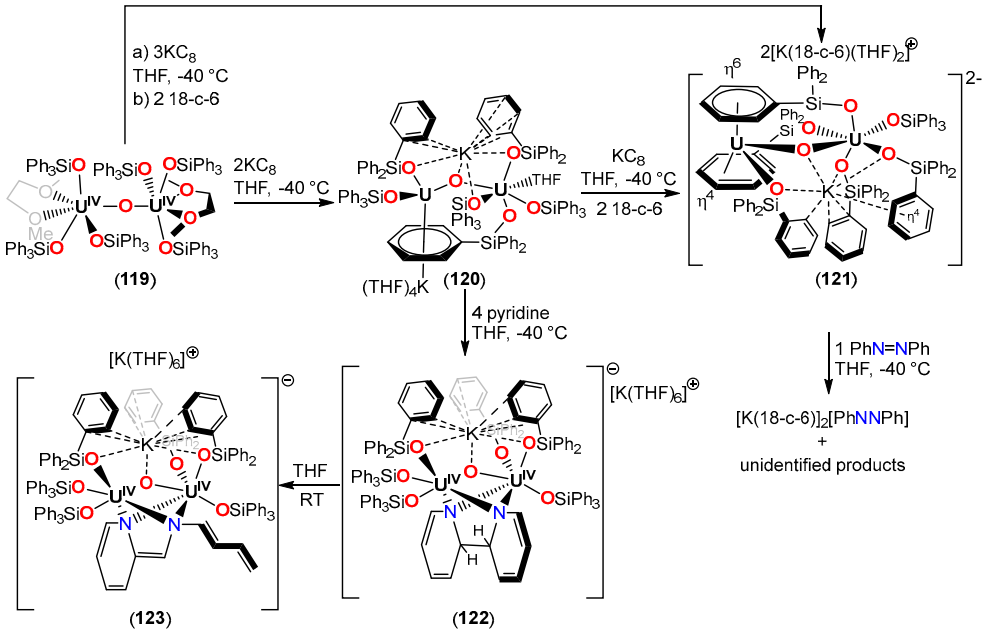

Scheme 31. Reactivity of masked multi-metallic masked U(II)/U(I) complexes.

Based on the charge balance, compound (**120**) is formally a bridging oxo 'U(II)/U(IV)' complex. Nevertheless, a structural analysis shows that the arene coordinated to one of the U–centres, and is consistent with a cyclohexadiene-like geometry (two short and two long C–C bonds and torsion angles of 14.0(7)° and 19.3(7)°) similar to $[K(2.2.2\text{-}crypt)][U^{(II)}(\kappa^1\text{-}O\text{:}\eta^6\text{-}TDA)_2]$ (**82**) (Schemes 21 and 28) and the Th(IV) complex (**91**) (Scheme 23) [206]. EPR studies, SQUID magnetomentry, and computational investigations show that a 'U^{IV}/U^{IV}' complex with a doubly occupied U-arene δ-bond, i.e., a doubly reduced arene, is the most likely scenario. Nevertheless, the description of a 'U(II)/U(IV)' complex with the two electrons of the U(II) centre stored in the δ-bond is equally valid. On the other hand, complex (**121**) features two planar arenes, one coordinating to the U–centre in an η^6 fashion and the other in an η^4. A sextet ground state (S = 5/2) was calculated for complex (**121**), pointing to a 'U(III)/U(IV)' system consistent with EPR spectroscopy and SQUID studies. Two electrons are located on the η^6-arene (Scheme 31), with the δ-bond having an 80% U–character [217].

Complex (**120**) reacts with four equivalents of pyridine to produce the oxo-bridged U(IV)/U(IV) dimer (**122**), where two pyridine molecules have been reductively coupled to form the de-aromatised bridging bis-amido [2,2'-dihydro-bipy]$^{2-}$ ligand. Complex (**122**) reacts further upon reaching RT with the cleavage of one of the 6-membered rings, to produce complex (**123**). Finally, complex (**121**) reduces PhN=NPh to the $[PhNNPh]^{2-}$ dianion, but no uranium-containing products could be isolated (Scheme 31) [217].

The reactivity shown in Scheme 31 underlines the roles that redox-active ligands (RALs) can play in obfuscating the 'true' valency of the metal centre, and to a certain degree, mimic the reactivity of low-valent actinide complexes [218].

3.3. Isolation and Reactivity of a U(I) Complex

During CV studies to investigate the redox chemistry of [U(η^5-Cp^{iPr5})$_2$I] (**75**) and determine the U(III)/U(II) redox couple value for this system (see also above and Section 4), an irreversible redox process centred at *ca* −2.85 V vs. Fc*/Fc*$^+$ (Fc* = [Fe(η^5-Cp*)$_2$; −3.28 V vs. Fc/Fc$^+$] close to the cathodic solvent breakdown was observed [196]. This suggested that a U(I) complex might be accessible. Indeed, both the U(III) complex (**75**) and the U(II) complex (**76-U**) can be reduced with KC_8, in the presence of [2.2.2.-crypt] in hexane at RT, to yield the only known bent U(I) complex [K(2.2.2-crypt][U^I(η^5-Cp^{iPr5})$_2$] (**124**) (Scheme 32) [219]. In this case, the reduction to (**124**), either from (**75**) or (**76-U**), does not proceed in the absence of chelator [2.2.2-crypt]. The Cp^{iPr5}(cent)-U-Cp^{iPr5}(cent) angle of 163.4° in (**124**) is somewhat less obtuse than the corresponding angle of 167.82° found in the bent uranocene [U^{III}(η^5-Cp^{iPr5})$_2$]$^+$[B(C$_6$F$_5$)$_4$]$^-$ [199]. In this family of U(III) to U(I) complexes, there is a monotonic increase in the Cp^{iPr5}(cent)–U bond distance after the reduction from 2.472 Å in [U^{III}(η^5-Cp^{iPr5})$_2$]$^+$[B(C$_6$F$_5$)$_4$]$^-$ (**125**) [199] to 2.504 Å in [U^{II}(η^5-Cp^{iPr5})$_2$] (**76-U**) [196], and, finally, to 2.575 Å (*avg*) in [K(2.2.2-crypt][U^I(η^5-Cp^{iPr5})$_2$] (**124**) [219]. Computational investigations suggest that the ground state electronic configuration is 5f^3(7s/6d$_{z2}$)^1(6d$_{x2-y2}$/6d$_{xy}$)^1, with three electrons occupying atomic 5f orbitals, one electron occupying a quasi σ-symmetric orbital with strong admixing of 7s and dz2 atomic orbitals (as in the case of (**76-U**)), and the last electron located in a quasi-δ-symmetric 6d$_{x2-y2}$/6d$_{xy}$ set of orbitals, with significant delocalization into the ligands. The X-band EPR spectrum of powdered samples of (**124**) at 10K shows a rhombic signal, whereas (**75**) is EPR-silent at this temperature. AC SQUID measurements show that the (**124**) exhibits some SMM behaviours, while measurements in the DC regime of $\chi_M T$ suggest a complicated manifold of thermally-accessible excited states.

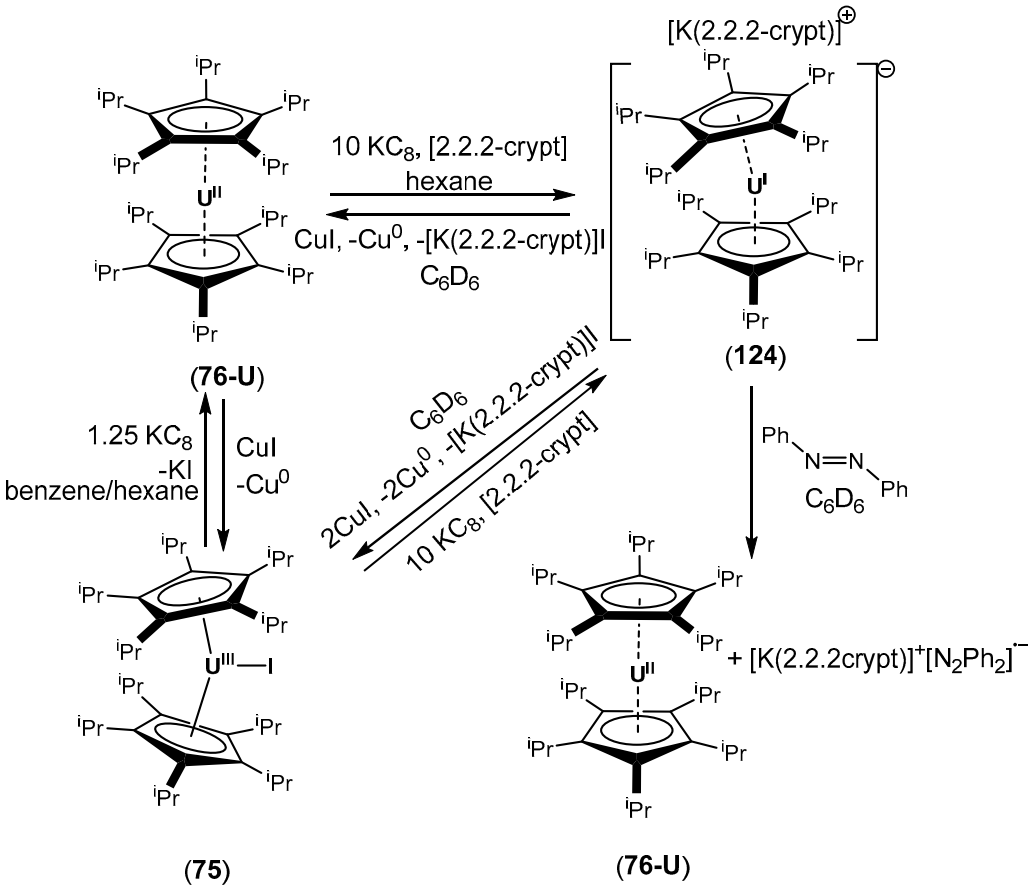

Scheme 32. Isolation and reactivity of the first U(I) complex (**124**).

The possibility of (**124**) being a U(II)-hydride complex was discounted by its reaction with CCl_4 that did not show any signs of $CHCl_3$ formation. Complex (**124**) reacts with one or two equivalents of CuI to produce the U(II) complex (**76-U**) or the U(III) precursor (**76**), respectively. Solutions of the U(I) complex (**124**) decompose instantly in THF, but disproportionately in C_6D_6 over the course of 5 days at RT to the U(II) complex (**76-U**), [K(2.2.2-crypt)]Cp^{iPr5} and U metal. When (**124**) reacts with, it undergoes an 1 e^- oxidation to the U(II) complex (**76-U**), while azobenzene is reduced to the $[Ph_2N_2]^{-\bullet}$ radical anion. This latter reactivity contrasts with the reactivity of the U(II) complex [K(2.2.2-crypt)][UN''_3] (**88-U**) and Ph_2N_2 [212], and is most likely attributable to the steric bulk by the Cp^{iPr5} ligand [219].

4. Cyclic Voltammetry (CV) Studies of Low Valent U and Th Complexes

Despite the rich reductive chemistry of the low-valent Th and U complexes highlighted above, informative cyclic voltammetry (CV) studies measuring the values of the relevant Th(IV)/Th(III) and An(III)/An(II) (An = U, Th) redox potentials were rare [203], and for many years, based on calculated estimates [220], especially for thorium. One reason is the high reactivity of these divalent and trivalent species, which makes them sensitive to the experimental conditions of the technique. For example, in the first CV studies conducted by Cloke et al. [221] to determine Th(IV)/Th(III) redox potential values, it was found that the electrolyte $[N(n\text{-}Bu)_4]^+[B(C_6F_5)_4]^-$, used successfully in CV studies of mixed sandwich U(III) complexes in THF [81], was incompatible. On the other hand, commercially available $[N(n\text{-}Bu)_4]^+[BPh_4]^-$ have enabled successful CV investigations into these highly-reduced species [146,191,196,198,207]. A summary of the measured $E_{1/2}$ values for the Th(IV)/Th(III) and An(III)/An(II) (An = U, Th) redox couples is given in Table 3.

Table 3. Experimentally determined Th(IV)/Th(III) and An(III)/An(II) (An = Th, U) reduction potentials. [a] vs Fc/Fc^+, [b] using 0.05M $[N(n\text{-}Bu)_4][BPh_4]$/THF; [c] using 100 mM $[N(n\text{-}Bu)_4][BPh_4]$/THF; [d] only cathodic current response observed; [e] using 50 mM $[N(n\text{-}Bu)_4][BPh_4]$/THF; [f] using 100 mM $[N(n\text{-}Bu)_4][PF_6]$/THF; [g] using 60 mM $[N(n\text{-}Bu)_4][BPh_4]$/THF irreversible process with ΔEpp = 884 mV at 200 $mV.s^{-1}$ scan rate; [h] vs. Fc^*/Fc^{*+} (Fc^* = decamethyl-ferrocene) 100 mM $[N(n\text{-}Bu)_4][PF_6]$/THF; [i] 100 mM $[N(n\text{-}Bu)_4][BPh_4]$/THF at 100 $mV.s^{-1}$ vs. Fc/Fc^+.

Compound	$E_{1/2}$ Th(IV)/Th(III) [a]	$E_{1/2}$ An(III)/(II) [a]
$[Th^{IV}(\eta^5\text{-}Cp'')_3Cl]$ (**6-Cl**) [191,221]	−2.96 [b] / −2.93 [c]	
$[Th^{III}(\eta^5\text{-}Cp'')_3]$ (**5**) [191,221]	−2.96 [b] / −2.93 [c]	−2.85 [c]
$[Th^{IV}(\eta^5\text{-}Cp'')_3Br]$ (**124**) [191]	−2.89 [c]	
$[Th^{IV}(\eta^5\text{-}Cp')_3Cl]$ (**125**) [191]	−3.14 [c]	
$[Th^{IV}(\eta^5\text{-}Cp')_3Br]$ (**126**) [191]	−3.17 [c,d]	
$[Th^{IV}(\eta^5\text{-}Cp^{Me4})_3Br]$ (**15-Br**) [191]	−3.34 [c]	
$[Th^{III}(\eta^5\text{-}Cp^{Me4})_3]$ (**15**) [191]		−3.28 [c]
$[K(18\text{-}c\text{-}6)(THF)_2][Th^{II}(\eta^5\text{-}Cp'')_3]$ (**30**) [191]		−2.84 [c]
$[K(2.2.2\text{-}crypt)][Th^{II}(\eta^5\text{-}Cp'')_3]$ (**30**) [221]		−2.85 [c]
$[Th^{IV}(\eta^8\text{-}COT^{TIPS2})(\eta^5\text{-}Cp^*)Cl]$ (**53-Cl**) [221]	−3.32 [b]	
$[Th^{IV}(\eta^8\text{-}COT^{TBDMS2})_2]$ (**9-Th**) [221]	−3.23 [b]	
$[U^{III}(\eta^5\text{-}Cp'')_3]$ (**67′-U**) [191]		−2.73 [c]
$[K(18\text{-}c\text{-}6)(THF)_2][U^{II}(\eta^5\text{-}Cp'')_3]$ (**68′′-U**) [191]		−2.71 [c]
$[U^{III}(\eta^5\text{-}Cp')_3]$ (**67′-U**) [191]		−2.26 [e]
$[K(2.2.2\text{-}crypt)][U^{II}(\eta^5\text{-}Cp')_3]$ (**68′-U**) [191]		−2.27 [e]
$[U^{III}(\eta^5\text{-}Cp^{Me4})_3]$ (**73**) [191]		−3.11 [c]
$[U^{III}\{(^{Ad,Me}ArO)_3Mes\}]$ (**77**) [203]		−2.495 [f]
$[U^{III}(^{Ad}TBPN_3)]$ (**84**) [146]		−2.40 [h]
$[U^{III}[\{OSi(O^tBu)_2Ar\}_3\text{-arene}](THF)]$ (**86**) [207]		−2.52 [i]
$[U^{III}(\eta^5\text{-}Cp^{iPr5})_2I]$ (**75**) [196]		−2.33 [g]

Based on the above values, reduction of [$Th^{III}(\eta^5$-$Cp'')_3$] (**5**) was achieved with all the alkali metals (except Fr) either in the presence of [2.2.2-crypt] (Li, Rb, Cs) or 18-c-6 (Na).

As can be seen from entries 1 and 3 in the table above, the leaving halide (chloride or bromide) plays a minimal role in the reduction in Th(IV) complexes to Th(III); on the other hand the electron-donating properties of the supporting ligands have a more profound effect, especially in the case of thorium complexes, with more electron-donating ligands pushing the measured $E_{1/2}$'s to more negative values. This is exemplified by $[CpMe4]^-$ Th(IV)/Th(III) supported complexes (entries 6 and 7), as well as the Th(IV) complexes supported by silyl-substituted COT ligands (entries 10 and 11). In the case of U(III)/U(II) redox couples, complex [U^{III} (η^5-$Cp^{Me4})_3$] has the most negative value [191,221].

The U(III)/U(II) redox couple in complex (**85**) was determined to be at −2.52 V vs. Fc/Fc^+ [207], a value close to the one found for (**77**) [203]. This was also confirmed by CV studies of the U(II) products (**86**) and (**86-crypt**), which both showed the same current response at this voltage. Complexes (**115**)/(**115-crypt**) (i.e., [K(2.2.2-crypt.][U^{III}[{OSi($O^tBu)_2Ar\}_3$-$(arene)^{2-}$](THF)]; Scheme 30) also feature a process with the same values as (**85**), (**86**)/(**86-crypt**) signifying that in a solution it can behave as a U(II) complex, a fact that is reflected by their $3e^-$ reactivity with CHT (Scheme 30) and further showcased by the fine balance between ligand vs. metal-based unpaired spin electron density (or somewhere in the middle, e.g., U-arene δ-bonds) [207]. Interestingly, in this series of U complexes, a second reductive process appears at −3.34 V vs. Fc/Fc^+, which is very close to the one found for the [$U^{II}(\eta^5$-$Cp^{iPr5})_2$](**76-U**)/[$U^{I}(\eta^5$-$Cp^{iPr5})_2]^-$(**124**) [196] redox couple (Scheme 32, Section 3.3). Nevertheless, whether this process was metal- or ligand- based is ambiguous.

Spectroelectrochemical studies of the thorium complexes listed in Table 3 further showed that both the +3 and +2 oxidation states could be accessed in situ via electrolysis, although the respective complexes were not stable under these conditions. The most important conclusion is that a $2e^-$ Th(IV) to Th(II) reduction is not taking place; instead, such a reduction involves two, one electron processes via the intermediacy of the corresponding Th(III) complex. This was also confirmed via the reaction of [$Th(\eta^5$-$Cp'')_3Br$] (**6-Br**) with Ba metal in THF: in the absence of chelates 2.2.2-cryptand or 18-c-6 only blue (**5**) is formed, whereas in the presence of these chelates, the green (**30**) is spectroscopically observed via the intermediacy of blue (**5**) [191].

The measured $E_{1/2}$ values in Table 3, show that low-valent An(III) and An(II) complexes (An = Th, U) are strongly reducing organometallic reagents. As such, this study has investigated whether they can be used to access lanthanide complexes in the +2 formal oxidation states. in situ EPR studies showed that (**5**) or (**67′′-U**) are insufficient to reduce either [$La^{III}(\eta^5$-$Cp'')_3$] (**67′′-La**) or [$Y^{III}(\eta^5$-$Cp')_3$] (**67′-Y**) to their La(II) or Y(II) derivatives ($I(^{139}La) = 7/2$, $I(^{89}Y) = 1/2$). Conversely, both [K(2.2.2.-crypt)][$An^{II}(\eta^5$-$Cp'')_3$] (An = Th (**30**), U (**68′′-U**)) reduce (**67′′-La**) and (**67′-Y**) to the corresponding Ln(II) complexes with the concomitant formation of [$An^{III}(\eta^5$-$Cp'')_3$] (An = Th (**5**), U (**67′′-U**)). Similarly, [K(2.2.2.-crypt)][$Y^{II}(\eta^5$-$Cp')_3$] (**62′-Yb)** and [K(2.2.2.-crypt)][$La^{II}(\eta^5$-$Cp'')_3$] (**68′′-La**) are able to reduce [$Th^{III}(\eta^5$-$Cp'')_3$] (**5**) to the Th(II) complex (**30**). Based on these studies, upper and lower bounds for the La(III)/La(II) and Y(III)/Y(II) redox potentials could be estimated: [K(2.2.2.-crypt)] [$An^{II}(\eta^5$-$Cp'')_3$] $</\approx$ [K(2.2.2.-crypt)][$Y^{II}(\eta^5$-$Cp')_3$] (**68′-Y**) $\approx$ [K(2.2.2.-crypt)][$La^{II}(\eta^5$-$Cp'')_3$] (**68′′-La**) < [$An^{III}(\eta^5$-$Cp'')_3$] [222]. In agreement with these studies, is the experimentally-determined $E_{1/2}$ redox value for (**68′-Y**) that was found to be −3.06 V vs. Fc/Fc^+ (for (**68′′-La**); only a cathodic current response is observed at −3.36 V vs. Fc/Fc^+) [223].

5. Conclusions

The prior discussion showcases recent advances in the exciting field of molecular U and Th complexes in oxidation states $\leq$ +3. From the early, well-defined Th(III) complexes reported by Lappert and Cloke, the newly emerging examples of both U and Th low-valent complexes underline the multifaced importance of ligand-metal complementarity to

tame such unusual oxidation states, determine ground state electronic configuration, and establish and control new patterns of reactivity, which in some cases involve metal-ligand cooperativity. Although, as a new field, the chemistry of these reactive species is still being explored, they have proven capable of promoting reductive events, with the number of transferred electrons (typically 1–3) modulated by the supporting ligands. This opens new prospectives in the activation of small molecules and similar important substrates and such investigations will undoubtedly be aided by CV experiments. These have proved useful in experimentally determining the actual values of these rare Th(IV)/Th(III), U(III)/U(II), and U(II)/U(I) redox couples; with the aid of electrochemistry-derived predictor tools [224], they can guide further explorations into their reactivity.

Although studies in the reactivity of these low-valent complexes are limited compared to U(III)-mediated transformations, small molecule activation, and, recently, catalysis [175] from the discussion above, the potential for these extremely low valent complexes to promote new chemical transformations is clear, especially when taking into considering their high reduction potentials. Central to this is the ligand's role and ability to control and modulate multi-electron transfers to substrates, as well as to determine the ground state electronic configuration of the actinide. However, for an effective catalysis, cycling the high-valent oxidised An^{n+} (An = Th, U; $n \geq 3$) products to their more reactive low-valent An^{n+} (An = Th, U; $n \leq 3$)-reduced couples pose challenges. One obvious solution would be to use electrochemical methods. However, another plausible way to circumvent our method of effective catalysis could take inspiration from the reports by Marks et al., as their work proposes the formation of Th(III) complexes from the photochemical elimination of H_2 from Th(IV) hydrides and alkyls [16,17], and suggests using photo-reductants. For example, acridine photo-reductants [225] have been recently synthesised with $E_{1/2}$ redox potential of their excited state of −2.91 to −3.6 V vs. SCE (*ca* −2.5 to −3.1 V vs. Fc/Fc^+), values that are in the range for the $An^{n+}/An^{(n-1)+}$ (An = Th (n = 4, 3) U (n = 3)) redox couples, shown in Table 3.

Finally, these U and Th low-valent complexes offer an overall fundamental understanding of the f-elements and are the basis to extend these motifs to the trans-uranic elements. As salient examples, we mentioned the isostructural to (**68″-U**) (Scheme 19) An(II) (An = Np, Pu) ionic complexes $[K(2.2.2\text{-crypt.})][An^{II}(\eta^5\text{-}Cp'')_3]$ (**68″-Np**) [226] and (**68″-Pu**) [227]; the former features a $5f^4 6d^1$ ground electronic state configuration, while the latter is a borderline case between a $5f^4 6d^1$ and a $5f^6 6d^0$ one (see also Table 1), with its HOMO having an appreciable $6dz^2$ character according to calculations [227,228]. With new synthetic methods [229–235] offering access to $AnX_{4-n}(coordinating\text{-}solvent)_y$ starting materials (n = 0, 1; coordinating-solvent = DME, THF, pyridine, CH_3CN; X = halide or N″ (n = 1, y = 0); An = transuranic element), low-valent molecular complexes of the heavier actinides [236–244] will further expand our knowledge and understanding of the f-elements.

Funding: We are thankful for partial funding from the National and Kapodistrian University of Athens, grant number 19497.

Conflicts of Interest: The authors declare no conflict of interest.

References

1. Jones, R.G.; Karmas, G.; Martin, G.A.; Gilman, H. Uranium(IV) Amides, Alkoxides and Mercaptides 42S5 Organic and Biological Chemistry [Contribution from the Organic Compounds of Uranium. II. Uranium(IV) Amides, Alkoxides and Mercaptides. *J. Am. Chem. Soc.* **1956**, *78*, 4285–4286. [CrossRef]
2. Gilman, H. Some Personal Notes on More Than One-Half Century of Organometallic Chemistry. In *Advances in Organometallic Chemistry*; Stone, F.G.A., Robert, W., Eds.; Elsevier: Amsterdam, The Netherlands, 1969; Volume 7, pp. 1–52. ISBN 978-0-12-031107-1.
3. Hickam, S.; Ray, D.; Szymanowski, J.E.S.; Li, R.Y.; Dembowski, M.; Smith, P.; Gagliardi, L.; Burns, P.C. Neptunyl Peroxide Chemistry: Synthesis and Spectroscopic Characterization of a Neptunyl Triperoxide Compound, $Ca_2[NpO_2(O_2)_3]\cdot 9H_2O$. *Inorg. Chem.* **2019**, *58*, 12264–12271. [CrossRef] [PubMed]

4. Loftier, S.T.; Meyer, K. Actinides. In *Comprehensive Coordination Chemistry III*; Elsevier: Amsterdam, The Netherlands, 2021; Volumes 1–9, pp. 471–521. ISBN 9780081026885.
5. Woen, D.H.; Evans, W.J. Expanding the +2 Oxidation State of the Rare-Earth Metals, Uranium, and Thorium in Molecular Complexes. In *Handbook on the Physics and Chemistry of Rare Earths*; Elsevier B.V.: Amsterdam, The Netherlands, 2016; Volume 50, pp. 337–394.
6. Jantunen, K.C.; Scott, B.L.; Kiplinger, J.L. A Comparative Study of the Reactivity of Zr(IV), Hf(IV) and Th(IV) Metallocene Complexes: Thorium Is Not a Group IV Metal after All. *J. Alloys Compd.* **2007**, *444–445*, 363–368. [CrossRef]
7. Cantat, T.; Graves, C.R.; Jantunen, K.C.; Burns, C.J.; Scott, B.L.; Schelter, E.J.; Morris, D.E.; Hay, J.; Kiplinger, J.L. Evidence for the Involvement of 5f Orbitals in the Bonding and Reactivity of Organometallic Actinide Compounds: Thorium(IV) and Uranium(IV) Bis(Hydrazonato) Complexes. *J. Am. Chem. Soc.* **2008**, *130*, 17537–17551. [CrossRef]
8. Gardner, B.M.; Cleaves, P.A.; Kefalidis, C.E.; Fang, J.; Maron, L.; Lewis, W.; Blake, A.J.; Liddle, S.T. The Role of 5f-Orbital Participation in Unexpected Inversion of the σ-Bond Metathesis Reactivity Trend of Triamidoamine Thorium(Iv) and Uranium(Iv) Alkyls. *Chem. Sci.* **2014**, *5*, 2489–2497. [CrossRef]
9. Zhang, L.; Hou, G.; Zi, G.; Ding, W.; Walter, M.D. Influence of the 5f Orbitals on the Bonding and Reactivity in Organoactinides: Experimental and Computational Studies on a Uranium Metallacyclopropene. *J. Am. Chem. Soc.* **2016**, *138*, 5130–5142. [CrossRef]
10. Liu, H.; Ghatak, T.; Eisen, M.S. Organoactinides in Catalytic Transformations: Scope, Mechanisms and Quo Vadis. *Chem. Commun.* **2017**, *53*, 11278–11297. [CrossRef]
11. Liu, H.; Saha, S.; Eisen, M.S. Recent Advances in Organo- Lanthanides and Actinides Mediated Hydroaminations. *Coord. Chem. Rev.* **2023**, *493*, 215284. [CrossRef]
12. Karmel, I.S.R.; Batrice, R.J.; Eisen, M.S. Catalytic Organic Transformations Mediated by Actinide Complexes. *Inorganics* **2015**, *3*, 392–428. [CrossRef]
13. Nugent, L.J.; Baybarz, R.D.; Burnett, J.L.; Ryan, J.L. Electron-Transfer and f-d Absorption Bands of Some Lanthanide and Actinide Complexes and the Standard (II-III) Oxidation Potential for Each Member of the Lanthanide and Actinide Series'. *J. Phys. Chem.* **1973**, *77*, 1528–1539. [CrossRef]
14. Ortu, F.; Formanuik, A.; Innes, J.R.; Mills, D.P. New Vistas in the Molecular Chemistry of Thorium: Low Oxidation State Complexes. *Dalton Trans.* **2016**, *45*, 7537–7549. [CrossRef] [PubMed]
15. Kanellakopulos, B.; Dornber~er, E.; Baumgmrtner, F. Das erste dreiwertige thorium in einem aromatenkomplex: Tris(cyclopentadienyl) thorium(III) Einleitung. *Inorg. Nucl. Chem. Lett.* **1974**, *10*, 155–160. [CrossRef]
16. Kalina, D.G.; Marks, T.J.; Wachter, W.A. Photochemical Synthesis of Low-Valent Organothorium Complexes. Evidence for Photoinduced β-Hydride Elimination. *J. Am. Chem. Soc.* **1977**, *99*, 3877–3879. [CrossRef]
17. Bruno, J.W.; Kalina, D.G.; Mintz, E.A.; Marks, T.J. Mechanistic Study of Photoinduced β-Hydride Elimination. The Facile Photochemical Synthesis of Low-Valent and Uranium Organometallics. *J. Am. Chem. Soc.* **1982**, *104*, 1860–1869. [CrossRef]
18. Blake, P.C.; Lappert, M.F.; Atwood, J.L.; Zhang, H. The Synthesis and Characterisation, Including X-Ray Diffraction Study, of [Th{η-$C_5H_3(SiMe_3)_2$}$_3$]; the First Thorium(III) Crystal Structure. *J. Chem. Soc. Chem. Commun.* **1986**, 1148–1149. [CrossRef]
19. Blake, P.C.; Lappert, M.F.; Taylor, R.G.; Atwood, J.L.; Zhang, H. Some Aspects of the Coordination and Organometallic Chemistry of Thorium and Uranium (MIII, MIV, UV) in +3 and +4 Oxidation States. *Inorg. Chim. Acta* **1987**, *139*, 13–20. [CrossRef]
20. Blake, P.C.; Edelstein, N.M.; Hitchcock, P.B.; Kot, W.K.; Lappert, M.F.; Shalimoff, G.V.; Tian, S. Synthesis, Properties and Structures of the Tris(Cyclopentadienyl)Thorium(III) Complexes [Th{η^5-$C_5H_3(SiMe_2R)_{2\text{-}1,3}$}$_3$] (R = Me or TBu). *J. Organomet. Chem.* **2001**, *636*, 124–129. [CrossRef]
21. Kot, W.K.; Shalimoff, G.V.; Edelstein, N.M.; Edelman, M.A.; Lappert, M.F. [ThIII(H5-$C_5H_3(SiMe_3)_2$]$_3$], an Actinide Compound with a 6d1 Ground State. *J. Am. Chem. Soc.* **1988**, *110*, 986–987. [CrossRef]
22. Parry, J.S.; Cloke, F.G.N.; Coles, S.J.; Hursthouse, M.B. Synthesis and Characterization of the First Sandwich Complex of: Trivalent Thorium: A Structural Comparison with the Uranium Analogue. *J. Am. Chem. Soc.* **1999**, *121*, 6867–6871. [CrossRef]
23. Walensky, J.R.; Martin, R.L.; Ziller, J.W.; Evans, W.J. Importance of Energy Level Matching for Bonding in Th^{3+}-Am^{3+} Actinide Metallocene Amidinates, $(C_5Me_5)_2$[^{i}PrNC(Me)N^{i}Pr]An. *Inorg. Chem.* **2010**, *49*, 10007–10012. [CrossRef]
24. Evans, W.J.; Walensky, J.R.; Ziller, J.W.; Rheingold, A.L. Insertion of Carbodiimides and Organic Azides into Actinide—Carbon Bonds. *Organometallics* **2009**, *28*, 3350–3357. [CrossRef]
25. Siladke, N.A.; Webster, C.L.; Walensky, J.R.; Takase, M.K.; Ziller, J.W.; Grant, D.J.; Gagliardi, L.; Evans, W.J. Actinide Metallocene Hydride Chemistry: C-H Activation in Tetramethylcyclopentadienyl Ligands to Form [μ-H^5-$C_5Me_3H(CH_2)$-Kc]$^{2-}$ Tuck-over Ligands in a Tetrathorium Octahydride Complex. *Organometallics* **2013**, *32*, 6522–6531. [CrossRef]
26. Langeslay, R.R.; Chen, G.P.; Windorff, C.J.; Chan, A.K.; Ziller, J.W.; Furche, F.; Evans, W.J. Synthesis, Structure, and Reactivity of the Sterically Crowded Th^{3+} Complex $(C_5Me_5)_3$Th Including Formation of the Thorium Carbonyl, [$(C_5Me_5)_3$Th(CO)][BPh_4]. *J. Am. Chem. Soc.* **2017**, *139*, 3387–3398. [CrossRef]
27. Broach, R.W.; Schultz, A.J.; Williams, J.M.; Brown, G.M.; Manriquez, J.M.; Fagan, P.J.; Marks, T.J. Molecular Structure of an Unusual Organoactinide Hydride Determined Solely by Neutron Diffraction. *Science (1979)* **1979**, *203*, 173–174. [CrossRef] [PubMed]
28. Formanuik, A.; Ariciu, A.M.; Ortu, F.; Beekmeyer, R.; Kerridge, A.; Tuna, F.; McInnes, E.J.L.; Mills, D.P. Actinide Covalency Measured by Pulsed Electron Paramagnetic Resonance Spectroscopy. *Nat. Chem.* **2017**, *9*, 578–583. [CrossRef]

29. Birnoschi, L.; Oakley, M.S.; McInnes, E.J.L.; Chilton, N.F. Relativistic Quantum Chemical Investigation of Actinide Covalency Measured by Electron Paramagnetic Resonance Spectroscopy. *J. Am. Chem. Soc.* **2024**, *146*, 14660–14671. [CrossRef]
30. Denning, R.G.; Harmer, J.; Green, J.C.; Irwin, M. Covalency in the 4f Shell of Tris-Cyclopentadienyl Ytterbium ($YbCp_3$)-A Spectroscopic Evaluation. *J. Am. Chem. Soc.* **2011**, *133*, 20644–20660. [CrossRef]
31. Altman, A.B.; Brown, A.C.; Rao, G.; Lohrey, T.D.; Britt, R.D.; Maron, L.; Minasian, S.G.; Shuh, D.K.; Arnold, J. Chemical Structure and Bonding in a Thorium(Iii)-Aluminum Heterobimetallic Complex. *Chem. Sci.* **2018**, *9*, 4317–4324. [CrossRef] [PubMed]
32. Rao, G.; Altman, A.B.; Brown, A.C.; Tao, L.; Stich, T.A.; Arnold, J.; David Britt, R. Metal Bonding with 3d and 6d Orbitals: An EPR and ENDOR Spectroscopic Investigation of Ti^{3+}-Al and Th^{3+}-Al Heterobimetallic Complexes. *Inorg. Chem.* **2019**, *58*, 7978–7988. [CrossRef]
33. Boronski, J.T.; Seed, J.A.; Hunger, D.; Woodward, A.W.; van Slageren, J.; Wooles, A.J.; Natrajan, L.S.; Kaltsoyannis, N.; Liddle, S.T. A Crystalline Tri-Thorium Cluster with σ-Aromatic Metal–Metal Bonding. *Nature* **2021**, *598*, 72–75. [CrossRef]
34. Lin, X.; Mo, Y. On the Bonding Nature in the Crystalline Tri-Thorium Cluster: Core-Shell Syngenetic σ-Aromaticity. *Angew. Chem.—Int. Ed.* **2022**, *61*, e202209658. [CrossRef] [PubMed]
35. Tomeček, J.; Liddle, S.T.; Kaltsoyannis, N. Actinide-Actinide Bonding: Electron Delocalisation and σ-Aromaticity in the Tri-Thorium Cluster [{Th(η^8-C_8H_8)(μ-Cl)$_2$}$_3$$K_2$]. *ChemPhysChem* **2023**, *24*, e202300366. [CrossRef] [PubMed]
36. Szczepanik, D.W. Bonding in a Crystalline Tri-Thorium Cluster: Not σ-Aromatic But Still Unique. *Angew. Chem.—Int. Ed.* **2022**, *61*, e202204337. [CrossRef] [PubMed]
37. Huh, D.N.; Roy, S.; Ziller, J.W.; Furche, F.; Evans, W.J. Isolation of a Square-Planar Th(III) Complex: Synthesis and Structure of [Th($OC_6H_2{}^tBu_2$-2,6-Me-4)4]$^{1-}$. *J. Am. Chem. Soc.* **2019**, *141*, 12458–12463. [CrossRef]
38. MacDonald, M.R.; Fieser, M.E.; Bates, J.E.; Ziller, J.W.; Furche, F.; Evans, W.J. Identification of the +2 Oxidation State for Uranium in a Crystalline Molecular Complex, [K(2.2.2-Cryptand)][($C_5H_4SiMe_3$)$_3$U]. *J. Am. Chem. Soc.* **2013**, *135*, 13310–13313. [CrossRef]
39. Wedal, J.C.; Bekoe, S.; Ziller, J.W.; Furche, F.; Evans, W.J. In Search of Tris(Trimethylsilylcyclopentadienyl) Thorium. *Dalton Trans.* **2019**, *48*, 16633–16640. [CrossRef]
40. Langeslay, R.R.; Fieser, M.E.; Ziller, J.W.; Furche, F.; Evans, W.J. Synthesis, Structure, and Reactivity of Crystalline Molecular Complexes of the {[$C_5H_3(SiMe_3)_2$]$_3$Th}$^{1-}$ Anion Containing Thorium in the Formal +2 Oxidation State. *Chem. Sci.* **2015**, *6*, 517–521. [CrossRef]
41. Formanuik, A.; Ortu, F.; Inman, C.J.; Kerridge, A.; Castro, L.; Maron, L.; Mills, D.P. Concomitant Carboxylate and Oxalate Formation From the Activation of CO_2 by a Thorium(III) Complex. *Chem.—Eur. J.* **2016**, *22*, 17976–17979. [CrossRef]
42. Formanuik, A.; Ortu, F.; Beekmeyer, R.; Kerridge, A.; Adams, R.W.; Mills, D.P. White Phosphorus Activation by a Th(III) Complex. *Dalton Trans.* **2016**, *45*, 2390–2393. [CrossRef]
43. Formanuik, A.; Ortu, F.; Liu, J.; Nodaraki, L.E.; Tuna, F.; Kerridge, A.; Mills, D.P. Double Reduction of 4,4′-Bipyridine and Reductive Coupling of Pyridine by Two Thorium(III) Single-Electron Transfers. *Chem.—Eur. J.* **2017**, *23*, 2290–2293. [CrossRef]
44. Liu, J.; Seed, J.A.; Formanuik, A.; Ortu, F.; Wooles, A.J.; Mills, D.P.; Liddle, S.T. Thorium(IV) Alkyl Synthesis from a Thorium(III) Cyclopentadienyl Complex and an N-Heterocyclic Olefin. *J. Organomet. Chem.* **2018**, *857*, 75–79. [CrossRef]
45. Wedal, J.C.; Cajiao, N.; Neidig, M.L.; Evans, W.J. Anion-Induced Disproportionation of Th(III) Complexes to Form Th(II) and Th(IV) Products. *Chem. Commun.* **2022**, *58*, 5289–5291. [CrossRef] [PubMed]
46. Langeslay, R.R.; Fieser, M.E.; Ziller, J.W.; Furche, F.; Evans, W.J. Expanding Thorium Hydride Chemistry Through Th^{2+}, Including the Synthesis of a Mixed-Valent Th^{4+}/Th^{3+} Hydride Complex. *J. Am. Chem. Soc.* **2016**, *138*, 4036–4045. [CrossRef]
47. Evans, W.J.; Nyce, G.W.; Johnston, M.A.; Ziller, J.W. How Much Steric Crowding Is Possible in Tris(H5-Pentamethylcyclopentadienyl) Complexes? Synthesis and Structure of (C_5Me_5)$_3$UCl and (C_5Me_5)$_3$$UF^1$. *J. Am. Chem. Soc.* **2000**, *122*, 12019–12020. [CrossRef]
48. Evans, W.J.; Forrestal, K.J.; Ziller, J.W. Activity of [Sm(C_5Me_5)$_3$] in Ethylene Polymerization and Synthesis of [U(C_5Me_5)$_3$], the First Tris(Pentamethylcyclopentadienyl) 5f-Element Complex. *Angew. Chem. (Int. Ed. Engl.)* **1997**, *36*, 774–776. [CrossRef]
49. Evans, W.J.; Perotti, J.M.; Kozimor, S.A.; Champagne, T.M.; Davis, B.L.; Nyce, G.W.; Fujimoto, C.H.; Clark, R.D.; Johnston, M.A.; Ziller, J.W. Synthesis and Comparative η 1-Alkyl and Sterically Induced Reduction Reactivity of (C_5Me_5)$_3$Ln Complexes of La, Ce, Pr, Nd, and Sm. *Organometallics* **2005**, *24*, 3916–3931. [CrossRef]
50. Ren, W.; Lukens, W.W.; Zi, G.; Maron, L.; Walter, M.D. Is the Bipyridyl Thorium Metallocene a Low-Valent Thorium Complex? A Combined Experimental and Computational Study. *Chem. Sci.* **2013**, *4*, 1168–1174. [CrossRef]
51. Wang, S.; Wang, D.; Li, T.; Heng, Y.; Hou, G.; Zi, G.; Walter, M.D. Synthesis, Structure, and Reactivity of the Uranium Bipyridyl Complex [{η^5-1,2,4-(Me_3Si)$_3$$C_5H_2$}$_2$U(Bipy)]. *Organometallics* **2022**, *41*, 1543–1557. [CrossRef]
52. Wang, S.; Li, T.; Heng, Y.; Wang, D.; Hou, G.; Zi, G.; Walter, M.D. Small-Molecule Activation Mediated by [η^5-1,3-(Me_3Si)$_2$$C_5H_3$]$_2$U(Bipy). *Inorg. Chem.* **2022**, *61*, 6234–6251. [CrossRef]
53. Zhang, L.; Zhang, C.; Hou, G.; Zi, G.; Walter, M.D. Small-Molecule Activation Mediated by a Uranium Bipyridyl Metallocene. *Organometallics* **2017**, *36*, 1179–1187. [CrossRef]
54. Button, Z.E.; Higgins, J.A.; Suvova, M.; Cloke, F.G.N.; Roe, S.M. Mixed Sandwich Thorium Complexes Incorporating Bis(Tri-Isopropylsilyl)Cyclooctatetraenyl and Pentamethylcyclopentadienyl Ligands: Synthesis, Structure and Reactivity. *Dalton Trans.* **2015**, *44*, 2588–2596. [CrossRef] [PubMed]
55. Yu, C.; Liang, J.; Deng, C.; Lefèvre, G.; Cantat, T.; Diaconescu, P.L.; Huang, W. Arene-Bridged Dithorium Complexes: Inverse Sandwiches Supported by a Δbonding Interaction. *J. Am. Chem. Soc.* **2020**, *142*, 21292–21297. [CrossRef] [PubMed]

56. Hsueh, F.C.; Chen, D.; Rajeshkumar, T.; Scopelliti, R.; Maron, L.; Mazzanti, M. Two-Electron Redox Reactivity of Thorium Supported by Redox-Active Tripodal Frameworks. *Angew. Chem.—Int. Ed.* **2024**, *63*, e202317346. [CrossRef]
57. Andersen, R.A. Tris((HexamethyldisiIyl)Amido)Uranium(III): Preparation and Coordination Chemistry. *Inorg. Chem.* **1979**, *18*, 1507–1509. [CrossRef]
58. Brennan, J.G.; Andersen, R.A.; Zalkin, A. Chemistry of Trivalent Uranium Metallocenes: Electron-Transfer Reactions with Carbon. Formation of $[(RC_5H_4)_3U]_2[\mu\text{-}\eta^1,\eta^2\text{-}CS_2]$. *Inorg. Chem.* **1986**, *25*, 1756–1760. [CrossRef]
59. Patel, D.; Wooles, A.J.; Hashem, E.; Omorodion, H.; Baker, R.J.; Liddle, S.T. Comments on Reactions of Oxide Derivatives of Uranium with Hexachloropropene to Give UCl4. *New J. Chem.* **2015**, *39*, 7559–7562. [CrossRef]
60. Schlesinger, H.I.; Brown, B.C. Uranium(IV) Borohydride1. *J. Am. Chem. Soc.* **1953**, *75*, 219–221. [CrossRef]
61. Haaland, A.; Shorokhov, D.J.; Tutukin, A.V.; Volden, H.V.; Swang, O.; McGrady, G.S.; Kaltsoyannis, N.; Downs, A.J.; Tang, C.Y.; Turner, J.F.C. Molecular Structures of Two Metal Tetrakis(Tetrahydroborates), $Zr(BH_4)_4$ and $U(BH_4)_4$: Equilibrium Conformations and Barriers to Internal Rotation of the Triply Bridging BH_4 Groups. *Inorg. Chem.* **2002**, *41*, 6646–6655. [CrossRef] [PubMed]
62. Carmichael, C.D.; Jones, N.A.; Arnold, P.L. Low-Valent Uranium Iodides: Straightforward Solution Syntheses of UI3 and UI4 Etherates. *Inorg. Chem.* **2008**, *47*, 8577–8579. [CrossRef]
63. Monreal, M.J.; Thomson, R.K.; Cantat, T.; Travia, N.E.; Scott, B.L.; Kiplinger, J.L. UI_4(1,4-Dioxane)$_2$, $[UCl_4$(1,4-Dioxane)$]_2$, and UI_3(1,4-Dioxane)$_{1.5}$: Stable and Versatile Starting Materials for Low- and High-Valent Uranium Chemistry. *Organometallics* **2011**, *30*, 2031–2038. [CrossRef]
64. Boreen, M.A.; Parker, B.F.; Lohrey, T.D.; Arnold, J. A Homoleptic Uranium(III) Tris(Aryl) Complex. *J. Am. Chem. Soc.* **2016**, *138*, 15865–15868. [CrossRef]
65. Der Sluys, V.; Burns, C.J.; Sattleberger, A.P. First Example Ot a Neutral Homoleptic Uranium Alkyl. Synthesis, Properties, and Structure of $U[CH(SIMe_3)_2]_3$. *Organometallics* **1989**, *8*, 855–857. [CrossRef]
66. Claude Berthet, J.; Lance, M.; Nierlich, M.; Ephritikhine, M. Synthesis of the Uranium Triflates $U(OTf)_3$ and $U(OTf)_4$—Crystal Structure of $[U(OTf)_2(OPPh_3)_4][OTf]$. *Eur. J. Inorg. Chem.* **1999**, *1999*, 2005–2007. [CrossRef]
67. Evans, W.J.; Nyce, G.W.; Forrestal, K.J.; Ziller, J.W. Multiple Syntheses of $(C_5Me_5)_3U$. *Organometallics* **2002**, *21*, 1050–1055. [CrossRef]
68. Avens, L.R.; Burns, C.J.; Butcher, R.J.; Clark, D.L.; Gordon, J.C.; Schake, A.R.; Scott, B.L.; Watkin, J.G.; Zwick, B.D. Mono(Pentamethylcyclopentadienyl)Uranium(III) Complexes: Synthesis, Properties, and X-Ray Structures of $(\eta\text{-}C_5Me_5)UI_2(THF)_3$, $(\eta\text{-}C_5Me_5)UI_2(Py)_3$, and $(\eta\text{-}C_5Me_5)U[N(SiMe_3)_2]_2$. *Organometallics* **2000**, *19*, 451–457. [CrossRef]
69. Baker, R.J. The Coordination and Organometallic Chemistry of UI_3 and $U\{N(SiMe_3)_2\}_3$: Synthetic Reagents Par Excellence. *Coord. Chem. Rev.* **2012**, *256*, 2843–2871. [CrossRef]
70. Fetrow, T.V.; Grabow, J.P.; Leddy, J.; Daly, S.R. Convenient Syntheses of Trivalent Uranium Halide Starting Materials without Uranium Metal. *Inorg. Chem.* **2021**, *60*, 7593–7601. [CrossRef]
71. Droidwski, J.; Du Preez, J.G.H. Synthesis and Characterization of Uranium Triiodide Tetrakis(Acetonitrile). *Inorg. Chim. Acta* **1994**, *218*, 203–205.
72. Evans, W.J.; Kozimor, S.A.; Ziller, J.W.; Fagin, A.A.; Bochkarev, M.N. Facile Syntheses of Unsolvated Ul_3 and Tetramethylcyclopentadienyl Uranium Halides. *Inorg. Chem.* **2005**, *44*, 3993–4000. [CrossRef]
73. Schnaars, D.D.; Wu, G.; Hayton, T.W. Reactivity of UH_3 with Mild Oxidants. *Dalton Trans.* **2008**, *69*, 6121–6126. [CrossRef]
74. Arnold, P.L.; Stevens, C.J.; Farnaby, J.H.; Gardiner, M.G.; Nichol, G.S.; Love, J.B. New Chemistry from an Old Reagent: Mono- and Dinuclear Macrocyclic Uranium(III) Complexes from $[U(BH_4)_3(THF)_2]$. *J. Am. Chem. Soc.* **2014**, *136*, 10218–10221. [CrossRef] [PubMed]
75. Avens, L.R.; Bott, S.G.; Clark, D.L.; Sattelberger, A.P.; Watkin, J.G.; Zwick, B.D. A Convenient Entry into Trivalent Actinide Chemistry: Synthesis and Characterization of $AnI_3(THF)_4$ and $An[N(SiMe_3)_2]_3$ (An = U, Np, Pu). *Inorg. Chem.* **1994**, *33*, 2248–2256. [CrossRef]
76. Evans, W.J.; Miller, K.A.; DiPasquale, A.G.; Rheingold, A.L.; Stewart, T.; Bau, R. A Crystallizable F-Element Tuck-in Complex: The Tuck-in Tuck-over Uranium Metallocene $[(C_5Me_5)U\{\mu\text{-}\eta^5\text{:}\eta^1\text{:}\eta^1\text{-}C_5Me_3(CH_2)_2\}(\mu\text{-}H)_2U\text{-}(C_5Me_5)_2]$. *Angew. Chem.—Int. Ed.* **2008**, *47*, 5075–5078. [CrossRef] [PubMed]
77. Pierre, H.S.L.; Heinemann, F.W.; Meyer, K. Well-Defined Molecular Uranium(Iii) Chloride Complexes. *Chem. Commun.* **2014**, *50*, 3962–3964. [CrossRef] [PubMed]
78. Tsoureas, N.; Summerscales, O.T.; Cloke, F.G.N.; Roe, S.M. Steric Effects in the Reductive Coupling of CO by Mixed-Sandwich Uranium(III) Complexes. *Organometallics* **2013**, *32*, 1353–1362. [CrossRef]
79. Kahan, R.J.; Cloke, F.G.N.; Roe, S.M.; Nief, F. Activation of Carbon Dioxide by New Mixed Sandwich Uranium(III) Complexes Incorporating Cyclooctatetraenyl and Pyrrolide, Phospholide, or Arsolide Ligands. *New J. Chem.* **2015**, *39*, 7602–7607. [CrossRef]
80. Summerscales, O.T.; Frey, A.S.P.; Cloke, F.G.N.; Hitchcock, P.B. Reductive Disproportionation of Carbon Dioxide to Carbonate and Squarate Products Using a Mixed-Sandwich U(III) Complex. *Chem. Commun.* **2009**, 198–200. [CrossRef]
81. Tsoureas, N.; Castro, L.; Kilpatrick, A.F.R.; Cloke, F.G.N.; Maron, L. Controlling Selectivity in the Reductive Activation of CO_2 by Mixed Sandwich Uranium(Iii) Complexes. *Chem. Sci.* **2014**, *5*, 3777–3788. [CrossRef]
82. Summerscales, O.T.; Cloke, F.G.N.; Hitchcock, P.B.; Green, J.C.; Hazari, N. Reductive Cyclotetramerization of CO to Squarate by a U(III) Complex: The x-Ray Crystal Structure of $[U\ (\eta\text{-}C_8H_6\{Si^iPr_{3\text{-}1,4}\}_2)(\eta\text{-}C_5Me_4H)]_2(\mu\text{-}\eta^2\text{:}\eta^2\text{-}C_4O_4)$. *J. Am. Chem. Soc.* **2006**, *128*, 9602–9603. [CrossRef]

83. Inman, C.J.; Frey, A.S.P.; Kilpatrick, A.F.R.; Cloke, F.G.N.; Roe, S.M. Carbon Dioxide Activation by a Uranium(III) Complex Derived from a Chelating Bis(Aryloxide) Ligand. *Organometallics* **2017**, *36*, 4539–4545. [CrossRef]
84. Frey, A.S.; Cloke, F.G.N.; Hitchcock, P.B.; Day, I.J.; Green, J.C.; Aitken, G. Mechanistic Studies on the Reductive Cyclooligomerisation of CO by U(III) Mixed Sandwich Complexes; the Molecular Structure of $[U(\eta\text{-}C_8H_6\{Si^iPr_3\text{-}1,4\}_2)(\eta\text{-}Cp^*)]_2(\mu\text{-}\eta^1\text{:}\eta^1\text{-}C_2O_2)$. *J. Am. Chem. Soc.* **2008**, *130*, 13816–13817. [CrossRef] [PubMed]
85. Kahan, R.J.; Farnaby, J.H.; Tsoureas, N.; Cloke, F.G.N.; Hitchcock, P.B.; Coles, M.P.; Roe, S.M.; Wilson, C. Sterically Encumbered Mixed Sandwich Compounds of Uranium(III): Synthesis and Reactivity with Small Molecules. *J. Organomet. Chem.* **2018**, *857*, 110–122. [CrossRef]
86. Summerscales, O.T.; Cloke, F.G.N.; Hitchcock, P.B.; Green, J.C.; Hazari, N. Reductive Cyclotrimerization of Carbon to the Deltate Dianion by an Organometallic Uranium Complex. *Science (1979)* **2006**, *311*, 829–831. [CrossRef]
87. Lam, O.P.; Meyer, K. Uranium-Mediated Carbon Dioxide Activation and Functionalization. *Polyhedron* **2012**, *32*, 1–9. [CrossRef]
88. Lam, O.P.; Bart, S.C.; Kameo, H.; Heinemann, F.W.; Meyer, K. Insights into the Mechanism of Carbonate Formation through Reductive Cleavage of Carbon Dioxide with Low-Valent Uranium Centers. *Chem. Commun.* **2010**, *46*, 3137–3139. [CrossRef]
89. Schmidt, A.C.; Nizovtsev, A.V.; Scheurer, A.; Heinemann, F.W.; Meyer, K. Uranium-Mediated Reductive Conversion of CO_2 to CO and Carbonate in a Single-Vessel, Closed Synthetic Cycle. *Chem. Commun.* **2012**, *48*, 8634–8636. [CrossRef]
90. Schmidt, A.; Heinemann, F.W.; Kefalidis, C.E.; Maron, L.; Roesky, P.W.; Meyer, K. Activation of SO_2 and CO_2 by Trivalent Uranium Leading to Sulfite/Dithionite and Carbonate/Oxalate Complexes. *Chem.—Eur. J.* **2014**, *20*, 13501–13506. [CrossRef]
91. Arnold, P.L.; Turner, Z.R.; Bellabarba, R.M.; Tooze, R.P. Carbon Monoxide Coupling and Functionalisation at a Simple Uranium Coordination Complex. *Chem. Sci.* **2011**, *2*, 77–79. [CrossRef]
92. Cooper, O.; Camp, C.; Pécaut, J.; Kefalidis, C.E.; Maron, L.; Gambarelli, S.; Mazzanti, M. Multimetallic Cooperativity in Uranium-Mediated CO_2 Activation. *J. Am. Chem. Soc.* **2014**, *136*, 6716–6723. [CrossRef]
93. Ward, R.J.; Kelley, S.P.; Lukens, W.W.; Walensky, J.R. Reduction of CO_2 and CS_2 with Uranium(III) Metallocene Aryloxides. *Organometallics* **2022**, *41*, 1579–1585. [CrossRef]
94. Camp, C.; Chatelain, L.; Kefalidis, C.E.; Pécaut, J.; Maron, L.; Mazzanti, M. CO_2 Conversion to Isocyanate via Multiple N-Si Bond Cleavage at a Bulky Uranium(III) Complex. *Chem. Commun.* **2015**, *51*, 15454–15457. [CrossRef] [PubMed]
95. Gardner, B.M.; Stewart, J.C.; Davis, A.L.; Mcmaster, J.; Lewis, W.; Blake, A.J.; Liddle, S.T. Homologation and Functionalization of Carbon Monoxide by a Recyclable Uranium Complex. *Proc. Natl. Acad. Sci. USA* **2012**, *109*, 9265–9270. [CrossRef] [PubMed]
96. Matson, E.M.; Forrest, W.P.; Fanwick, P.E.; Bart, S.C. Functionalization of Carbon Dioxide and Carbon Disulfide Using a Stable Uranium(III) Alkyl Complex. *J. Am. Chem. Soc.* **2011**, *133*, 4948–4954. [CrossRef] [PubMed]
97. Mansell, S.M.; Kaltsoyannis, N.; Arnold, P.L. Small Molecule Activation by Uranium Tris(Aryloxides): Experimental and Computational Studies of Binding of N_2, Coupling of CO, and Deoxygenation Insertion of CO_2 under Ambient Conditions. *J. Am. Chem. Soc.* **2011**, *133*, 9036–9051. [CrossRef] [PubMed]
98. Mougel, V.; Camp, C.; Pécaut, J.; Copéret, C.; Maron, L.; Kefalidis, C.E.; Mazzanti, M. Siloxides as Supporting Ligands in Uranium(III)-Mediated Small-Molecule Activation. *Angew. Chem.—Int. Ed.* **2012**, *51*, 12280–12284. [CrossRef]
99. Castro-Rodriguez, I.; Meyer, K. Carbon Dioxide Reduction and Carbon Monoxide Activation Employing a Reactive Uranium(III) Complex. *J. Am. Chem. Soc.* **2005**, *127*, 11242–11243. [CrossRef]
100. Tsoureas, N.; Cloke, F.G.N. Activation of Carbon Suboxide (C_3O_2) by U(III) to Form a Cyclobutane-1,3-Dione Ring. *Chem. Commun.* **2018**, *54*, 8830–8833. [CrossRef]
101. Frey, A.S.P.; Cloke, F.G.N.; Hitchcock, P.B.; Green, J.C. Activation of P4 by $U(\eta^5\text{-}C_5Me_5)(\eta^8\text{-}C_8H_6(SiiPr_3)_2\text{-}1,4)(THF)$; The X-Ray Structure of $[U(\eta^5\text{-}C_5Me_5)(\eta^8\text{-}C_8H_6(SiiPr_3)_2\text{-}1,4)]_2(\mu\text{-}\eta^2\text{:}\eta^2\text{-}P_4)$. *New J. Chem.* **2011**, *35*, 2022–2026. [CrossRef]
102. Tsoureas, N.; Kilpatrick, A.F.R.; Summerscales, O.T.; Nixon, J.F.; Cloke, F.G.N.; Hitchcock, P.B. The First Example of the Two-Electron Reduction of a Phosphaalkyne—Synthesis and Structural Characterisation of the Diuranium(IV) Pentalene Complex $[(U\{\eta^5\text{-}C_5Me_5\}\{\eta^8\text{-}C_8H_4(SiiPr_3\text{-}1,4)_2\})_2(\mu\text{-}\eta^2\text{:}\eta^1\text{-}TBuCP)]$. *Eur J Inorg. Chem.* **2013**, *2013*, 4085–4089. [CrossRef]
103. Hoerger, C.J.; Heinemann, F.W.; Louyriac, E.; Maron, L.; Grützmacher, H.; Meyer, K. Formation of a Uranium-Bound N1-Cyaphide (CP-) Ligand via Activation and C-O Bond Cleavage of Phosphaethynolate (OCP-). *Organometallics* **2017**, *36*, 4351–4354. [CrossRef]
104. Hoerger, C.J.; Heinemann, F.W.; Louyriac, E.; Rigo, M.; Maron, L.; Grützmacher, H.; Driess, M.; Meyer, K. Cyaarside (CAs^-) and 1,3-Diarsaallendiide ($AsCAs^{2-}$) Ligands Coordinated to Uranium and Generated via Activation of the Arsaethynolate Ligand ($OCAs^-$). *Angew.Chem.—Int. Ed.* **2019**, *58*, 1679–1683. [CrossRef] [PubMed]
105. Mansell, S.M.; Farnaby, J.H.; Germeroth, A.I.; Arnold, P.L. Thermally Stable Uranium Dinitrogen Complex with Siloxide Supporting Ligands. *Organometallics* **2013**, *32*, 4214–4222. [CrossRef]
106. Roussel, P.; Scott, P. Complex of Dinitrogen with Trivalent Uranium. *J. Am. Chem. Soc.* **1998**, *120*, 1070–1071. [CrossRef]
107. Roussel, P.; Errington, W.; Kaltsoyannis, N.; Scott, P. Back Bonding without σ-Bonding: A Unique π-Complex of Dinitrogen with Uranium. *J. Organomet. Chem.* **2001**, *635*, 69–74. [CrossRef]
108. Cloke, F.G.N.; Hitchcock, P.B. Reversible Binding and Reduction of Dinitrogen by a Uranium(III) Pentalene Complex. *J. Am. Chem. Soc.* **2002**, *124*, 9352–9353. [CrossRef]
109. Odom, A.L.; Arnold, P.L.; Cummins, C.C. Heterodinuclear Uranium/Molybdenum Dinitrogen Complexes. *J. Am. Chem. Soc.* **1998**, *120*, 5836–5837. [CrossRef]
110. Evans, W.J.; Kozimor, S.A.; Ziller, J.W. A Monometallic f Element Complex of Dinitrogen: $(C_5Me_5)_3U(\eta^1\text{-}N_2)$. *J. Am. Chem. Soc.* **2003**, *125*, 14264–14265. [CrossRef]

111. Korobkov, I.; Gambarotta, S.; Yap, G.P.A. A Highly Reactive Uranium Complex Supported by the Calix[4]Tetrapyrrole Tetraanion Affording Dinitrogen Cleavage, Solvent Deoxygenation, and Polysilanol Depolymerization. *Angew. Chem.—Int. Ed.* **2002**, *41*, 3433–3436. [CrossRef]
112. Falcone, M.; Chatelain, L.; Scopelliti, R.; Živković, I.; Mazzanti, M. Nitrogen Reduction and Functionalization by a Multimetallic Uranium Nitride Complex. *Nature* **2017**, *547*, 332–335. [CrossRef]
113. Jori, N.; Keener, M.; Rajeshkumar, T.; Scopelliti, R.; Maron, L.; Mazzanti, M. Dinitrogen Cleavage by a Dinuclear Uranium(Iii) Complex. *Chem. Sci.* **2023**, *14*, 13485–13494. [CrossRef]
114. Jori, N.; Rajeshkumar, T.; Scopelliti, R.; Živković, I.; Sienkiewicz, A.; Maron, L.; Mazzanti, M. Cation Assisted Binding and Cleavage of Dinitrogen by Uranium Complexes. *Chem. Sci.* **2022**, *13*, 9232–9242. [CrossRef] [PubMed]
115. Batov, M.S.; del Rosal, I.; Scopelliti, R.; Fadaei-Tirani, F.; Zivkovic, I.; Maron, L.; Mazzanti, M. Multimetallic Uranium Nitride Cubane Clusters from Dinitrogen Cleavage. *J. Am. Chem. Soc.* **2023**, *145*, 26435–26443. [CrossRef] [PubMed]
116. Jori, N.; Moreno, J.J.; Shivaraam, R.A.K.; Rajeshkumar, T.; Scopelliti, R.; Maron, L.; Campos, J.; Mazzanti, M. Iron Promoted End-on Dinitrogen-Bridging in Heterobimetallic Complexes of Uranium and Lanthanides. *Chem. Sci.* **2024**, *15*, 6842–6852. [CrossRef]
117. Falcone, M.; Barluzzi, L.; Andrez, J.; Fadaei Tirani, F.; Zivkovic, I.; Fabrizio, A.; Corminboeuf, C.; Severin, K.; Mazzanti, M. The Role of Bridging Ligands in Dinitrogen Reduction and Functionalization by Uranium Multimetallic Complexes. *Nat. Chem.* **2019**, *11*, 154–160. [CrossRef]
118. Arnold, P.L.; Ochiai, T.; Lam, F.Y.T.; Kelly, R.P.; Seymour, M.L.; Maron, L. Metallacyclic Actinide Catalysts for Dinitrogen Conversion to Ammonia and Secondary Amines. *Nat. Chem.* **2020**, *12*, 654–659. [CrossRef]
119. Wang, P.; Douair, I.; Zhao, Y.; Wang, S.; Zhu, J.; Maron, L.; Zhu, C. Facile Dinitrogen and Dioxygen Cleavage by a Uranium(III) Complex: Cooperativity Between the Non-Innocent Ligand and the Uranium Center. *Angew. Chem.—Int. Ed.* **2021**, *60*, 473–479. [CrossRef]
120. Halter, D.P.; Heinemann, F.W.; Bachmann, J.; Meyer, K. Uranium-Mediated Electrocatalytic Dihydrogen Production from Water. *Nature* **2016**, *530*, 317–321. [CrossRef] [PubMed]
121. Halter, D.P.; Heinemann, F.W.; Maron, L.; Meyer, K. The Role of Uranium-Arene Bonding in H_2O Reduction Catalysis. *Nat. Chem.* **2018**, *10*, 259–267. [CrossRef]
122. Arnold, P.L.; Mansell, S.M.; Maron, L.; McKay, D. Spontaneous Reduction and C-H Borylation of Arenes Mediated by Uranium(III) Disproportionation. *Nat. Chem.* **2012**, *4*, 668–674. [CrossRef]
123. Barluzzi, L.; Falcone, M.; Mazzanti, M. Small Molecule Activation by Multimetallic Uranium Complexes Supported by Siloxide Ligands. *Chem. Commun.* **2019**, *55*, 13031–13047. [CrossRef]
124. Castro-Rodriguez, I.; Nakai, H.; Zakharov, L.N.; Rheingold, A.L.; Meyer, K. A Linear, O-Coordinated H1-CO_2 Bound to Uranium. *Science (1979)* **2004**, *305*, 1757–1759. [CrossRef]
125. Tsoureas, N.; Maron, L.; Kilpatrick, A.F.R.; Layfield, R.A.; Cloke, F.G.N. Ethene Activation and Catalytic Hydrogenation by a Low-Valent Uranium Pentalene Complex. *J. Am. Chem. Soc.* **2020**, *142*, 89–92. [CrossRef] [PubMed]
126. Camp, C.; Cooper, O.; Andrez, J.; Pécaut, J.; Mazzanti, M. CS2 Activation at Uranium(Iii) Siloxide Ate Complexes: The Effect of a Lewis Acidic Site. *Dalton Trans.* **2015**, *44*, 2650–2656. [CrossRef]
127. Lam, O.P.; Heinemann, F.W.; Meyer, K. C-C Bond Formation through Reductive Coupling of CS_2 to Yield Uranium Tetrathiooxalate and Ethylenetetrathiolate Complexes. *Angew. Chem.—Int. Ed.* **2011**, *50*, 5965–5968. [CrossRef]
128. Lam, O.P.; Franke, S.M.; Heinemann, F.W.; Meyer, K. Reactivity of U-E-U (E = S, Se) toward CO_2, CS_2, and COS: New Mixed-Carbonate Complexes of the Types U-CO_2E-U (E = S, Se), U-CS_2E-U (E = O, Se), and U-COSSe-U. *J. Am. Chem. Soc.* **2012**, *134*, 16877–16881. [CrossRef]
129. Hoerger, C.J.; La Pierre, H.S.; Maron, L.; Scheurer, A.; Heinemann, F.W.; Meyer, K. Reductive Disproportionation of Nitric Oxide Mediated by Low-Valent Uranium. *Chem. Commun.* **2016**, *52*, 10854–10857. [CrossRef] [PubMed]
130. Siladke, N.A.; Meihaus, K.R.; Ziller, J.W.; Fang, M.; Furche, F.; Long, J.R.; Evans, W.J. Synthesis, Structure, and Magnetism of an f Element Nitrosyl Complex, $(C_5Me_4H)_3UNO$. *J. Am. Chem. Soc.* **2012**, *134*, 1243–1249. [CrossRef]
131. Frey, A.S.P.; Cloke, F.G.N.; Coles, M.P.; Hitchcock, P.B. UIII-Induced Reductive Co-Coupling of NO and CO to Form UIV Cyanate and Oxo Derivates. *Chem.—Eur. J.* **2010**, *16*, 9446–9448. [CrossRef]
132. Kefalidis, C.E.; Frey, A.S.P.; Roe, S.M.; Cloke, F.G.N.; Maron, L. Formation of Cyanates in Low-Valent Uranium Chemistry: A Synergistic Experimental/Theoretical Study. *Dalton Trans.* **2014**, *43*, 11202–11208. [CrossRef]
133. Matson, E.M.; Forrest, W.P.; Fanwick, P.E.; Bart, S.C. Synthesis and Reactivity of Trivalent Tp*U($CH_2Ph)_2$(THF): Insertion vs Oxidation at Low-Valent Uranium-Carbon Bonds. *Organometallics* **2013**, *32*, 1484–1492. [CrossRef]
134. Zuend, S.J.; Lam, O.P.; Heinemann, F.W.; Meyer, K. Carbon Dioxide Insertion into Uranium-Activated Dicarbonyl Complexes. *Angew. Chem.—Int. Ed.* **2011**, *50*, 10626–10630. [CrossRef] [PubMed]
135. David J Arney, G.S.; Burns, C.J. Synthesis and Structure of High-Valent Organouranium Containing Terminal Monooxo Functional. *J. Am. Chem. Soc* **1993**, *115*, 3939. [CrossRef]
136. Tsoureas, N.; Kilpatrick, A.F.R.; Inman, C.J.; Cloke, F.G.N. Steric Control of Redox Events in Organo-Uranium Chemistry: Synthesis and Characterisation of U(v) Oxo and Nitrido Complexes. *Chem. Sci.* **2016**, *7*, 4624–4632. [CrossRef] [PubMed]
137. King, D.M.; Tuna, F.; McMaster, J.; Lewis, W.; Blake, A.J.; McInnes, E.J.L.; Liddle, S.T. Single-Molecule Magnetism in a Single-Ion Triamidoamine Uranium(V) Terminal Mono-Oxo Complex. *Angew. Chem.—Int. Ed.* **2013**, *52*, 4921–4924. [CrossRef]

138. Smiles, D.E.; Wu, G.; Hayton, T.W. Synthesis of Uranium-Ligand Multiple Bonds by Cleavage of a Trityl Protecting Group. *J. Am. Chem. Soc.* **2014**, *136*, 96–99. [CrossRef]
139. Brown, J.L.; Fortier, S.; Lewis, R.A.; Wu, G.; Hayton, T.W. A Complete Family of Terminal Uranium Chalcogenides, $[U(E)(N\{SiMe_3\}_2)_3]^-$ (E = O, S, Se, Te). *J. Am. Chem. Soc.* **2012**, *134*, 15468–15475. [CrossRef]
140. Smiles, D.E.; Wu, G.; Hayton, T.W. Synthesis of Terminal Monochalcogenide and Dichalcogenide Complexes of Uranium Using Polychalcogenides, $[En]^{2-}$ (E = Te, n = 2; E = Se, n = 4), as Chalcogen Atom Transfer Reagents. *Inorg. Chem.* **2014**, *53*, 10240–10247. [CrossRef]
141. Kraft, S.J.; Walensky, J.; Fanwick, P.E.; Hall, M.B.; Bart, S.C. Crystallographic Evidence of a Base-Free Uranium(IV) Terminal Oxo Species. *Inorg. Chem.* **2010**, *49*, 7620–7622. [CrossRef]
142. Arnold, P.L.; Puig-Urrea, L.; Wells, J.A.L.; Yuan, D.; Cruickshank, F.L.; Young, R.D. Applications of Boroxide Ligands in Supporting Small Molecule Activation by U(Iii) and U(Iv) Complexes. *Dalton Trans.* **2019**, *48*, 4894–4905. [CrossRef]
143. Zi, G.; Jia, L.; Werkema, E.L.; Walter, M.D.; Gottfriedsen, J.P.; Andersen, R.A. Preparation and Reactions of Base-Free Bis(1,2,4-Tri-Tert-Butylcyclopentadienyl)Uranium Oxide, Cp′2UO. *Organometallics* **2005**, *24*, 4251–4264. [CrossRef]
144. Evans, W.J.; Kozimor, S.A.; Ziller, J.W. Bis(Pentamethylcyclopentadienyl) U(III) Oxide and U(IV) Oxide Carbene Complexes. *Polyhedron* **2004**, *23*, 2689–2694. [CrossRef]
145. Fortier, S.; Brown, J.L.; Kaltsoyannis, N.; Wu, G.; Hayton, T.W. Synthesis, Molecular and Electronic Structure of U V(O) $[N(SiMe_3)_2]_3$. *Inorg. Chem.* **2012**, *51*, 1625–1633. [CrossRef] [PubMed]
146. Deng, C.; Liang, J.; Sun, R.; Wang, Y.; Fu, P.X.; Wang, B.W.; Gao, S.; Huang, W. Accessing Five Oxidation States of Uranium in a Retained Ligand Framework. *Nat. Commun.* **2023**, *14*, 4657. [CrossRef] [PubMed]
147. Settineri, N.S.; Shiau, A.A.; Arnold, J. Two-Electron Oxidation of a Homoleptic U(Iii) Guanidinate Complex by Diphenyldiazomethane. *Chem. Commun.* **2018**, *54*, 10913–10916. [CrossRef]
148. King, D.M.; Tuna, F.; McInnes, E.J.L.; McMaster, J.; Lewis, W.; Blake, A.J.; Liddle, S.T. Isolation and Characterization of a Uranium(VI)-Nitride Triple Bond. *Nat. Chem.* **2013**, *5*, 482–488. [CrossRef] [PubMed]
149. King, D.M.; Tuna, F.; McInnes, E.J.L.; McMaster, J.; Lewis, W.; Blake, A.J.; Liddle, S.T. Synthesis and Structure of a Terminal Uranium Nitride Complex. *Science (1979)* **2012**, *337*, 717–720. [CrossRef]
150. King, D.M.; Atkinson, B.E.; Chatelain, L.; Gregson, M.; Seed, J.A.; Wooles, A.J.; Kaltsoyannis, N.; Liddle, S.T. Uranium-Nitride Chemistry: Uranium-Uranium Electronic Communication Mediated by Nitride Bridges. *Dalton Trans.* **2022**, *51*, 8855–8864. [CrossRef]
151. Du, J.; King, D.M.; Chatelain, L.; Lu, E.; Tuna, F.; McInnes, E.J.L.; Wooles, A.J.; Maron, L.; Liddle, S.T. Thorium- and Uranium-Azide Reductions: A Transient Dithorium-Nitride: Versus Isolable Diuranium-Nitrides. *Chem. Sci.* **2019**, *10*, 3738–3745. [CrossRef]
152. Cleaves, P.A.; King, D.M.; Kefalidis, C.E.; Maron, L.; Tuna, F.; McInnes, E.J.L.; McMaster, J.; Lewis, W.; Blake, A.J.; Liddle, S.T. Two-Electron Reductive Carbonylation of Terminal Uranium(V) and Uranium(VI) Nitrides to Cyanate by Carbon Monoxide. *Angew. Chem.—Int. Ed.* **2014**, *53*, 10412–10415. [CrossRef]
153. Evans, W.J.; Kozimor, S.A.; Ziller, J.W. Chemistry: Molecular Octa-Uranium Rings with Alternating Nitride and Azide Bridges. *Science (1979)* **2005**, *309*, 1835–1838. [CrossRef]
154. Thomson, R.K.; Cantat, T.; Scott, B.L.; Morris, D.E.; Batista, E.R.; Kiplinger, J.L. Uranium Azide Photolysis Results in C-H Bond Activation and Provides Evidence for a Terminal Uranium Nitride. *Nat. Chem.* **2010**, *2*, 723–729. [CrossRef] [PubMed]
155. Barluzzi, L.; Scopelliti, R.; Mazzanti, M. Photochemical Synthesis of a Stable Terminal Uranium(VI) Nitride. *J. Am. Chem. Soc.* **2020**, *142*, 19047–19051. [CrossRef] [PubMed]
156. Palumbo, C.T.; Scopelliti, R.; Zivkovic, I.; Mazzanti, M. C-H Bond Activation by an Isolated Dinuclear U(III)/U(IV) Nitride. *J. Am. Chem. Soc.* **2020**, *142*, 3149–3157. [CrossRef] [PubMed]
157. Barluzzi, L.; Hsueh, F.C.; Scopelliti, R.; Atkinson, B.E.; Kaltsoyannis, N.; Mazzanti, M. Synthesis, Structure, and Reactivity of Uranium(vi) Nitrides. *Chem. Sci.* **2021**, *12*, 8096–8104. [CrossRef]
158. Staun, S.L.; Wu, G.; Lukens, W.W.; Hayton, T.W. Synthesis of a Heterobimetallic Actinide Nitride and an Analysis of Its Bonding. *Chem. Sci.* **2021**, *12*, 15519–15527. [CrossRef]
159. Tatebe, C.J.; Zeller, M.; Bart, S.C. [2π+2π] Cycloaddition of Isocyanates to Uranium(IV) Imido Complexes for the Synthesis of U(IV) K2-Ureato Compounds. *Inorg. Chem.* **2017**, *56*, 1956–1965. [CrossRef]
160. Evans, W.J.; Miller, K.A.; Ziller, J.W.; Greaves, J. Analysis of Uranium Azide and Nitride Complexes by Atmospheric Pressure Chemical Ionization Mass Spectrometry. *Inorg. Chem.* **2007**, *46*, 8008–8018. [CrossRef] [PubMed]
161. Meyer, K.; Mindiola, D.J.; Baker, T.A.; Davis, W.M.; Cummins, C.C. Uranium Hexakisamido Complexes. *Angew. Chem.—Int. Ed.* **2000**, *39*, 3063–3066. [CrossRef]
162. Anderson, N.H.; Yin, H.; Kiernicki, J.J.; Fanwick, P.E.; Schelter, E.J.; Bart, S.C. Investigation of Uranium Tris(Imido) Complexes: Synthesis, Characterization, and Reduction Chemistry of $[U(NDIPP)_3(Thf)_3]$. *Angew. Chem.* **2015**, *127*, 9518–9521. [CrossRef]
163. Anderson, N.H.; Odoh, S.O.; Yao, Y.; Williams, U.J.; Schaefer, B.A.; Kiernicki, J.J.; Lewis, A.J.; Goshert, M.D.; Fanwick, P.E.; Schelter, E.J.; et al. Harnessing Redox Activity for the Formation of Uranium Tris(Imido) Compounds. *Nat. Chem.* **2014**, *6*, 919–926. [CrossRef]
164. Hayton, T.W.; Boncella, J.M.; Scott, B.L.; Batista, E.R.; Hay, P.J. Synthesis and Reactivity of the Imido Analogues of the Uranyl Ion. *J. Am. Chem. Soc.* **2006**, *128*, 10549–10559. [CrossRef] [PubMed]

165. Hayton, T.W.; Boncella, J.M.; Scott, B.L.; Palmer, P.D.; Batista, E.R.; Hay, J.P. Synthesis of Imido Analogs of the Uranyl Ion. *Science (1979)* **2005**, *310*, 1941–1943. [CrossRef] [PubMed]
166. Lam, O.P.; Franke, S.M.; Nakai, H.; Heinemann, F.W.; Hieringer, W.; Meyer, K. Observation of the Inverse Trans Influence (ITI) in a Uranium(V) Imide Coordination Complex: An Experimental Study and Theoretical Evaluation. *Inorg. Chem.* **2012**, *51*, 6190–6199. [CrossRef] [PubMed]
167. Anderson, N.H.; Xie, J.; Ray, D.; Zeller, M.; Gagliardi, L.; Bart, S.C. Elucidating Bonding Preferences in Tetrakis(Imido)Uranate(VI) Dianions. *Nat. Chem.* **2017**, *9*, 850–855. [CrossRef]
168. Andersen, R.A.; Brennan, J.G. Electron-Transfer Reactions of Trivalent Uranium. Preparation and Structure of (MeC5H4)3U=NPh and $[(MeC_5H_4)_3U]_2[\mu\text{-}\eta^1,\eta^1\text{-PhNCO}]$. *J. Am. Chem. Soc.* **1985**, *107*, 514–516. [CrossRef]
169. Tsoureas, N.; Cloke, F.G.N. Mixed Sandwich Imido Complexes of Uranium(V) and Uranium(IV): Synthesis, Structure and Redox Behaviour. *J. Organomet. Chem.* **2018**, *857*, 25–33. [CrossRef]
170. Vlaisavljevich, B.; Diaconescu, P.L.; Lukens, W.L.; Gagliardi, L.; Cummins, C.C. Investigations of the Electronic Structure of Arene-Bridged Diuranium Complexes. *Organometallics* **2013**, *32*, 1341–1352. [CrossRef]
171. Mullane, K.C.; Cheisson, T.; Nakamaru-Ogiso, E.; Manor, B.C.; Carroll, P.J.; Schelter, E.J. Reduction of Carbonyl Groups by Uranium(III) and Formation of a Stable Amide Radical Anion. *Chem.—Eur. J.* **2018**, *24*, 826–837. [CrossRef]
172. Arnold, P.L. Uranium-Mediated Activation of Small Molecules. *Chem. Commun.* **2011**, *47*, 9005–9010. [CrossRef]
173. Boreen, M.A.; Arnold, J. The Synthesis and Versatile Reducing Power of Low-Valent Uranium Complexes. *Dalton Trans.* **2020**, *49*, 15124–15138. [CrossRef]
174. Liddle, S.T. Progress in Nonaqueous Molecular Uranium Chemistry: Where to Next? *Inorg. Chem.* **2024**, *63*, 9366–9384. [CrossRef] [PubMed]
175. Hartline, D.R.; Meyer, K. From Chemical Curiosities and Trophy Molecules to Uranium-Based Catalysis: Developments for Uranium Catalysis as a New Facet in Molecular Uranium Chemistry. *JACS Au* **2021**, *1*, 698–709. [CrossRef] [PubMed]
176. Gardner, B.M.; Liddle, S.T. Small-Molecule Activation at Uranium(III). *Eur. J. Inorg. Chem.* **2013**, *2013*, 3753–3770. [CrossRef]
177. Liddle, S.T. The Renaissance of Non-Aqueous Uranium Chemistry. *Angew. Chem.* **2015**, *127*, 8726–8764. [CrossRef]
178. Lam, O.P.; Heinemann, F.W.; Meyer, K. A New Diamantane Functionalized Tris(Aryloxide) Ligand System for Small Molecule Activation Chemistry at Reactive Uranium Complexes. *C. R. Chim.* **2010**, *13*, 803–811. [CrossRef]
179. Andrews, L.; Zhou, M.; Liang, B.; Li, J.; Bursten, B.E. Reactions of Laser-Ablated U and Th with CO_2: Neon Matrix Infrared Spectra and Density Functional Calculations of OUCO, OThCO, and Other Products. *J. Am. Chem. Soc.* **2000**, *122*, 11440–11449. [CrossRef]
180. Mclaren, A.B.; Kanellakopulos, B.; Dornberger, E. Unexpected chemistry in the reduction of uranium cyclopentadienides. *Inorg. Nucl. Chem. Lett.* **1980**, *16*, 223–225. [CrossRef]
181. Diaconescu, P.L.; Arnold, P.L.; Baker, T.A.; Mindiola, D.J.; Cummins, C.C. Arene-Bridged Diuranium Complexes: Inverted Sandwiches Supported by δ Backbonding. *J. Am. Chem. Soc.* **2000**, *122*, 6108–6109. [CrossRef]
182. Evans, W.J.; Kozimor, S.A.; Ziller, J.W.; Kaltsoyannis, N. Structure, Reactivity, and Density Functional Theory Analysis of the Six-Electron Reductant, $[(C_5Me_5)_2U]_2(\mu\text{-}\eta^6{:}\eta^6\text{-}C_6H_6)$, Synthesized via a New Mode of $(C_5Me_5)_3M$ Reactivity. *J. Am. Chem. Soc.* **2004**, *126*, 14533–14547. [CrossRef]
183. Liddle, S.T. Inverted Sandwich Arene Complexes of Uranium. *Coord. Chem. Rev.* **2015**, *293–294*, 211–227. [CrossRef]
184. Evans, W.J. Tutorial on the Role of Cyclopentadienyl Ligands in the Discovery of Molecular Complexes of the Rare-Earth and Actinide Metals in New Oxidation States. *Organometallics* **2016**, *35*, 3088–3100. [CrossRef]
185. Macdonald, M.R.; Bates, J.E.; Ziller, J.W.; Furche, F.; Evans, W.J. Completing the Series of +2 Ions for the Lanthanide Elements: Synthesis of Molecular Complexes of Pr^{2+}, Gd^{2+}, Tb^{2+}, and Lu^{2+}. *J. Am. Chem. Soc.* **2013**, *135*, 9857–9868. [CrossRef] [PubMed]
186. Nicholas, H.M.; Mills, D.P. Lanthanides: Divalent Organometallic Chemistry. In *Encyclopedia of Inorganic and Bioinorganic Chemistry*; Wiley: New York, NY, USA, 2017; pp. 1–10.
187. Cassani, M.C.; Lappert, M.F.; Laschi, F. First Identification by EPR Spectra of Lanthanum(II) Organometallic (and $E_{1/2}$ for $La^{3+} \rightarrow La^{2+}$) in the C-O Bond Activation of Dimethoxyethane. *Chem. Commun.* **1997**, 1563–1564. [CrossRef]
188. Hitchcock, P.B.; Lappert, M.F.; Maron, L.; Protchenko, A.V. Lanthanum Does Form Stable Molecular Compounds in the +2 Oxidation State. *Angew. Chem.—Int. Ed.* **2008**, *47*, 1488–1491. [CrossRef] [PubMed]
189. Windorff, C.J.; MacDonald, M.R.; Meihaus, K.R.; Ziller, J.W.; Long, J.R.; Evans, W.J. Expanding the Chemistry of Molecular U^{2+} Complexes: Synthesis, Characterization, and Reactivity of the $\{[C_5H_3(SiMe_3)_2]_3U\}^-$ Anion. *Chem.—Eur. J.* **2016**, *22*, 772–782. [CrossRef]
190. Windorff, C.J.; Evans, W.J. 29Si NMR Spectra of Silicon-Containing Uranium Complexes. *Organometallics* **2014**, *33*, 3786–3791. [CrossRef]
191. Wedal, J.C.; Barlow, J.M.; Ziller, J.W.; Yang, J.Y.; Evans, W.J. Electrochemical Studies of Tris(Cyclopentadienyl)Thorium and Uranium Complexes in the +2, +3, and +4 Oxidation States. *Chem. Sci.* **2021**, *12*, 8501–8511. [CrossRef]
192. Huh, D.N.; Ziller, J.W.; Evans, W.J. Chelate-Free Synthesis of the U(II) Complex, $[(C_5H_3(SiMe_3)_2)_3U]^{1-}$, Using Li and Cs Reductants and Comparative Studies of La(II) and Ce(II) Analogs. *Inorg. Chem.* **2018**, *57*, 11809–11814. [CrossRef]
193. Parry, J.; Carmona, E.; Coles, S.; Hursthouse, M. Synthesis and Single Crystal X-Ray Diffraction on the First Isolable Carbonyl Complex of an Actinide, $(C_5Me_4H)_3U(CO)$. *J. Am. Chem. Soc.* **1995**, *117*, 2649–2650. [CrossRef]

194. Ryan, A.J.; Angadol, M.A.; Ziller, J.W.; Evans, W.J. Isolation of U(Ii) Compounds Using Strong Donor Ligands, C5Me4H and $N(SiMe_3)_2$, Including a Three-Coordinate U(Ii) Complex. *Chem. Commun.* **2019**, *55*, 2325–2327. [CrossRef]
195. Jenkins, T.F.; Woen, D.H.; Mohanam, L.N.; Ziller, J.W.; Furche, F.; Evans, W.J. Tetramethylcyclopentadienyl Ligands Allow Isolation of Ln(II) Ions across the Lanthanide Series in [K(2.2.2-Cryptand)][$(C_5Me_4H)_3$Ln] Complexes. *Organometallics* **2018**, *37*, 3863–3873. [CrossRef]
196. Guo, F.; Tsoureas, N.; Huang, G.; Tong, M.; Mansikkamäki, A.; Layfield, R.A. Isolation of a Perfectly Linear Uranium(II) Metallocene. *Angew. Chem.* **2020**, *132*, 2319–2323. [CrossRef]
197. Streitweiser, A.; Muller-Westerhoff, U. Bis(Cyclooctatetraeny Uranium (Uranocene). *J. Am. Chem. Soc.* **1968**, *90*, 7364. [CrossRef]
198. Boreen, M.A.; Lussier, D.J.; Skeel, B.A.; Lohrey, T.D.; Watt, F.A.; Shuh, D.K.; Long, J.R.; Hohloch, S.; Arnold, J. Structural, Electrochemical, and Magnetic Studies of Bulky Uranium(III) and Uranium(IV) Metallocenes. *Inorg. Chem.* **2019**, *58*, 16629–16641. [CrossRef] [PubMed]
199. Guo, F.S.; Chen, Y.C.; Tong, M.L.; Mansikkamäki, A.; Layfield, R.A. Uranocenium: Synthesis, Structure, and Chemical Bonding. *Angew. Chem.—Int. Ed.* **2019**, *58*, 10163–10167. [CrossRef]
200. McClain, K.R.; Gould, C.A.; Marchiori, D.A.; Kwon, H.; Nguyen, T.T.; Rosenkoetter, K.E.; Kuzmina, D.; Tuna, F.; Britt, R.D.; Long, J.R.; et al. Divalent Lanthanide Metallocene Complexes with a Linear Coordination Geometry and Pronounced 6s-5d Orbital Mixing. *J. Am. Chem. Soc.* **2022**, *144*, 22193–22201. [CrossRef]
201. Lapierre, H.S.; Scheurer, A.; Heinemann, F.W.; Hieringer, W.; Meyer, K. Synthesis and Characterization of a Uranium(II) Monoarene Complex Supported by δ-Backbonding. *Angew. Chem.—Int. Ed.* **2014**, *53*, 7158–7162. [CrossRef]
202. Bart, S.C.; Heinemann, F.W.; Anthon, C.; Hauser, C.; Meyer, K. A New Tripodal Ligand System with Steric and Electronic Modularity for Uranium Coordination Chemistry. *Inorg. Chem.* **2009**, *48*, 9419–9426. [CrossRef]
203. Lapierre, H.S.; Kameo, H.; Halter, D.P.; Heinemann, F.W.; Meyer, K. Coordination and Redox Isomerization in the Reduction of a Uranium(III) Monoarene Complex. *Angew. Chem.—Int. Ed.* **2014**, *53*, 7154–7157. [CrossRef]
204. Fieser, M.E.; Palumbo, C.T.; La Pierre, H.S.; Halter, D.P.; Voora, V.K.; Ziller, J.W.; Furche, F.; Meyer, K.; Evans, W.J. Comparisons of Lanthanide/Actinide +2 Ions in a Tris(Aryloxide)Arene Coordination Environment. *Chem. Sci.* **2017**, *8*, 7424–7433. [CrossRef]
205. Billow, B.S.; Livesay, B.N.; Mokhtarzadeh, C.C.; McCracken, J.; Shores, M.P.; Boncella, J.M.; Odom, A.L. Synthesis and Characterization of a Neutral U(II) Arene Sandwich Complex. *J. Am. Chem. Soc.* **2018**, *140*, 17369–17373. [CrossRef] [PubMed]
206. Straub, M.D.; Ouellette, E.T.; Boreen, M.A.; Britt, R.D.; Chakarawet, K.; Douair, I.; Gould, C.A.; Maron, L.; Del Rosal, I.; Villarreal, D.; et al. A Uranium(II) Arene Complex That Acts as a Uranium(I) Synthon. *J. Am. Chem. Soc.* **2021**, *143*, 19748–19760. [CrossRef]
207. Keener, M.; Shivaraam, R.A.K.; Rajeshkumar, T.; Tricoire, M.; Scopelliti, R.; Zivkovic, I.; Chauvin, A.S.; Maron, L.; Mazzanti, M. Multielectron Redox Chemistry of Uranium by Accessing the +II Oxidation State and Enabling Reduction to a U(I) Synthon. *J. Am. Chem. Soc.* **2023**, *145*, 16271–16283. [CrossRef] [PubMed]
208. Wedal, J.C.; Furche, F.; Evans, W.J. Density Functional Theory Analysis of the Importance of Coordination Geometry for 5f36d1versus 5f4Electron Configurations in U(II) Complexes. *Inorg. Chem.* **2021**, *60*, 16316–16325. [CrossRef]
209. Green, M.L.H.; Parkin, G. Application of the Covalent Bond Classification Method for the Teaching of Inorganic Chemistry. *J. Chem. Educ.* **2014**, *91*, 807–816. [CrossRef]
210. Wedal, J.C.; Bekoe, S.; Ziller, J.W.; Furche, F.; Evans, W.J. C−H Bond Activation via U(II) in the Reduction of Heteroleptic Bis(Trimethylsilyl)Amide U(III) Complexes. *Organometallics* **2020**, *39*, 3425–3432. [CrossRef]
211. Modder, D.K.; Scopelliti, R.; Mazzanti, M. Accessing a Highly Reducing Uranium(III) Complex through Cyclometalation. *Inorg. Chem.* **2024**, *63*, 9527–9538. [CrossRef]
212. Modder, D.K.; Palumbo, C.T.; Douair, I.; Scopelliti, R.; Maron, L.; Mazzanti, M. Single Metal Four-Electron Reduction by U(II) and Masked "u(II)" Compounds. *Chem. Sci.* **2021**, *12*, 6153–6158. [CrossRef]
213. Modder, D.K.; Palumbo, C.T.; Douair, I.; Fadaei-Tirani, F.; Maron, L.; Mazzanti, M. Delivery of a Masked Uranium(II) by an Oxide-Bridged Diuranium(III) Complex. *Angew. Chem.—Int. Ed.* **2021**, *60*, 3737–3744. [CrossRef]
214. Arliguie, T.; Lance, M.; Nierlich, M.; Vignerb, J.; Ephritikhinea, M. Inverse Cycloheptatrienyl Sandwich Complexes. Crystal Structure of $[U(BH_4)_2(OC_4H_8)_5][[(BH_4)_3U(\mu\text{-}\eta^7,\eta^7\text{-}C_7H_7)U(BH_4)_3]$. *J. Chem. Soc. Chem. Commun.* **1994**, 847–848. [CrossRef]
215. Arliguie, T.; Lance, M.; Nierlich, M.; Ephritikhine, M. Inverse Cycloheptatrienyl Sandwich Complexes of Uranium and Neodymium. *J. Chem. Soc. Dalton Trans.* **1997**, 2501–2504. [CrossRef]
216. Arliguie, T.; Lance, M.; Nierlich, M.; Vigner, J.; Ephritikhine, M. Synthesis and Crystal Structure of $[K(C_{12}H_{24}O_6)][U(\eta\text{-}C_7H_7)_2]$, The First Cycloheptatrienyl Sandwich Compound. *J. Chem. Soc. Chem. Commun.* **1995**, 183–184. [CrossRef]
217. Keerthi Shivaraam, R.A.; Keener, M.; Modder, D.K.; Rajeshkumar, T.; Živković, I.; Scopelliti, R.; Maron, L.; Mazzanti, M. A Route to Stabilize Uranium(II) and Uranium(I) Synthons in Multimetallic Complexes. *Angew. Chem.—Int. Ed.* **2023**, *62*, e202304051. [CrossRef]
218. Kiernicki, J.J.; Fanwick, P.E.; Bart, S.C. Utility of a Redox-Active Pyridine(Diimine) Chelate in Facilitating Two Electron Oxidative Addition Chemistry at Uranium. *Chem. Commun.* **2014**, *50*, 8189–8192. [CrossRef]
219. Barluzzi, L.; Giblin, S.R.; Mansikkamäki, A.; Layfield, R.A. Identification of Oxidation State +1 in a Molecular Uranium Complex. *J. Am. Chem. Soc.* **2022**, *144*, 18229–18233. [CrossRef]
220. Bratsch, S.G.; Lagowski, J.J. Actinide thermodynamic predictions. 3. Thermodynamics of compounds and aquo-ions of the 2+, 3+, and 4+ oxidation states and standard electrode potentials at 298.15 K. *J. Phys. Chem.* **1986**, *90*, 307–312. [CrossRef]

221. Inman, C.J.; Cloke, F.G.N. The Experimental Determination of Th(Iv)/Th(Iii) Redox Potentials in Organometallic Thorium Complexes. *Dalton Trans.* **2019**, *48*, 10782–10784. [CrossRef]
222. Moehring, S.A.; Evans, W.J. Evaluating Electron-Transfer Reactivity of Complexes of Actinides in +2 and +3 Oxidation States by Using EPR Spectroscopy. *Chem.—Eur. J.* **2020**, *26*, 1530–1534. [CrossRef] [PubMed]
223. Trinh, M.T.; Wedal, J.C.; Evans, W.J. Evaluating Electrochemical Accessibility of 4fn5d1and 4fn+1 Ln(II) Ions in $(C_5H_4SiMe_3)_3Ln$ and $(C_5Me_4H)_3Ln$ Complexes. *Dalton Trans.* **2021**, *50*, 14384–14389. [CrossRef]
224. Riedhammer, J.; Halter, D.P.; Meyer, K. Nonaqueous Electrochemistry of Uranium Complexes: A Guide to Structure-Reactivity Tuning. *Chem. Rev.* **2023**, *123*, 7761–7781. [CrossRef]
225. MacKenzie, I.A.; Wang, L.; Onuska, N.P.R.; Williams, O.F.; Begam, K.; Moran, A.M.; Dunietz, B.D.; Nicewicz, D.A. Discovery and Characterization of an Acridine Radical Photoreductant. *Nature* **2020**, *580*, 76–80. [CrossRef] [PubMed]
226. Su, J.; Windorff, C.J.; Batista, E.R.; Evans, W.J.; Gaunt, A.J.; Janicke, M.T.; Kozimor, S.A.; Scott, B.L.; Woen, D.H.; Yang, P. Identification of the Formal +2 Oxidation State of Neptunium: Synthesis and Structural Characterization of $\{NpII[C_5H_3(SiMe_3)_2]_3\}^{1-}$. *J. Am. Chem. Soc.* **2018**, *140*, 7425–7428. [CrossRef] [PubMed]
227. Windorff, C.J.; Chen, G.P.; Cross, J.N.; Evans, W.J.; Furche, F.; Gaunt, A.J.; Janicke, M.T.; Kozimor, S.A.; Scott, B.L. Identification of the Formal +2 Oxidation State of Plutonium: Synthesis and Characterization of $\{PuII[C_5H_3(SiMe_3)_2]_3\}^-$. *J. Am. Chem. Soc.* **2017**, *139*, 3970–3973. [CrossRef] [PubMed]
228. Wu, Q.Y.; Lan, J.H.; Wang, C.Z.; Cheng, Z.P.; Chai, Z.F.; Gibson, J.K.; Shi, W.Q. Paving the Way for the Synthesis of a Series of Divalent Actinide Complexes: A Theoretical Perspective. *Dalton Trans.* **2016**, *45*, 3102–3110. [CrossRef]
229. Goodwin, C.A.P.; Janicke, M.T.; Scott, B.L.; Gaunt, A.J. (An = Np, Pu) Preparation Bypassing An0Metal Precursors: Access to Np3+/Pu3+Nonaqueous and Organometallic Complexes. *J. Am. Chem. Soc.* **2021**, *143*, 20680–20696. [CrossRef]
230. Staun, S.L.; Stevens, L.M.; Smiles, D.E.; Goodwin, C.A.P.; Billow, B.S.; Scott, B.L.; Wu, G.; Tondreau, A.M.; Gaunt, A.J.; Hayton, T.W. Expanding the Nonaqueous Chemistry of Neptunium: Synthesis and Structural Characterization of $[Np(NR_2)_3Cl]$, $[Np(NR_2)_3Cl]^-$, and $[Np\{N(R)(SiMe_2CH_2)\}_2(NR_2)]$-(R = $SiMe_3$). *Inorg. Chem.* **2021**, *60*, 2740–2748. [CrossRef]
231. Pattenaude, S.A.; Anderson, N.H.; Bart, S.C.; Gaunt, A.J.; Scott, B.L. Non-Aqueous Neptunium and Plutonium Redox Behaviour in THF-Access to a Rare Np(III) Synthetic Precursor. *Chem. Commun.* **2018**, *54*, 6113–6116. [CrossRef] [PubMed]
232. Whitefoot, M.A.; Perales, D.; Zeller, M.; Bart, S.C. Synthesis of Non-Aqueous Neptunium(III) Halide Solvates from NpO_2. *Chem.—Eur. J.* **2021**, *27*, 18054–18057. [CrossRef]
233. Gaunt, A.J.; Enriquez, A.E.; Reilly, S.D.; Scott, B.L.; Neu, M.P. Structural Characterization of $Pu[N(SiMe_3)_2]_3$, a Synthetically Useful Nonaqueous Plutonium(III) Precursor. *Inorg. Chem.* **2008**, *47*, 26–28. [CrossRef]
234. Gaunt, A.J.; Reilly, S.D.; Enriquez, A.E.; Hayton, T.W.; Boncella, J.M.; Scott, B.L.; Neu, M.P. Low-Valent Molecular Plutonium Halide Complexes. *Inorg. Chem.* **2008**, *47*, 8412–8419. [CrossRef]
235. Lopez, L.M.; Uible, M.C.; Zeller, M.; Bart, S.C. Lewis Base Adducts of $NpCl_4$. *Chem. Commun.* **2024**, *60*, 5956–5959. [CrossRef] [PubMed]
236. Arnold, P.L.; Dutkiewicz, M.S.; Walter, O. Organometallic Neptunium Chemistry. *Chem Rev* **2017**, *117*, 11460–11475. [CrossRef]
237. Dutkiewicz, M.S.; Farnaby, J.H.; Apostolidis, C.; Colineau, E.; Walter, O.; Magnani, N.; Gardiner, M.G.; Love, J.B.; Kaltsoyannis, N.; Caciuffo, R.; et al. Organometallic Neptunium(III) Complexes. *Nat. Chem.* **2016**, *8*, 797–802. [CrossRef] [PubMed]
238. Goodwin, C.A.P.; Wooles, A.J.; Murillo, J.; Lu, E.; Boronski, J.T.; Scott, B.L.; Gaunt, A.J.; Liddle, S.T. Carbene Complexes of Neptunium. *J. Am. Chem. Soc.* **2022**, *144*, 9764–9774. [CrossRef] [PubMed]
239. Myers, A.J.; Tarlton, M.L.; Kelley, S.P.; Lukens, W.W.; Walensky, J.R. Synthesis and Utility of Neptunium(III) Hydrocarbyl Complex. *Angew. Chem.* **2019**, *131*, 15033–15037. [CrossRef]
240. Dutkiewicz, M.S.; Apostolidis, C.; Walter, O.; Arnold, P.L. Reduction Chemistry of Neptunium Cyclopentadienide Complexes: From Structure to Understanding. *Chem. Sci.* **2017**, *8*, 2553–2561. [CrossRef]
241. Shephard, J.J.; Berryman, V.E.J.; Ochiai, T.; Walter, O.; Price, A.N.; Warren, M.R.; Arnold, P.L.; Kaltsoyannis, N.; Parsons, S. Covalent Bond Shortening and Distortion Induced by Pressurization of Thorium, Uranium, and Neptunium Tetrakis Aryloxides. *Nat. Commun.* **2022**, *13*, 5923. [CrossRef]
242. Long, B.N.; Beltrán-Leiva, M.J.; Celis-Barros, C.; Sperling, J.M.; Poe, T.N.; Baumbach, R.E.; Windorff, C.J.; Albrecht-Schönzart, T.E. Cyclopentadienyl Coordination Induces Unexpected Ionic Am−N Bonding in an Americium Bipyridyl Complex. *Nat. Commun.* **2022**, *13*, 201. [CrossRef]
243. Goodwin, C.A.P.; Su, J.; Albrecht-Schmitt, T.E.; Blake, A.V.; Batista, E.R.; Daly, S.R.; Dehnen, S.; Evans, W.J.; Gaunt, A.J.; Kozimor, S.A.; et al. $[Am(C_5Me_4H)_3]$: An Organometallic Americium Complex. *Angew. Chem.* **2019**, *131*, 11821–11825. [CrossRef]
244. Goodwin, C.A.P.; Su, J.; Stevens, L.M.; White, F.D.; Anderson, N.H.; Auxier, J.D.; Albrecht-Schönzart, T.E.; Batista, E.R.; Briscoe, S.F.; Cross, J.N.; et al. Isolation and Characterization of a Californium Metallocene. *Nature* **2021**, *599*, 421–424. [CrossRef]